Mps1-dependent phosphorylation of the kinetochore protein Ndc80 is an intrinsic step in spindle checkpoint activation

Dissertation

submitted to the
Combined Faculties for the Natural Sciences and for Mathematics
of the Ruperto-Carola University of Heidelberg, Germany
for the degree of
Doctor of Natural Sciences

presented by
Stefan Kemmler

Dissertation

submitted to the
Combined Faculties for the Natural Sciences and for Mathematics
of the Ruperto-Carola University of Heidelberg, Germany
for the degree of
Doctor of Natural Sciences

presented by

Diplom-Biologist	Stefan Kemmler
born in:	Karlsruhe
Oral-examination:	17.12.2007

Mps1-dependent phosphorylation of the kinetochore protein Ndc80 is an intrinsic step in spindle checkpoint activation

Referees: Prof. Dr. Michael Brunner

PD Dr. Johannes Lechner

Diese Arbeit ist meinen Eltern gewidmet.

TABLE OF CONTENTS

ABBREVIATIONS

A	alanine
aa	amino acid
ade	adenine
Amp	ampicillin
ATP	adenosine triphosphate
bp	base pair
CBP	Calmoduline binding peptide
CEN	centromere
CHIP	chromatin immunoprecipitation
Chr	chromosome
°C	degree celsius
D	aspartate
DMSO	dimethyl sulfoxide
DNA	deoxyribonucleic acid
dNTP	deoxynucleosid 5´-triphosphate
DOC	deoxycholate
DTT	dithiothreitol
E. coli	*Escherichia coli*
EDTA	Ethylenediaminetetraacetic acid
EtOH	ethanol
FACS	Fluorescence activated cell sorting
FOA	5´-fluoroorotic acid
g	gram
GFP	Green Fluorescent Protein
h	hour
his	histidine
IP	immunoprecipitation
IPTG	isopropyl-beta-D-thiogalactopyranoside
k	1000
kb	kilo base
kDa	kilo Dalton
LB	Luria-Bertani media
leu	leucine
LiAc	lithium acetate
lys	lysine
M	molar
MALDI	Matrix Assisted Laser Desorption/Ionisation
Mbp	mega base pairs

min	minute
ml	milliliter
mg	milligram
µg	microgramm
µl	microliter
µM	micromolar
MT	microtubule
ng	nanogram
NZ	nocodazole
o/n	over night
OD587	optical density at 587 nm
ON	oligonucleotide
ORF	open reading frame
p	plasmid
PAGE	polyacrylamide gel electrophoresis
PBS	Phosphate Buffered Saline
PCR	polymerase chain reaction
PEG	Polyethylene glycol
PMSF	phenylmetanosulfonylfluoride
ProA	Protein A
PMSF	phenylmethylsulphonyl fluoride
PVDF	polyvinylidendifluoride
rpm	rotations per min
RT	room temperature
S	serine
S. cerevisiae	*Saccharomyces cerevisiae*
SDS	sodium dodecyl sulfate
sec	second
SPB	spindle pole body
t	time
T	threonine
TAP	tandem affinity purification
trp	tryptophane
ts	temperature sensitive
U	unit
ura	uracil
WB	Western Blot
WT	wild-type
Y	yeast strain

SUMMARY

The kinetochore is a multi-protein complex which supports chromosome segregation in mitosis by mediating the connection between centromeric DNA and the mitotic spindle. In addition, it serves as a docking platform for the spindle checkpoint proteins. The spindle checkpoint is a surveillance mechanism which monitors the proper assembly of the mitotic spindle apparatus. It allows the transition from meta- into anaphase only if all kinetochores are bipolarly attached to the spindle microtubules and if tension across the spindle is applied.

The tetrameric Ndc80-complex (Ndc80, Nuf2, Spc24, Spc25) is part of the kinetochore. It is highly conserved and was shown to be required for the spindle checkpoint in *S. cerevisiae* (Janke et al. 2001). The kinase Mps1 has also been implicated in spindle checkpoint control (Hartwick et al. 1996). In mammalian cells, the kinetochore localisation of Mps1 depends on the presence of the Ndc80-complex (Stucke et al. 2004). Furthermore, endogenous Mps1 was found as a faint Coomassie-stained protein band in a Ndc80-complex pull down from yeast (C. Jaeger, unpublished results). Based on these observations, the goal of the present studies was to elucidate whether components of the *S. cerevisiae* Ndc80-complex are phosphorylated by Mps1 and if this phosphorylation has an influence on the regulation of the spindle checkpoint. The following observations were made:

1. Mps1 physically interacts with Ndc80

- Mps1 weakly associates with the kinetochore by ChIP-analysis in *S. cerevisiae*.
- Mps1 physically interacts with the Ndc80-complex after spindle checkpoint activation by Mps1-overexpression.
- Mps1 specifically interacts with the conserved, globular N-terminus of Ndc80 *in vitro*.

2. Mps1 phosphorylates Ndc80

- Mps1 phosphorylates the N-terminus of Ndc80 *in vitro*.
- Ndc80-phosphorylation depends on Mps1 *in vivo*.

3. Ndc80-phosphorylation activates the spindle assembly checkpoint

- Ndc80 in its non-phosphorylated state (ndc80^{14A}) is checkpoint deficient.
- constitutive pseudo-phosphorylation of Ndc80 (ndc80^{14D}) causes lethality due to a permanently activated spindle checkpoint (cell cycle arrest in mitosis). This checkpoint activation specifically depends on the checkpoint proteins Mad2 and Bub1.

⇒ Ndc80-phosphorylation by Mps1 is an intrinsic step of the spindle checkpoint pathway!

4. The kinetochore of ndc80^{14D}-cells is functional

- The expression levels and the kinetochore localisation of the ndc80^{14D} protein are comparable to the wild-type protein.
- The ndc80^{14D}-protein is able to compete with the wild-type protein for binding-sites at the kinetochore.
- the spindle in ndc80^{14D}-cells is under tension, a state which can only be achieved in the presence of an intact kinetochore.

⇒ the observed checkpoint activation is specifically caused by the introduced point mutations rather than by a defective ndc80^{14D}-protein.

5. Mps1-activity is required downstream of Ndc80

- The ndc80^{14D} mutant is unable to activate the spindle checkpoint in Mps1-depleted cells.

⇒ Mps1 has a second function in spindle checkpoint activation downstream of Ndc80-phosphorylation which might involve the phosphorylation of the checkpoint protein Mad1.

The results which were obtained in the current work provide evidence that Mps1 specifically phosphorylates Ndc80 and that Ndc80-phosphorylation is the mechanism by which the spindle checkpoint is activated in the presence of unattached kinetochores in early stages of mitosis.
The functional characterisation of Ndc80-phosphorylation allows for a refinement of the current model of the spindle assembly checkpoint (Figure 34).

ZUSAMMENFASSUNG

Das Kinetochor ist ein Multiprotein Komplex, der die Chromosomen-Segregation in der Mitose vermittelt, indem er die Verbindung zwischen Centromer-DNA und der mitotischen Spindel herstellt. Darüber hinaus fungiert das Kinetochor als Plattform für die Proteine des Spindel Checkpoints. Der Spindel Checkpoint ist ein Kontrollmechanismus, der den korrekten Aufbau der mitotischen Spindel überwacht. Er lässt den Übergang von der Meta- in die Anaphase nur zu, wenn alle Kinetochore bipolar an Spindel-Mikrotubuli angeheftet sind und wenn die Spindel unter Spannung steht. Der tetramere Ndc80-Komplex (Ndc80, Nuf2, Spc24, Spc25) ist Teil des Kinetochors. Er ist hoch konserviert und wird für den Spindel Checkpoint in *S. cerevisiae* benötigt (Janke et al. 2001). Neben dem Ndc80-Komplex wurde auch die Kinase Mps1 mit dem Spindel Checkpoint in Verbindung gebracht (Hartwick et al. 1996). In Säugerzellen ist die Kinetochor Lokalisation von Mps1 abhängig von der Anwesenheit des Ndc80-Komplex (Stucke et al. 2004). Darüber hinaus wurde endogenes Mps1 als schwache Coomassie-gefärbte Proteinbande in einer Aufreinigung des Ndc80-Komplex aus Hefe gefunden (C. Jaeger, nicht publizierte Daten).

Basierend auf diesen Beobachtungen war das Ziel der vorliegenden Arbeit herauszufinden, ob Komponenten des *S. cerevisiae* Ndc80-Komplex von Mps1 phosphoryliert werden und ob diese Phosphorylierung die Aktivität des Spindel Checkpoints reguliert.

Folgende Ergebnisse wurden erzielt:

1. Mps1 interagiert physisch mit Ndc80

- Mps1 assoziiert schwach mit dem Kinetochor in *S. cerevisiae* (ChIP-Analyse).
- Mps1 interagiert physisch mit dem Ndc80-Komplex *in vivo* nach Spindle Checkpoint Aktivierung durch Mps1-Überexpression.
- Mps1 bindet spezifisch an den konservierten, globulären N-Terminus von Ndc80 *in vitro*.

2. Mps1 phosphoryliert Ndc80

- Mps1 phosphoryliert den N-Terminus von Ndc80 *in vitro*.
- Die Phosphorylierung von Ndc80 ist abhängig von Mps1 *in vivo*.

3. Ndc80-Phosphorylierung aktiviert den Spindle Assembly Checkpoint

- Ndc80 in seiner nicht-phosphorlierten Form ($ndc80^{14A}$) ist Checkpoint defizient.
- konstitutive Pseudo-Phosphorylierung von Ndc80 ($ndc80^{14D}$) verursacht einen lethalen Phänotyp aufgrund eines permanent aktivierten Spindel Checkpoints (Zellzyklus-Arrest in der Metaphase). Diese Checkpoint-Aktivierung ist spezifisch abhängig von den Checkpoint Proteinen Mad2 und Bub1.

⇒ Ndc80-Phosphorylierung durch Mps1 ist ein integraler Schritt im Spindle Checkpoint!

4. Das Kinetochor von $ndc80^{14D}$-Zellen ist funktional

- Die Protein-Level und die Kinetochor Lokalisation des $ndc80^{14D}$-Proteins sind vergleichbar mit dem Wildtyp Protein.
- Das $ndc80^{14D}$-Protein ist in der Lage, mit dem Ndc80-Wildtyp Protein um Bindungsstellen am Kinetochor zu kompetitieren.
- Die Spindel in $ndc80^{14D}$-Zellen steht unter Spannung, ein Zustand, der nur in Anwesenheit eines intakten Kinetochors erreicht werden kann.

⇒ die beobachtete Spindel Checkpoint Aktivierung wird spezifisch durch die eingeführten Punktmutationen ausgelöst und nicht durch ein defektes $ndc80^{14D}$-Protein.

5. Mps1-Aktivität wird „downstream" von Ndc80 benötigt

- in Mps1-depletierten Zellen ist die $ndc80^{14D}$ Mutante nicht in der Lage, den Spindel Checkpoint zu aktivieren.

⇒ Mps1 hat neben der Ndc80-Phosphorylierung eine zweite Funktion im Zusammenhang mit der Aktivierung des Spindel Checkpoints, welche die Phosphorylierung des Checkpoint Proteins Mad1 beinhalten könnte.

Die Resultate, die im Verlauf der vorliegenden Arbeit erzielt werden konnten, liefern Hinweise darauf, daß Ndc80 spezifisch von Mps1 phosphoryliert wird und daß die Ndc80-Phosphorylierung der Mechanismus ist, durch den der Spindel Checkpoint in der Anwesenheit von freien Kinetochoren aktiviert wird.
Die funktionelle Charakterisierung der Ndc80-Phosphorylierung erlaubt eine Verfeinerung des heutigen Modells des Spindel Assembly Checkpoint (Figure 34).

1 INTRODUCTION

1.1 *S. cerevisiae* as a model organism

In the present work, *Saccharomyces cerevisiae* (*S. cerevisiae,* baker's yeast, budding yeast) was used as a model organism to study the role of the kinetochore in spindle checkpoint regulation. Because of its relative low complexity, *S. cerevisiae* is one of the most important eukaryotic model organism for the investigation of basic cellular processes which are often highly conserved. The small genome, the fast growth rate and the ease of genetic manipulation make it a convenient organism for biological studies. In the last decades, the cell cycle and its complex regulation could be dissected on the molecular level. *S. cerevisiae* proliferates in a haploid or in a diploid state. In the haploid state, the phenotype of mutants or gene deletions can be easily studied without having a second copy of the gene present in the cell. In respect to the kinetochore research field, yeast is particularly useful since its centromeric DNA is only 125 bp in length and therefore relatively simple compared to the complex mammalian centromere which spans a region of several Mbp. In addition, the yeast kinetochore is comprised of approximately 65 different proteins - a small number compared to the situation in higher eukaryotic organisms.

1.2 The *S. cerevisiae* cell cycle

In order to grow and divide, a cell needs to coordinate numerous essential processes in space and time. Among those, the duplication of the genetic material and its distribution between mother and daughter cell are essential for viability. In unicellular organisms like yeast, errors in the regulation of these events often leads to cell death. In multicellular organisms, developmental defects or cancer can be the consequence of a misregulated cell cycle. Therefore, the dissection of the processes which regulate the cell cycle are of particular interest. To ensure the correct progression through the cell cycle, several regulatory mechanisms are active of which reversible protein phosphorylation and the proteasome dependent degradation of proteins are of major importance. These processes are highly conserved among eukaryotic organisms.

The eukaryotic cell cycle (Figure 1) ensures the coordinated growth of a cell and its division into mother and daughter cell. It consists of 4 phases which are passed in a cyclic sequence. The genetic material is duplicated in S-phase (S = Synthesis). The replication of the DNA is initiated

at so called origins of replication. Each origin is activated only once during S-phase which ensures that the DNA is duplicated exactly once per cell cycle. Beside DNA-replication, the duplication of the spindle pole body (SPB) and kinetochores is essential for the separation of the genetic material in mitosis. The duplication of the SPB, the equivalent of the mammalian centrosome, follows a conservative mechanism which is initiated in late G_1-phase by the activity of two protein kinases, Cdc28 and Mps1. In contrast to mammalian cells, the SPBs of yeast are embedded in the nuclear envelope. The molecular mechanism of kinetochore-duplication is unknown. Morphologically, the beginning of S-phase is characterised by the appearance of a small bud.

When DNA-replication is completed, the cell enters the G_2-phase (G = Gap) which is rather short in budding yeast. The cell increases in mass due to RNA and protein biosynthesis. Furthermore, the maturation of the SPBs is completed and their separation is initiated.

The G_2-phase is followed by mitosis, which controls the faithful segregation of the genetic material into mother and daughter cell. It can be further subdivided into five consecutive and morphologically distinct phases: prophase, prometaphase, metaphase, anaphase and telophase. Unlike in mammalian cells, the nuclear envelope does not break down in *S. cerevisiae* ("closed mitosis"). In prophase, the chromatin condenses to form distinct chromosomes which can be seen by light microscopy. The degree of chromatin condensation in yeast is low compared to other eukaryotic organisms. Between the spindle pole bodies, the mitotic spindle apparatus forms. At the same time, the two SPBs migrate to opposite poles of the nucleus. In prometaphase, the spindle microtubules attach to the kinetochores (K-fibers). Other microtubules emanating from the poles overlap in the middle of the mitotic spindle and form the so called interpolar microtubules which are involved in the elongation of the mitotic spindle in late anaphase. In metaphase, the two SPBs have reached opposite poles and the sister kinetochores are attached to microtubules emanating from opposing poles. In yeast, each kinetochore is attached to a single microtubule fiber. In contrast, each kinetochore of higher eukaryotes interacts with several (up to 24) microtubules (McEwen 1997). Only if all kinetochores of the cell are attached to microtubules and tension is applied across the mitotic spindle, the cell enters the next phase of the cell cycle. Proper bipolar attachment is monitored by the so called spindle assembly checkpoint (Figure 2). At this stage, a short metaphase spindle can be seen between the two SPBs. Once sister kinetochores are attached to the spindle, tension is created which slightly pulls the sister kinetochores apart (about 1 μm). Since the sister chromatids are held together by the cohesin

complex, the centromer regions are separated and can be visualised by fluorescence microscopy as two distinct dots when labeled with GFP (4.2.16). However, this separation of centromeric regions in metaphase is highly dynamic since the opposing force of the cohesins pulls the centromeres back together. This process is termed “chromosome breathing” (He et al. 2000). In mammalian cells, all chromosomes align in the so called metaphase plate. However, this situation could not be shown for *S. cerevisiae.*

In anaphase, both sister chromatids of a chromosome are separated and move to opposite poles of the mitotic spindle. This process is regulated via Cdc20, the substrate specifying subunit of the anaphase promoting complex (APC) which is inhibited by the spindle checkpoint until bipolar attachment is reached (Figure 3). The APC is a ubiquitin-ligase which is activated at the meta-to-anaphase transition when all kinetochores are properly attached to the mitotic spindle and tension is applied. The action of the APC^{Cdc20} leads to the proteasome dependent proteolysis of several key regulators like Pds1. The degradation of Pds1 allows the activation of the protease Esp1 which cleaves the cohesin subunit Scc1 (Sister chromatid cohesion 1) which in turn initiates chromosome segregation. The Pds1-protein levels are therefore a good marker for the activity of the spindle checkpoint since Pds1 is degraded upon spindle checkpoint inactivation at the meta-to-anaphase transition. The movement of the chromatids towards the poles is supported by the shortening of the kinetochore microtubules (anaphase A) and by the overall elongation of the mitotic spindle (anaphase B).

In telophase, each cell body contains a complete set of chromosomes. The segregation of the chromosomes is followed by cytokinesis which separates the cytoplasm and thus creates a mother and a daughter cell. The cell cycle is completed by the G_1-phase. The length of this phase is influenced by the cell size which increases due to the synthesis of RNA and proteins which in turn prepares the cell for the next round of DNA-replication. The progression from G_1-phase into the next S-phase is controlled by a pathway called START which represents a point of no return. Once START is reached, the cell is committed to S-phase and a whole new cell cycle. Because G_1-, S- und G_2-phase lie between two mitotic divisions they are together referred to as interphase.

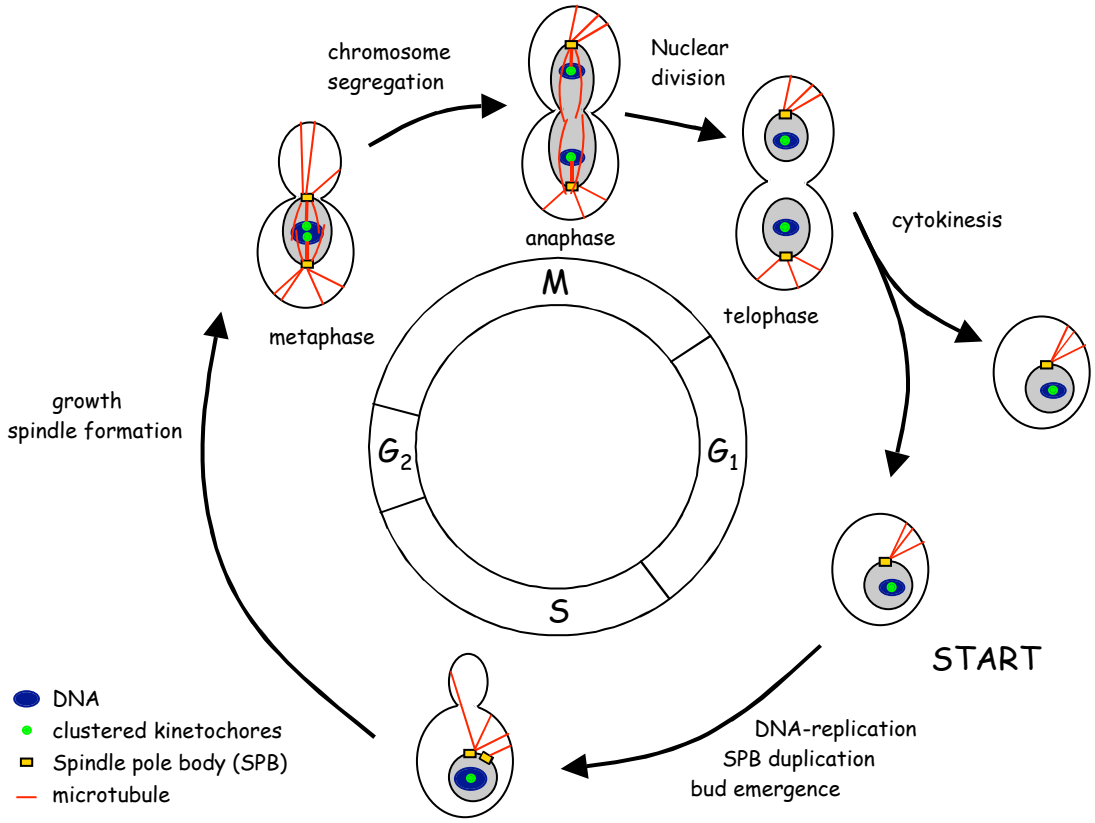

Figure 1: The *S. cerevisiae* cell cycle.

The genetic information is duplicated in S-phase (synthesis) and subsequently distributed between mother and daughter cell in mitosis. Both phases are separated by the G_1- and G_2-phase during which the cell increases in mass due to RNA- and protein-biosynthesis. Cytokinesis separates the cytoplasm and thus creates a mother and a daughter cell.

1.3 Mitotic checkpoints

For cell viability it is essential that individual steps of the cell cycle are precisely orchestrated. The cell has to ensure that a critical process is initiated only after the upstream events have been successfully completed. The tight regulation of cell growth and cell division is monitored by so called cell cycle checkpoints which inhibit cell cycle progression until the cell is ready for the entry into the next phase (Elledge 1996; Murray 1994). In mitosis, two of those evolutionary conserved checkpoints control the accurate segregation of sister chromatids into mother and daughter cell. The spindle assembly checkpoint monitors the bipolar attachment of the sister kinetochores to microtubules emanating from opposing spindle poles and the establishment of tension across the mitotic spindle apparatus (Figure 2). The spindle positioning checkpoint (1.3.2)

regulates the correct positioning of the spindle along the mother-bud axis. Both checkpoints inhibit the onset of anaphase until the mitotic spindle is properly assembled and positioned.

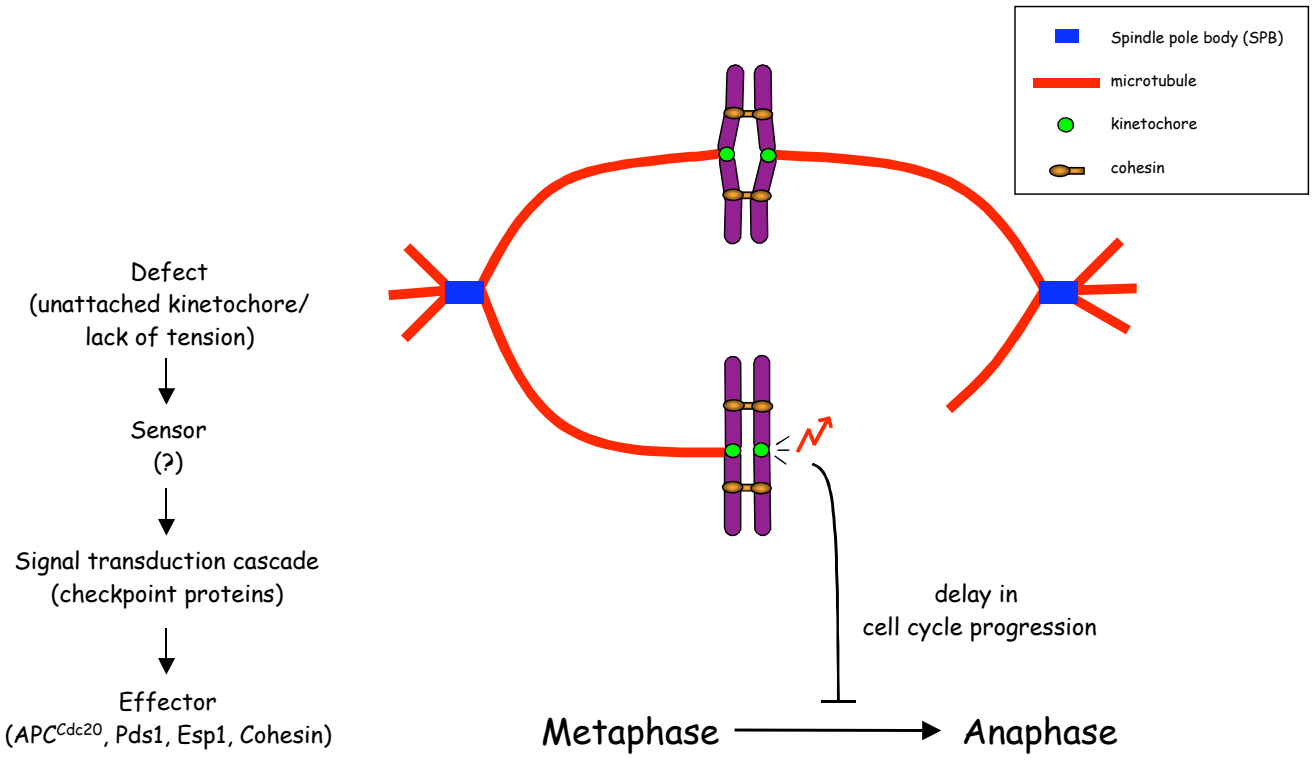

Figure 2: The meta-to-anaphase transition is controlled by the spindle assembly checkpoint.

The spindle assembly checkpoint delays cell cycle progression from meta- to anaphase in response to unattached kinetochores or the lack of tension.

1.3.1 The spindle assembly checkpoint (Mad2-checkpoint)

1.3.1.1 Microtubule-Attachment

In the last 16 years, the spindle assembly checkpoint has been extensively studied. In 1991, two independent genetic screens led to the identification of genes which bypass the mitotic arrest in response to spindle poisons (Hoyt et al. 1991; Li et al. 1991). The genes identified by those screens included the MAD (mitotic-arrest deficient) and the BUB (budding uninhibited by benzimidazole) genes (Table 1). The products of these genes are part of a highly conserved regulatory pathway which monitors the assembly of the mitotic spindle apparatus and the accurate segregation of sister chromatids during mitosis (Hardwick 1998; Musacchio and Salmon

2007). Therefore, it was termed the spindle assembly checkpoint (Figure 3). Mutations in these genes lead to errors in chromosome segregation and thus cause genetic instability, a hallmark of many cancer cells. The consequences of a defective spindle assembly checkpoint indicate that the investigation of the exact molecular mechanisms underlying this pathway are of major importance.

The inhibition of cell cycle progression in response to unattached kinetochores is mediated via the anaphase promoting complex and its substrate specifying subunit Cdc20 (APC^{Cdc20}). Elegant studies have demonstrated that a single unattached kinetochore is sufficient to delay the cell cycle at the meta-to-anaphase transition (Rieder et al. 1995). As a response, the checkpoint protein Mad2 is recruited to unattached kinetochores (Chen et al. 1996; Li and Benzra 1996). Mad1 is required for the kinetochore localisation of Mad2. Mad2 exists in two conformations, C-Mad2 ("closed") and O-Mad2 ("open"). In its closed form, Mad2 interacts with Mad1 (Mad1/C-Mad2) and acts as a template recruiting O-Mad2, a process known as conformational dimerisation. O-Mad2 is then able to bind Cdc20 which in turn induces a conformational change in Mad2 (from O-Mad2 to C-Mad2). The C-Mad2/Cdc20-dimer is thought to promote the formation of more C-Mad2/Cdc20-dimers in an autocatalytic prion-like reaction. This mechanism amplifies the checkpoint signal which leads to the inhibition of the APC and therefore to a checkpoint mediated cell cycle arrest in metaphase (De Antoni et al. 2005; Yu 2006). This so called "Mad2-template model of checkpoint activation" provides a molecular mechanism to explain the observation that a single kinetochore is sufficient to activate the spindle checkpoint. Beside the direct inactivation of Cdc20 by Mad2, there is another protein-complex which inhibits the ability of Cdc20 to activate the APC. Unattached kinetochores contribute to the creation of the so called mitotic checkpoint complex (MCC), which consists of Mad2, Mad3 and Bub3. Within the MCC, both Mad2 and Mad3 bind Cdc20 directly. The MCC was shown to be a 3000-fold stronger APC^{Cdc20}-inhibitor *in vitro* compared with recombinant Mad2 alone.

Once bipolar attachment of all kinetochores is achieved, Mad2 is inactivated, liberating Cdc20 which can now bind and activate the APC. The APC^{Cdc20} is a multiprotein E3 ubiquitin ligase responsible for the proteasome dependent destruction of a range of cell cycle regulators at the meta-to-anaphase transition (Table 1). The key target for anaphase onset is the securin Pds1, the inhibitor of the separase Esp1. When Pds1 is degraded, Esp1 is activated and cleaves Scc1, a subunit of the cohesin complex which is responsible for the connection of the sister chromatids ("chromosomal glue"). The cleavage of the cohesin complex eliminates the forces which hold

together the sisters and thus leads to their segregation towards opposite poles of the mitotic spindle. The degradation of proteins at the meta-to-anaphase transition is irreversible and thus gives the cell cycle a direction.

Although it is clear that unattached kinetochores in metaphase cause cell cycle arrest via the inhibition of the APC^{Cdc20}, the primary signal that activates the checkpoint on the molecular level could not be identified so far.

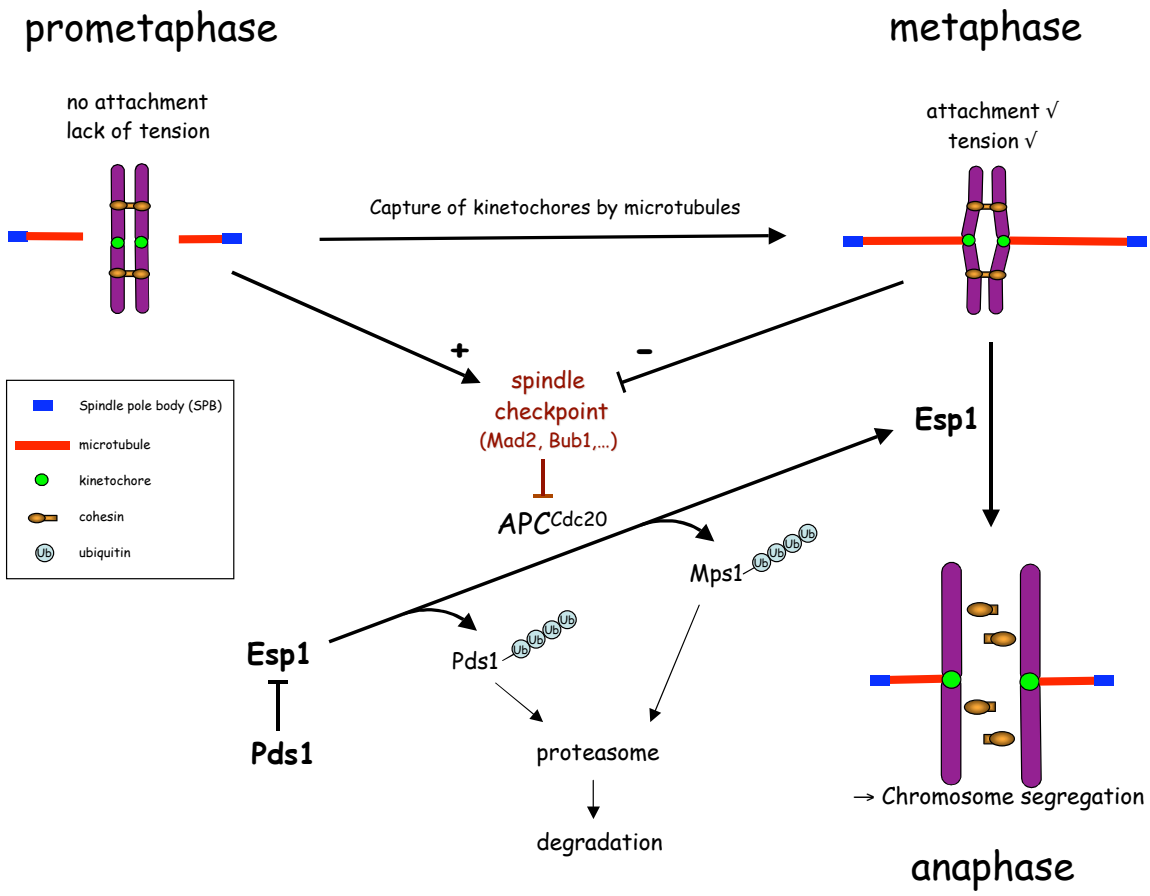

Figure 3: The spindle assembly checkpoint.

In prometaphase, the spindle assembly checkpoint is active due to the presence of unattached kinetochores which inhibits Cdc20 and therefore the anaphase promoting complex (APC). Esp1 is a protease, the activity of which is required to remove sister chromatid cohesion at the meta-to-anaphase transition. Prior to anaphase, Esp1 is kept inactive by its inhibitor Pds1 (Securin). Once bipolar attachment is created in metaphase, tension is applied to the mitotic spindle which negatively regulates the checkpoint. As a consequence, Cdc20 is no longer kept inactive and can now associate with the APC which leads to its activation. The APC^{Cdc20} is a E3 ubiquitin ligase which targets Pds1 for proteolytic destruction by the proteasome. The decrease in Pds1-levels leads to the activation of Esp1 which in turn cleaves the cohesin complex. The loss of sister chromatid cohesion initiates the onset of anaphase and chromosome segregation. The degradation of Mps1 by the APC^{Cdc20} irreversibly inactivates the spindle checkpoint in anaphase (Palframan et al. 2006).

1.3.1.2 Kinetochore-Tension

As illustrated in Figure 4, kinetochores can be attached to the mitotic spindle in a syntelic manner. In this case, all kinetochores are fully attached. However, the initiation of sister chromatid segregation at this stage would lead to missegregation of chromosomes and therefore to aneuploidy. In order to prevent cell cycle progression, the spindle assembly checkpoint responds not only to the lack of attachment but also to the absence of tension (McIntosh et al. 1991; Li and Nicklas 1995) which allows the checkpoint to distinguish between sister kinetochores attached to microtubules emanating from the same pole (syntelic attachment, Figure 4B) and kinetochores which are bipolarly attached (amphitelic attachment, Figure 4A). Therefore, tension is an indirect indication of bipolarity.

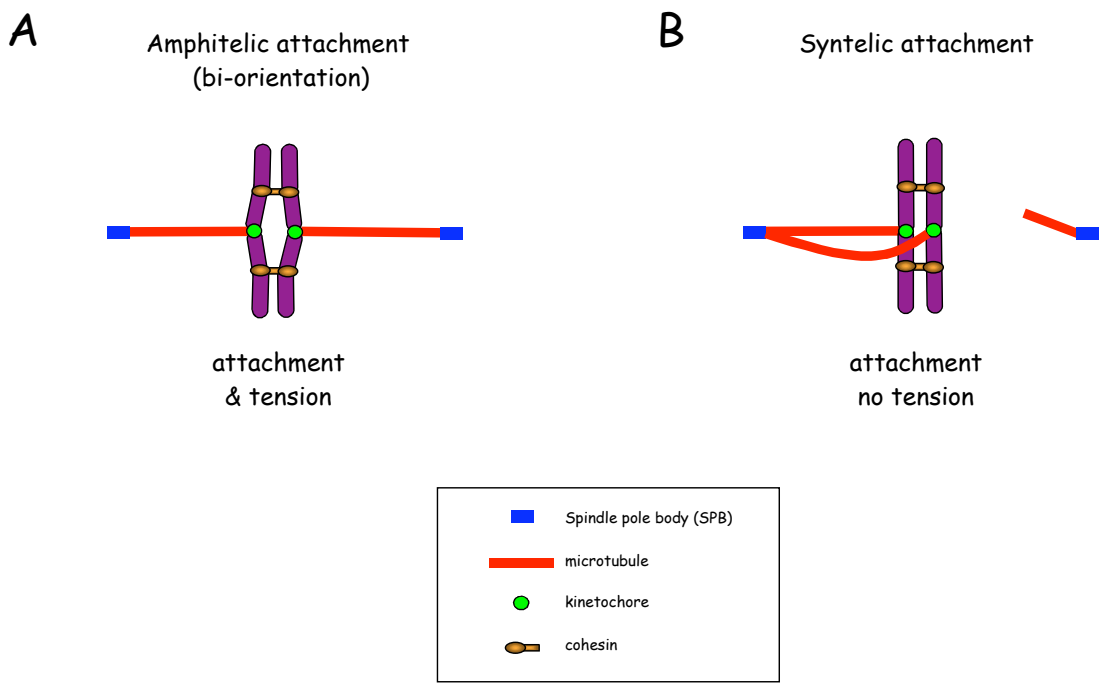

Figure 4: Kinetochore-microtubule attachments.

(A) *Amphitelic attachment.* Each kinetochore is attached to microtubules emanating from opposing spindle poles.
(B) *Syntelic attachment.* Both sister kinetochores attach to microtubules emanating from the same pole.

One striking difference between the checkpoint response to lack of tension and that to lack of attachment is the recruitment of the Mad and Bub proteins. Mad2 e.g. localises to unattached kinetochores but not to attached kinetochores which lack tension (Waters et al. 1998). On the

other hand, Bub1 and Mad1 are stably associated with kinetochores lacking either attachment or tension (Skoufias et al. 2001; Taylor et al. 2001). The molecular mechanism sensing tension is poorly characterised. In mutants which are defective in DNA-replication (e.g. *cdc6*) or sister chromatid cohesion the spindle checkpoint gets activated (Stern and Murray 2001; Biggins and Murray 2001). In both cases, kinetochores are attached to microtubules however tension cannot be created. The presence of a phospho-epitope at unattached kinetochores which can no longer be detected upon proper bipolar attachment (Gorbsky and Ricketts 1993) suggests that phosphorylation of a kinetochore component might act as a signal regulating the tension branch of the spindle assembly checkpoint (see 1.6).

The activity of the type-B Aurora kinase Ipl1 was shown to be important for sensing tension at kinetochores and for the establishment of a bipolar spindle (Biggins and Murray 2001; Tanaka et al. 2002, Table 1). Temperature sensitive *ipl1* mutants proceed through the cell cycle in the presence of syntelically attached kinetochores without detectable spindle checkpoint delay which leads to a monopolar distribution of the sister chromatids with a preference for the daughter cell (Biggins et al. 1999; Tanaka et al. 2002). Furthermore, it was shown that the activation of the spindle checkpoint in response to microtubule depolymerisation is independent of Ipl1. Ipl1 supports the formation of bipolarity by resolving syntelically attached kinetochores by a yet unknown mechanism. The resulting unattached kinetochore triggers the spindle assembly checkpoint giving the cell time for the formation of amphitelic kinetochore attachments (Pinsky et al. 2003; Pinsky et al. 2006). The molecular mechanism of Ipl1-inactivation after the establishment of a bipolar spindle is currently unknown. One possible mode of inactivation implies the mechanical dissociation of Ipl1 from the kinetochore once tension is created (Tanaka et al. 2002).

The activation of the spindle checkpoint in response to microtubule depolymerisation by nocdazole is stronger than the cell cycle delay caused by the absence of tension. Furthermore, microtubule attachment is stabilised by tension (Nicklas et al. 2001). The inter-relation between attachment and tension makes it difficult to conclude which is the primary defect monitored by the spindle checkpoint.

In anaphase, sister chromatids get separated and are therefore no longer under tension. At this stage, the cell has to make sure that the checkpoint is not re-activated. A recent study (Palframan et al. 2006) demonstrates that in yeast, the degradation of Mps1 by the APC^{Cdc20} irreversibly inactivates the spindle checkpoint in anaphase. In mammalian cells, phosphorylation of Mad2

disrupts the formation of the mitotic checkpoint complex by preventing the interaction of Mad2 with Mad1 and Cdc20 which is thought to contribute to the checkpoint inactivation in anaphase (Wassmann et al. 2003).

Protein	Structural features	Comments	References
Mad1	Coiled-coil	Binds to Mad2 and recruits Mad2 to kinetochores; also localises Mad2 to the nuclear periphery in interphase; Phosphorylated by Mps1 and Bub1 *in vitro*	Chen et al. 1998; Hardwick and Murray 1995; Hardwick et al. 1996
Mad2	Horma domain	Binds to Mad1; binds to Cdc20 and inhibits APC^{Cdc20} activity; exists in two confirmations (C-Mad2 when bound to Mad1 or Cdc20 and O-Mad2 when unbound); localises to kinetochores	Martin-Lluesma et al. 2002; Waters et al. 1998; Li and Benezra 1996
Mad3	GLEBS-motif	Binds to Bub3; binds to Cdc20 and inhibits APC *in vitro;* yeast Mad3 lacks the kinase domain; localises to kinetochores	Skoufias et al. 2001; Millband and Hardwick 2002
Bub1	GLEBS-motif; Serine/threonine kinase	Binds to Bub3, Mad1 and Cdc20; reported substrates include Bub3, hMad1; kinase activity is not required for checkpoint function; Protein-levels are cell cycle regulated	Taylor et al. 2001; Bernard et al. 2001
Bub2	GAP	Regulates spindle positioning checkpoint in S. cerevisiae; essential for cytokinesis in *S. pombe*	Hu and Elledge 2002; Pereira et al. 2000
Bub3	Seven WD40 repeats	Interacts with Bub3-binding domains in Bub1 and BubR1; localises to kinetochores	Campbell and Hardwick 2003
Mps1	Dual-specific kinase	Role in recruitment of checkpoint proteins like Mad1/Mad2 to kinetochores; in budding yeast also required for spindle pole body duplication; reported substrates include Mad1, Spc110	Stucke et al. 2002; Castillo et al. 2002; Abrieu et al. 2001
Cdc20	C-box; D-box; KEN-box	Binds to Mad2, Mad3, APC; activates APC; phosphorylated by Cdk1 in mammals	Kallio et al. 2002; Tang et al. 2001
APC	E3 ubiquitin ligase	targets mitotic regulators like Pds1 or Mps1 for destruction by the proteasome; downstream effector of the spindle assembly checkpoint	Zachariae and Nasmyth 1999
Pds1	-	binds and inhibits Esp1; target of the APC^{Cdc20}	Ciosk et al. 1998
Esp1	protease	cleaves the cohesin subunit Scc1 upon activation at the meta-to-anaphase transition	Uhlmann et al. 2000
Cohesin	-	protein-complex of Scc1, Smc1 and Smc3; chromosomal glue holding sister chromatids together; clevage of Scc1 required for sister chromatid separation	Michaelis et al. 1997
Ipl1	Serine/threonine kinase	Ensures bipolar orientation; proposed to sense tension at kinetochores; chromosomal passenger protein	Cheeseman et al. 2002

Table 1: Proteins involved in spindle checkpoint signalling.

1.3.2 The spindle positioning checkpoint (Bub2-checkpoint)

Accurate segregation of sister chromatids into mother and daughter cell requires a proper positioning of the spindle apparatus in respect to the mother-bud axis. A surveillance mechanism, the so called spindle positioning checkpoint is in charge of responding to spindle misalignment by delaying both mitotic exit and cytokinesis giving the cell time to correct the defects (Figure 5). It functions independent of the spindle assembly checkpoint and monitors the entry of the old spindle pole body (SPB) into the bud (Goh and Kilmartin 1993; Gardner et al. 2001). If the

mitotic spindle is mispositioned, the spindle checkpoint arrests the cell in metaphase. One of the key players in this pathway is Bub2 which monitors the position of the SPBs (Bloechner et al. 2000; Bardin et al. 2000; Pereira et al. 2002). Bub2 is asymmetrically located to the SPB facing the bud (Cerutti and Simanis 1999; Pereira et al. 2000; Bloechner et al. 2000) and keeps Tem1 inactive. Tem1 is a GTPase which triggers the mitotic exit network (MEN) (Furge et al. 1998; Geymonat et al. 2002). Once the old SPB enters the bud, Bub2 is inactivated which in turn initiates anaphase (Figure 5). In loss-of-function mutants of this signal cascade, the mitotic spindle is misoriented and elongates in the mother cell (Palmer et al. 1992; Schuyler and Pellman 2001; Segal and Bloom 2001). Table 1 summarises the main features of the key regulators of the mitotic checkpoints.

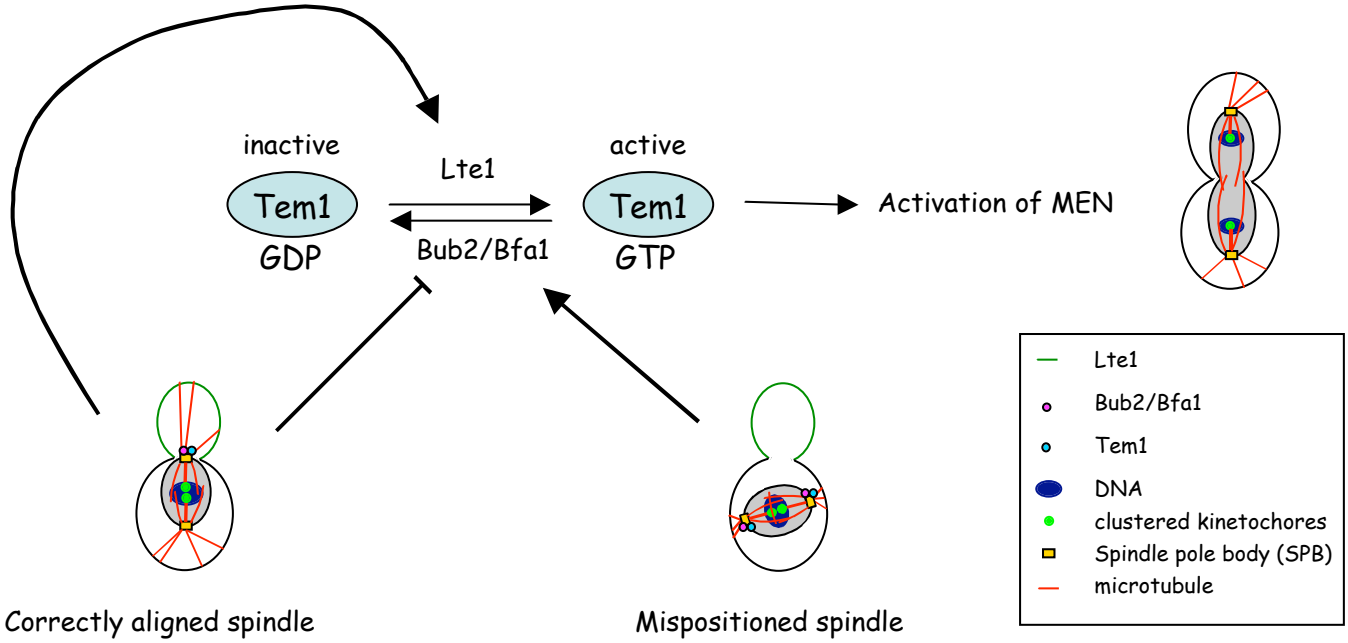

Figure 5: The spindle positioning checkpoint.

The spindle positioning checkpoint is a signal cascade which regulates the exit from mitosis. In the presence of a misaligned spindle, the Bub2/Bfa1 complex associates to both spindle pole bodies and delays mitotic progression by inhibiting Tem1. Once the spindle is correctly positioned, the old SPB enters the bud which leads to the dissociation of Bub2/Bfa1 from the mother SPB and to the exposure of Tem1 to its activator Lte1 which is located at the cortex of the bud. Tem1 in its GTP-bound form activates the mitotic exit network (MEN). In late anaphase, the Bub2/Bfa1 dimer dissociates from the bud directed SPB and Lte1 relocates from the cortex to the cytoplasm.

1.4 The kinetochore

1.4.1 Centromere DNA

The centromere DNA (CEN DNA) is a chromosomal region which serves as a platform for the assembly of the kinetochore. The structure of centromeres of various organisms can differ significantly. In *S. cerevisiae,* is consists of only 125 bp (Figure 6). Because of its little size, it is termed "point kinetochore". In contrast, the centromeric DNA region of higher eucaryotes is significantly bigger and much more complex. The human centromere DNA for example spanns around 2-4 Mbp of highly repetitive DNA ("regional centromere").

The CEN DNA of budding yeast is well characterised and can be divided into three characteristic regions, CDEI, CDEII and CDEIII (CDE= Centromere-DNA-element) (Fitzgerald-Hayes et al. 1982). CDEI is only 8 bp long (A/GTCACG/ATG) and highly conserved among the 16 yeast chromosomes. CDEII is AT-rich and consists of 78-86 bp (Clarke and Carbon 1980). The sequence of CDEII seems to be less important than its leghth and AT-content. CDEIII is 26 bp in leghth and is absolutely essential for accurate choromosome segregation. Like CDEI, its sequence is highly conserved among the 16 chromosomes of *S.cerevisiae.* A single point mutation in the central CCG-triplet leads to complete loss of centromere function (Ng and Carbon 1987).

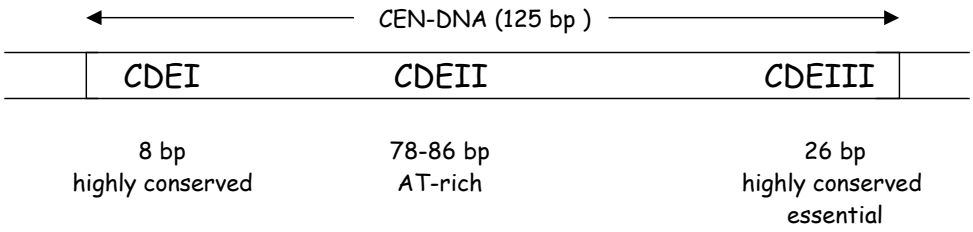

Figure 6: *S. cerevisiae* CEN-DNA

Sequence elements present at all 16 chromosomes of *S. cerevisiae* are denoted CDEI, CDEII and CDEIII. See text for details.

1.4.2 Kinetochore proteins

The *S. cerevisiae* kinetochore is the most simple one among the eukaryotic model organisms. It is composed of at least 65 different proteins which are organised in subcomplexes (McAinsh et al. 2003). Together, they form a stable protein-structure which connects the chromosomes to the microtubules. Furthermore, it serves as a docking platform for numerous regulatory factors like the spindle checkpoint proteins, motor proteins or the Aurora kinase Ipl1. The interaction of the kinetochore proteins has been studied extensively by yeast two hybrid screens, chromatin-immuno precipitation (ChIP) and affinity chromatography (Ito et al. 2001; Uetz et al. 2000; DeWulf et al. 2003; Westermann et al. 2003). Figure 7 summarises the current model of the *S. cerevisiae* kinetochore.

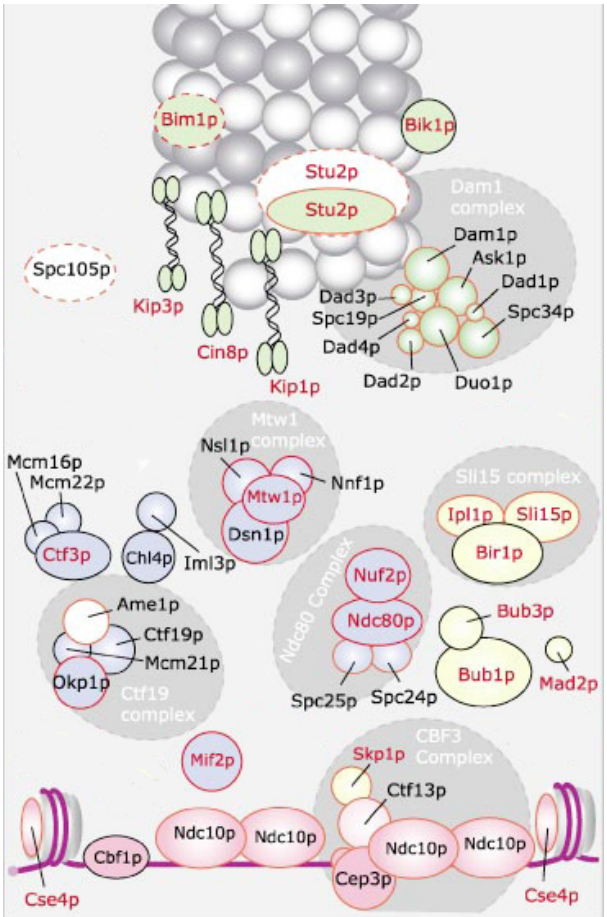

Figure 7: The *S. cerevisiae* kinetochore.

The yeast kinetochore is composed of distinct subcomplexes which are estimated to be at least 5 MDa in size. Image adapted and modified from McAinsh et al. 2003.

Cbf1 (Centromere binding factor 1)

Cbf1 binds to the CDEI-element as a dimer (Bram and Kronberg 1987; Baker et al. 1989). It contains a helix-loop-helix domain which is required for dimerisation as well as for DNA-binding. Although Cbf1 is non-essential, its deletion (Δcbf1) causes a 10 fold increased chromosome loss rate, hypersensitivity to spindle drugs like benomyl or thiabendazole (Baker and Masison 1990; Cai and Davis 1990) and changes in chromatin structure of centromeric DNA and promoter-proximal regions which posess the palindromic CACGTG motif. (Kent et al. 2004).

Cse4 (Chromosome segregation 4)

Cse4 was first identified in a genetic synthetic lethal screen for factors that lead to a defect in chromosome segregation in combination with mutations in the CDEII-element (Xiao et al. 1993). A particular region of the protein which is approximately 100 amino acids in leghth shares high homology with the histone H3. This so called "histone-fold" is also found in CENP-A, a kinetochore protein of higher eucaryotes. It is believed that Cse4 replaces histone H3 at the centromeric region giving rise to a specialised nucleosome (Meluh et al. 1995; Stoler et al. 1995).

Mif2 (Mitotic Fidelity of chromosome transmission)

Mif2 is essential and shares high homology with CENP-C, a kinetochore protein in vertebrates. It contains a sequence motif which is extremely rich in prolines indicating that it might bind to AT-rich DNA-sequences like the CDEII-element. It is also physically connected to the specialised centromere nucleosome since Cse4 and histones co-purify in Mif2 affinity purifications (Westermann et al. 2003).

CBF3-complex

The CBF3-complex was first identified by its ability to bind to CDEIII-DNA *in vitro* (Lechner and Carbon 1991). It contains four proteins: Cbf3a (Ndc10), Cbf3b (Cep3), Cbf3c (Ctf13) and Cbf3d (Skp1) (Connelly and Hieter 1996; Doheny et al. 1993; Espelin et al. 1997; Goh and Kilmartin 1993; Lechner and Carbon 1991; Stemmann and Lechner 1996; Strunnikov et al.

1995). All components of the complex are essential for cell viability. The centromere association of all other kinetochore proteins identified so far depends on the presence of the CBF3-complex (Ortiz et al. 1999; Janke et al. 2001; Goshima and Yanagida 2000). Therefore, it is not surprising that mutations in one of the four proteins lead to segregation defects and detachment of the kinetochore from the microtubules (Jiang et al. 1993; Goh and Kilmartin 1993).
In addition to its kinetochore localisation, Ndc10 has been shown to bind to microtubules (Müller-Reichert et al. 2003; Bouck and Bloom 2005).

Okp1-complex

The Okp1-complex consists of two essential proteins (Okp1 and Ame1) and at least 9 more proteins (Ctf19, Mcm21, Mcm22, Mcm16, Mcm19, Ctf3, Chl4, Nkp1 and Nkp2) which are dispensable for growth (Cheesman et al. 2002; Measday et al. 2002; Ortiz et al. 1999). It forms a bridge between the proteins that are in contact with centromeric DNA and the subunits bound to microtubules during kinetochore assembly. According to their sedimentation characteristics, the proteins of the Okp1-complex can be further divided into two subcomplexes, the COMA-complex (Ctf19, Okp1, Mcm21 and Ame1) and the Ctf3-complex (all other proteins) (De Wulf et al. 2003).

Mtw1-complex

The Mtw1-complex comprises four proteins which are all essential for viability: Mtw1, Nsl1, Dsn1 and Nnf1 (Goshima and Yanagida 2000; Euskirchen et al. 2002; Pinsky et al. 2003; De Wulf et al. 2003; Scharfenberger et al. 2003). The Mtw1-complex is involved in the recruitment of outer kinetochore subunits that will bind to microtubules. Nsl1 and Mtw1 are required for proper attachment of the kinetochore to spindle microtubules (Scharfenberger et al. 2003; Pinsky et al. 2003). Mutations in the MTW1-gene lead to the loss of tension across the mitotic spindle apparatus (Goshima and Yanagida 2000). Furthermore, the metaphase spindle of the temperature sensitive *mtw1-1* mutant is elongated in comparison to wild-type cells (Goshima and Yanagida 2000).

Spc105-complex

The Spc105-complex contains Spc105 and Ydr532 (Nekrasov et al. 2003). Both proteins are essential. Spc105 has been shown to be required for accurate chromosome segregation.

Ndc80-complex

The Ndc80-complex contains four proteins: Ndc80, Nuf2, Spc24 and Spc25. All are essential for viability (Janke et al. 2001; Wigge and Kilmartin 2001). They were originally identified as spindle pole body components (Rout and Kilmartin 1990; Osborne et al. 1994; Wigge et al. 1998). However, detailed analyses showed that these four proteins form a complex which localises to the kinetochore. The human homologe of Ndc80 is Hec1 which stands for "highly expressed in cancer 1". The name indicates the importance of the protein for the proper regulation of the cell cycle. It was shown that mutations in members of the Ndc80-complex lead to complete detachment of the kinetochores from the mitotic spindle (Janke et al. 2001; Wigge and Kilmartin 2001). At restrictive temperature, the *S. cerevisiae* mutant *ndc80-1* arrests in mitosis with long anaphase spindles however the replicated DNA mass stays in the mother cell indicating that the Ndc80-complex plays an essential role in forming stable kinetochore-microtubule attachments. *Spc24-2* cells cannot sustain a mitotic arrest in response to microtubule depolymerisation by nocodazole at 37°C (Janke et al. 2001; McCleland et al. 2003) suggesting that the Ndc80-complex is required for spindle checkpoint activity.
All four subunits contain globular domains and extensive coiled-coil regions. The tetramerization domain of the complex is proposed to involve the C-terminal coiled-coils of the Ndc80/Nuf2 heterodimer as well as the N-termini of the Spc24/Spc25 coiled-coils (Figure 8, Ciferri et al. 2007).
Ndc80 was shown to be phosphorylated by the kinase Ipl1 in yeast and mammals (Cheeseman et al. 2002; De Luca et al. 2006). Ipl1 is involved in regulating kinetochore-microtubule attachments. The phosphorylation of Dam1 and Ndc80 by Ipl1 is proposed to weaken the interaction between the Dam1-complex and the Ndc80-complex thereby facilitating the formation of bipolar connections between kinetochores and the mitotic spindle (Shang et al. 2003). This finding indicates that phosphorylation of Ndc80 plays a role in regulating the attachment/detachment dynamics of kinetochore microtubules.

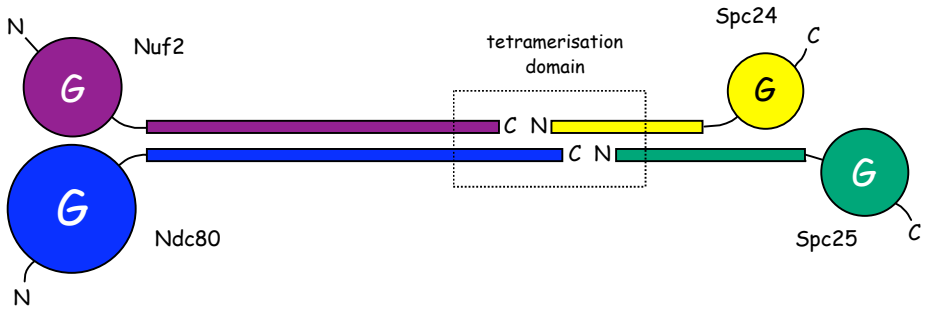

Figure 8: The Ndc80-complex.

The tetrameric Ndc80-complex has an elongated shape and contains two globular domains at each end of a central shaft which includes the coiled-coils of the Ndc80/Nuf2 and Spc24/Spc25-heterodimers. The tetramerisation domain involves the N-termini of the Spc24/Spc25 coiled-coil and the C-termini of the Ndc80/Nuf2-dimer (Ciferri et al. 2005).

The globular domain of Ndc80 contains the highly conserved HEC-domain ("highly expressed in cancer"), the function of which is currently unknown (Figure 9). In vertebrates, the Ndc80-complex is part of the outer plate of the kinetochore.

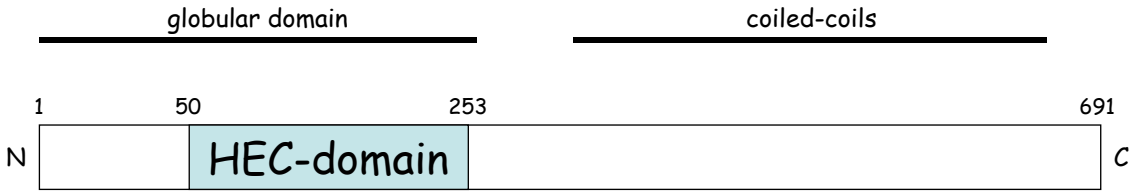

Figure 9: Domain structure of Ndc80.

Ndc80 contains a globular domain at the N-terminus which includes the evolutionary conserved HEC-domain ("highly expressed in cancer"). The biological function of the HEC-domain is currently unknown. The C-terminal part of the protein contains several coiled-coil regions which are known to promote binding to Nuf2.

DDD-complex

The DDD-complex (or Dam/Duo-complex) comprises at least 9 essential proteins: Dad1, Dad2, Dad3, Dad4, Dam1, Duo1, Spc34, Spc19, and Ask1 (Cheeseman et al. 2001; Janke et al. 2002; Li et al. 2002). Components of this complex localise to the kinetochore as well as to the spindle microtubules. Their kinetochore-localisation depends on the presence of microtubules (Li et al. 2002; Janke et al. 2002). Mutations in members of the DDD-complex cause monopolar distribution of the sister chromatids and disrupted spindles (Cheeseman et al. 2001; Janke et al.

2002) indicating that they play a role in spindle attachment, chromosome segregation and spindle stability. It was shown that the DDD-complex is a target for the kinase Ipl1 which is involved in the correction of syntelic attachments (Cheeseman et al. 2002).

Regulatory proteins

Ipl1 (Increase in Ploidy)

Ipl1 is a member of the Aurora kinase family and is proposed to sense tension at kinetochores and regulate kinetochore-microtubule attachments (Tanaka et al. 2002; Buvelot et al. 2003). It localises at the kinetochore until all chromosomes aquire a bipolar attachment to microtubules. In late anaphase it is found at the spindle midzone as part of the so called chromosomal passenger complex (Vagnarelli and Earnshaw 2004). It associates with Sli15 and is thought to contribute to the stabilisation of the mitotic spindle and cytokinesis (Zeng et al. 1999; Sullivan et al. 2001; Pinsky et al. 2006).
Ndc80 and Dam1 were shown to be substrates for Ipl1 in yeast and mammals (Cheeseman et al. 2002; De Luca et al. 2006). The phosphorylation those two kinetochore-components is proposed to destabilise the interaction between the Dam1-complex and the Ndc80-complex thereby promoting the establishment of bipolarly attached kinetochores (Shang et al. 2003).

Mps1 (Monopolar spindle 1)

Members of the Mps1 family of protein kinases are widely distributed among eukaryotic organisms. Mps1 is essential and was first discovered in the budding yeast *S. cerevisiae* (Winey et al. 1991). Subsequently, kinases structurally related to the dual-specific kinase Mps1 were described in *S. pombe* (Mph1p) (He et al. 1998), *A. thaliana* (PPK1) (Schutz and Winey 1998), *X. laevis* (XMps1) (Abrieu et al. 2001) and mammals (mMps1/Esk in mouse, hMps1/TTK/PYT in humans) (Douville et al. 1992; Fisk and Winey 2001; Mills et al. 1992; Lindberg et al. 1993).
The originally identified temperature sensitive allele *mps1-1* carries a single point mutation in the kinase domain which leads to a defect in spindle pole body (SPB) duplication at the restrictive temperature, resulting in mitotic cells with a single SPB (Winey et al. 1991). The presence of only one SPB leads to the formation of a monopolar spindle in mitosis. Normally, mutations that

give rise to a monopolar spindle activate the spindle checkpoint and cells arrest in mitosis (Weiss and Winey 1996). However, unlike other yeast mutants that fail in SPB duplication and hence establish a monopolar spindle, *mps1-1* cells do not show a cell cycle arrest (Weiss and Winey 1996). Instead, these mutants missegregate their chromosomes and exit mitosis, leading to decreased cell viability due to aneuploidy (Winey et al. 1991). In addition, *mps1-1* cells fail to arrest in response to microtubule-depolymerizing drugs like nocodazole, but instead exit mitosis as multibudded, polyploid cells (Weiss and Winey 1996; Stucke et al. 2002). This phenotype is common among *mad* and *bub* mutants (Li and Murray 1991; Hoyt et al. 1991), and indicated that Mps1 acts in the mitotic spindle checkpoint. Consistent with this is the finding that Mps1 is localised to kinetochores (Castillo et al. 2002).

Beside the phenotypes associated with the *mps1-1* mutant, overexpression studies of Mps1 gave a second clue for the involvement of the kinase in the mitotic spindle checkpoint. Overexpression of Mps1 induces phosphorylation of Mad1 and arrests wild-type cells in mitosis with morphologically normal spindles (Hardwick et al. 1996). Spindle checkpoint mutants overexpressing Mps1 pass through mitosis without delay suggesting that the arrest of wild-type cells results from an inappropriate activation of the checkpoint in cells whose spindle is fully functional.

In budding yeast, activation of the mitotic spindle checkpoint triggered upon spindle damage can be monitored by the phosphorylation state of Mad1 (Hardwick and Murray 1995). Mad1 is hyperphosphorylated in wild-type and in all of the *mad* and *bub* mutants after Mps1 overexpression, whereas in *mps1-1* cells, no modification of Mad1 was detected (Hardwick et al. 1996). In addition, Mps1 isolated from yeast is able to phosphorylate Mad1 *in vitro* (Hardwick et al. 1996). The molecular mechanism by which Mps1 activates the mitotic spindle checkpoint is currently unknown. As described above (1.3.1.2), Mps1 is a target of the APC^{Cdc20} which controls Mps1 protein levels during mitosis (Palframan et al. 2006). The proteasome dependent degradation of Mps1 irreversibly inactivates the spindle checkpoint in anaphase. Therefore, Mps1 plays a role in spindle checkpoint activation as well as in checkpoint silencing.

Other *in vitro* substrates of Mps1 include the SPB components Spc98, Spc110 and Spc42 (Castillo et al. 2002; Friedman et al. 2001; Pereira et al. 1998). The phosphorylated forms of these proteins depend on Mps1 activity *in vivo*, and Mps1 and Spc42 were found to bind each other by co-immuoprecipitation (Castillo et al. 2002).

In fission yeast *S. pombe*, the Mps1 ortholog, called Mph1 (Mps1-like pombe homolog), was

identified in a screen for genes whose overexpression leads to a mitotic arrest (He et al. 1998). Fission yeast Mph1 could complement the spindle checkpoint defect of a budding yeast *mps1-1* mutant, indicating that it represents a functional homolog (He et al. 1998). The Mph1 gene is not essential, but the deletion mutant shows defects in the mitotic spindle checkpoint response. Importantly, overexpression of Mph1 mimics activation of the checkpoint and imposes a metaphase arrest, which is dependent on the checkpoint protein Mad2 (He et al. 1998). It was shown that Mph1, together with Bub1 and Bub3, is required for kinetochore recruitment of Mad3 (Millband and Hardwick 2002). However, in contrast to budding yeast Mps1, Mph1 is not required for spindle pole body duplication.

Initial characterisations have also been reported for putative vertebrate homologs of yeast Mps1. Mps1 kinase has been implicated in the mitotic spindle checkpoint in *Xenopus* egg extracts and mammalian cells (Abrieu et al. 2001; Stucke et al. 2002). XMps1 was shown to localise to kinetochores and to be necessary for the establishment and maintenance of a mitotic spindle checkpoint mediated arrest reconstituted in *Xenopus* egg extracts (Abrieu et al. 2001). Furthermore, kinetochore recruitment of the checkpoint proteins XMad1, XMad2 and CENP-E was dependent on the kinase activity of XMps1, consistent with the yeast data that Mps1 kinases must act early in the checkpoint pathway (Abrieu et al. 2001).

In mammalian cells, Mps1 was shown to interact with the kinetochore via its N-terminal non-catalytic domain in early stages of mitosis. This association was shown to be dependent on the presence of Hec1 (Stucke et al. 2002). In addition, murine Mps1 was reported to localize to kinetochores in mitosis (Fisk and Winey 2001).

Microtubule-binding proteins

Microtubule-associated proteins are involved in the regulation of many microtubule-dependent events (Hunter and Wordeman 2000; Akhmanova and Hoogenraad 2005; Moore and Wordeman 2004; Tytell and Sorger 2006). Kip1 and Cin8 are required for the correct alignment and clustering of kinetochores in metaphase (Hildebrandt and Hoyt 2000; Hoyt et al. 1992). Kip3 takes part in the coordination of sister chromatid movements to the spindle poles during anaphase (Moore and Wordeman 2004) and Kar3 plays a role in the lateral sliding of minichromosomes along microtubules during the capture of newly formed kinetochores by microtubules (Tanaka et al. 2005).

Stu1 binds to interpolar microtubules and locates at the spindle midzone. It is required for interpolar microtubules to provide an outward force on the spindle poles (Yin et al. 2002).
The chromosomal passenger complex Sli15-Bir1 is proposed to be the tension sensor which translates the mechanical state of centromere-microtubule connections into the activation of Ipl1 (Sandall et al. 2006). In addition, Sli15-Bir1 is involved in the regulation of mitotic spindle disassembly (Buvelot et al. 2003).

1.5 Kinetochore structure

The most inner part of the kinetochore is represented by the CBF3-complex which promotes direct binding to the centromeric DNA together with Cse4 (Lechner and Carbon 1991; Meluh et al. 1998). The assembly of all other kinetochore-subcomplexes depend on the CBF3-complex. According to yeast two hybrid and chromatin-immuno precipitation data, the Okp1-, Mtw1- and Ndc80-complexes form the central layer which forms a bridge between the DNA-binding CBF3-complex and the microtubule associated DDD-complex. The kinetochore localisation of the DDD-complex depends on all other subcomplexes and on the presence of microtubules (Li et al. 2002; Enquist-Newman et al. 2001). The Ndc80- and the DDD-complex have been shown to be required for proper kinetochore-microtubule attachment (He et al. 2001; Janke et al. 2001; Janke et al. 2002; Jones et al. 2001).
The yeast kinetochore was shown to contain 2 Cse4-molecules. Using quantitative fluorescence microscopy, it was possible to determine the stoichometry of protein-complexes at the budding yeast kinetochore. By meassuring the relative fluoresence to Cse4-GFP, it was shown that the kinetochore is assembled from one CBF3-complex, eight Ndc80-complexes, six Mtw1-complexes, five Spc105-complexes and 16-20 DDD-complexes.
Due to its large size, the structure of the mammalian kinetochore can be visualised by electron microscopy. In contrast, the *S. cerevisiae* is to small for direct visualisation. However the centromeric region can be indirectly tagged with GFP by a method which was originally established by Michaelis and collegues (1997, see methods chapter for more details). Since in yeast the kinetochores of all 16 chromosomes are clustered, they can be seen as one distinct signal. This way the centromere region of *S. cerevisiae* can be investigated by fluorescence microscopy.

1.6 Phosphoepitopes at the kinetochore

The identification of the so called 3F3/2-antibody (Cyert et al. 1988) gave rise to the idea that phosphorylation of kinetochore components might act as a signal which regulates the activity of the spindle checkpoint. The antibody was raised against Xenopus egg extracts that were treated with ATP-γ-S. It was shown to specifically recognise a phosphoepitop at the mammalian kinetochore. Using this antibody as a tool, it was demonstrated that kinetochore phosphorylation is dependent on the absence of tension across the mitotic spindle (Gorbsky and Ricketts 1993). In prometaphase, when no tension is built up and unattached kinetochores are present, the 3F3/2-antibody specifically recognises an unknown phosphorylated substrate that co-localises with a known kinetochore marker (CREST-antigen). When cells proceed into metaphase, all kinetochores become attached to the mitotic spindle apparatus and tension is applied. At this stage, phosphorylation of the kinetochore can no longer be detected by the 3F3/2-antibody which clearly shows a dependency between kinetochore phosphorylation and the regulation of the spindle checkpoint. These data suggest that the phosphorylation of a yet unidentified kinetochore substrate may act as a signal for the checkpoint control pathway by which the transition from meta- into anaphase is inhibited until the mitotic spindle has properly assembled.
Using Xenopus egg extracts, it was shown that the depletion of the Polo-like kinase Plk1 leads to the loss of 3F3/2 kinase activity which can be rescued by the re-addition of recombinant Plk1. These data suggest that Plk1 is the kinase which creates the 3F3/2-phospho-epitope on mitotic kinetochores (Ahonen et al. 2005).

2 GOAL OF THE PRESENT WORK

The kinetochore is a multilayer proteinacous complex assembled on the centromere which was two distinct functions. The kinetochore forms the interface between centromeric DNA and the spindle microtubules and thus supports sister chromatid segregation in mitosis. In addition, it serves as a docking platform for the proteins of the spindle checkpoint pathway. This surveillance mechanism monitors the correct assembly of the spindle apparatus in mitosis. It inhibits the meta-to-anaphase transition untill bipolar attachment of all kinetochores to the spindle microtubules is achieved.

The tetrameric Ndc80-complex (Ndc80, Nuf2, Spc24, Spc25) is part of the kinetochore. It is highly conserved and was shown to be required for the spindle checkpoint in *S. cerevisiae* (Janke et al. 2001). The kinase Mps1 has also been implicated in spindle checkpoint control (Hartwick et al. 1996). In mammalian cells, Mps1 associates with the kinetochore dependent on the presence of the Ndc80-complex (Stucke et al. 2004).

The goal of the present thesis was to elucidate whether components of the *S. cerevisiae* Ndc80-complex are phosphorylated by Mps1 and if this phosphorylation has an influence on the regulation of the spindle checkpoint.

In a first step, the association of Mps1 with the Ndc80-complex should be examined in *S. cerevisiae*. In addition, it should be investigated if this association takes place at the kinetochore or in solution. In the next step, it should be tested whether Mps1 phosphorylates members of the Ndc80-complex. The final goal was to characterise Mps1-dependent Ndc80-complex phosphorylation in respect to spindle checkpoint function *in vivo*.

3 MATERIALS

3.1 Plasmids

General plasmids

pSK919 Δbar1::ADE2 (P-ORF-Term)
pSK950 pGal1-MPS1-TAP; LEU2; 2µ
pSK953 NDC80 (Promoter-ORF-Terminator) ARS / CEN4; URA 3
pSK954 pNDC80-NDC80 ORF-3HA-KanMX6-Term
pSK1029 MAD2 (P-ORF-Term) LEU2
pSK1037 pGal1.10-NDC80 Δaa1-116 S205A T248A T252A T255A T685A T690A-3HA
pSK1038 pGal1.10-Flag-NDC80 ORF-3HA
pSK1050 pGal1-myc; pGal10-Flag; LEU2
pSK1052 Flag-MPS1 AmpR
pSK1053 pGal1-myc; pGal10-Flag-NDC80 S4D T5D S6D T248D T252D S205D T21D S22D S37D T38D T43D T74D T79D T82D; LEU2
pSK1055 pGal1-myc; pGal10-Flag-NDC80; LEU2
pSK1063 pGal1-NDC80-3HA S4D T5D S6D T248D T252D S205D T21D S22D S37D T38D T43D T74D T79D T82D-Term. pYX243; LEU2
pSK1064 pGal10-Flag-NDC80; LEU2; 2µ
pSK1065 pGal10-Flag-NDC80 S4D T5D S6D T248D T252D S205D T21D S22D S37D T38D T43D T74D T79D T82D; LEU2; 2µ
pSK1069 Flag-MPS1; AmpR
pSK1070 Flag-MPS1; T7lac-Histag/MCS1-T7lac-Stag/MCS2-T7 term; KanR; ColA ori; lacI
pSK1074 pGal1-NDC80; pGal10-Flag; LEU2
pSK1075 pGal1-NDC80 S4D T5D S6D T248D T252D S205D T21D S22D S37D T38D T43D T74D T79D T82D; pGal10-Flag; LEU2
pSK1076 pGal1-MPS1-TAP; pGal10-Flag; LEU2
pSK1077 pGal1-MAD2-ORF; pGal10-Flag; LEU2
pSK1080 pGal1-MPS1-9myc ; pGal10-Flag; LEU2
pSK1082 BUB1 (P-ORF-Term) LEU2
pSK1083 10His-Nuf2
pSK1086 P-BUB2-Term CEN6 ARS LEU2
pSK1091 pNDC80-NDC80 S4D T5D S6D T248D T252D S205D T21D S22D S37D T38D T43D T74D T79D T82D-3HA-Term; LEU2
pSK1092 NDC80 (Promoter-ORF-Terminator) ARS / CEN4 ; URA 3
pSK1096 NDC80-eGFP
pSK1097 pNDC80-NDC80-eGFP-NDC80-Term S4D T5D S6D T248D T252D S205D T21D S22D S37D T38D T43D T74D T79D T82D LEU2
pSK1098 pNDC80-NDC80-eGFP-NDC80-Term LEU2
pSK1099 pNDC80-NDC80-eGFP-NDC80-Term S4D T5D S6D T248D T252D S205D T21D S22D S37D T38D T43D T74D T79D T82D LEU2
pSK1103 LYS2; CFP-TUB1
pSK1104 pNDC80-NDC80-3HA-Term S4D T5D S6D T248D T252D S205D T21D S22D S37D T38D T43D LEU2
pSK1105 pNDC80-NDC80-eGFP-NDC80-Term S4D T5D S6D T248D T252D S205D T21D S22D S37D T38D T43D LEU2
pSK1106 pMAD2-LYS2-Term.(MAD2) MAD2-disruption construct
pSK1107 pNDC80-NDC80-3HA-Term S205A T248A T252A S37A T38A T43A T21A S22A S4A T5A S6A T74A T79A T82A
pSK1108 pNDC80-NDC80-eGFP-Term S205A T248A T252A S37A T38A T43A T21A S22A S4A T5A S6A T74A T79A T82A
pSK1114 mCherry-TUB1; HIS3
pCJ092 tetR-GFP; ADE2
pMS746 bar1::loxP-HIS3-loxP
pSH47 pGal-CRE; ARS; CEN; URA3
pASF125 TUB1-GFP; URA3
pXH136 ChrV-tetO2x112-URA3-ChrV integration close to CEN5
pSB38 pGal-Mps1; URA3

pBL938 NDC80 (10His-ORF)
pBL941 10His-NDC80 aa1-257
pBL946 pNDC80-NDC80 ORF aa255-691-3HA-KanMX6-NDC80-Term
pBL959 pNDC80-NDC80 ORF aa116-691-3HA-KanMX6-NDC80-Term
pBL960 pNDC80-NDC80 ORF aa43-691-3HA-KanMX6-NDC80-Term
pAW920 Δmad2::HIS3
pAW925 Δbub2::HIS3
pRS415 CEN6 ARS LEU2

NDC80 Ser/Thr to Ala mutants: pNDC80-NDC80-ORF-3HA-KanMX6-NDC80-Term including point mutations...

pSK970 Δaa1-116 T248A T252A S255A
pSK971 Δaa1-116 T248A T252A S255A T685A T690A
pSK972 Δaa1-116 T248A T252A S255A T685A T690A T145A S150A
pSK973 Δaa1-116 T248A T252A S255A T685A T690A T145A S150A S205A
pSK974 Δaa1-116 T248A T252A S255A T685A T690A T145A S150A S205A T180A
pSK975 Δaa1-116 T248A T252A S255A T685A T690A T145A S150A S205A T180A S126A
pSK982 Δaa1-116 T145A S150A S205A
pSK983 Δaa1-116 S205A
pSK985 S205A
pSK991 T145A S150A S205A T248A T252A T255A T685A T690A
pSK997 T145A S150A S205A
pSK1000 Δaa1-116 S205A T248A T252A T255A T685A T690A
pSK1001 S205A T248A T252A T255A T685A T690A
pSK1003 T145A S150A S205A T248A T252A T255A
pSK1004 S205A T248A T252A T255A
pSK1012 Δaa1-116 S205A T248A T252A T255A
pSK1014 Δaa1-116 T145A S150A
pSK1015 T145A S150A
pSK1016 S205A T248A T252A T255A S37A T38A T43A
pSK1017 Δaa1-116 S205A T685A T690A
pSK1021 Δaa1-116 T145A S150A S205A T248A T252A T255A
pSK1022 S205A T248A T252A T255A S37A T38A T43A T21A S22A
pSK1023 S205A T248A T252A T255A S37A T38A T43A T21A S22A S4A T5A S6A
pSK1025 S37A T38A T43A T21A S22A S4A T5A S6A S205A
pSK1026 S37A T38A T43A T21A S22A S4A T5A S6A T145A S150A
pSK1027 S37A T38A T43A T21A S22A S4A T5A S6A T145A S150A S205A
pSK1028 Δaa1-116 S205A T248A T252A
pSK1031 S205A T248A T252A S37A T38A T43A
pSK1032 S205A T248A T252A S37A T38A T43A T21A S22A S4A T5A S6A
pSK1036 S205A T248A T252A S37A T38A T43A S4 T5 S6
pSK1039 S205A T248A T252A S37A T38A T43A T21A S22A S4A T5A S6A T74A T79A T82A
pSK1058 S37A T38A T43A T21A S22A S4A T5A S6A S205A T248A T252A
pSK1095 T248A T252A

NDC80 Ser/Thr to Asp mutants: pNDC80-NDC80-ORF-3HA-KanMX6-NDC80-Term including point mutations...

pSK976 S4D T5D S6D
pSK977 S4D T5D S6D T248D T252D
pSK978 S4D T5D S6D T248D T252D S205D

pSK979 S4D T5D S6D T248D T252D S205D T21D S22D
pSK980 S4D T5D S6D T248D T252D S205D T21D S22D S37D T38D T43D
pSK981 S4D T5D S6D T248D T252D S205D T21D S22D S37D T38D T43D T74D T79D T82D
pSK984 S4D T5D S6D T248D T252D S205D T21D S22D S37D T38D T43D T74D T79D T82D S97D S100D S106D
pSK986 S205D
pSK987 S4D T5D S6D T248D T252D S205D T21D S22D S37D T38D T43D T74D T79D T82D S97D S100D S106D T145D S150D
pSK992 S4D T5D S6D T248D T252D S205D T21D S22D S37D T38D T43D T74D T79D T82D S97D S100D S106D T145D S150D T54D S56D T58D
pSK993 T74D T79D T82D
pSK994 T74D T79D T82D S37D T38D T43D T21D S22D S4D T5D S6D
pSK995 S205D S248D T252D
pSK996 S205D S4D T5D S6D
pSK1002 T145D S150D S205D
pSK1011 S4D T5D S6D T21D S22D S37D T38D T43D T54D S56D T58D T74D T79D T82D S97D S100D S106D
pSK1013 S205D S248D T252D S37D T38D T43D
pSK1018 S37D T38D T43D
pSK1019 S37D T38D T43D S205D
pSK1020 S37D T38D T43D S145D S205D
pSK1024 S4D T5D S6D T21D S22D S37D T38D T43D S145D S205D
pSK1030 S4D T5D S6D T248D T252D T21D S22D S37D T38D T43D
pSK1034 T74D T79D T82D S205D S248D T252D
pSK1040 S205D S248D T252D S37D T38D T43D T21D S22D
pSK1041 S205D S248D T252D S37D T38D T43D S4D T5D S6D
pSK1042 S4D T5D S6D S205D T21D S22D S37D T38D T43D
pSK1043 S4D T5D S6D T248D T252D S205D T21D S22D S37D T38D T43D T54D S56D T58D
pSK1056 S4D T5D S6D T248D T252D T21D S22D S37D T38D T43D T74D T79D T82D
pSK1057 S4D T5D S6D S205D T21D S22D S37D T38D T43D T74D T79D T82D
pSK1059 S205D S248D T252D S37D T38D T43D S4D T5D S6D T74D T79D T82D
pSK1060 S205D S248D T252D S37D T38D T43D T21D S22D T74D T79D T82D
pSK1061 S4D T5D S6D T248D T252D S205D T21D S22D T74D T79D T82D
pSK1066 T74D T79D T82D S205D S248D T252D S4D T5D S6D
pSK1067 T74D T79D T82D S205D S248D T252D S37D T38D T43D
pSK1068 T74D T79D T82D S205D S248D T252D T21D S22D
pSK1089 S4D T5D S6D T248D T252D S205D T21D S22D S37D T38D T43D T74D T79D T82D

Plasmids used for epitop-tagging of yeast genes

pYM2 HAx3-His3MX6
pYM3 HAx6-klTRP1
pYM6 MYCx9-klTRP1
pYM7 ProtA-KanMX6
pYM10 TEV-ProtA-7xHIS-His3MX6
pYM12 eGFP-KanMX4
pYM19 9myc; His3MX6
pYM28 eGFP-His3MX6
pYM29 eGFP-klTRP1
pYM43 RedStar2; naTNT2
pCM79-2 pFA6a::3mcherry::hphNT1
pBS1479 TAPTag (CBP-TEV-ProtA)-TRP1-KL
pBS1539 TAP-tag (CBP-TEV-ProtA)-klURA3
pBL929 KanMX6-pGal-Ubi-R integration

3.2 *E.coli* strains

For amplification of plasmid DNA, the *E.coli* strain DH5α was used. Recombinant expression of yeast genes was done in BL21 (DE3). Both strains were grown at 37°C. During protein expression, the strain BL21 (DE3) was grown at 18-25°C depending on the stability and solubility of the expressed protein. The genotypes of the used strains are:

DH5α supE44 lacU169 (ϕ80lacZM15) hsdR17 recA1 endA1 gyrA96 thi1 relA1

BL21 (DE3) hsdS gal (λclts857 ind1 Sam7 nin5 lacUV5-t gene1)

3.3 *S. cerevisiae* strains

Strain	Genotype
YSK632	SPC24-ProA::His3MX6 ura3-1:pGal-Mps1-myc:URA3
YSK653	Δbar1::loxP
YSK658	Δbar1::loxP NUF2-6HA::klTRP1 SPC25-TAP:: URA3 NDC80-3myc-KanMX6
YSK663	Δbar1::loxP ura3-1:pGal-Mps1-myc:URA3
YSK658	Δbar1::loxP NUF2-6HA::klTRP1 SPC25-TAP:: URA3 NDC80-3myc-KanMX6 pSK950
YSK770	Δbar1::loxP ura3-1:pGal-Mps1-myc:URA3 SPC25-TAP:: TRP1-KL
YSK775	Δbar1::loxP Δndc80::ndc80 Δaa 1-116-3HA-KanMX6 ade2::tetR-GFP:ADE2
YSK776	Δbar1::loxP Δndc80::ndc80 Δaa 1-43-3HA-KanMX6 ade2::tetR-GFP:ADE2
YSK783	Δbar1::loxP Δndc80::ndc80 Δaa 1-116-3HA-KanMX6 ade2::tetR-GFP:ADE2 1.4kb left of CEN5-tetO2x112::URA3
YSK784	Δbar1::loxP Δndc80::ndc80 Δaa 1-43-3HA-KanMX6 ade2::tetR-GFP:ADE2 1.4kb left of CEN5-tetO2x112::URA3
YSK787	Δbar1::loxP Δndc80::HIS3 PDS1-9MYC:klTRP1 pSK953 (NDC80-shuffle strain)
YSK788	Δbar1::loxP Δndc80::NDC80-3HA-KanMX6 PDS1-9MYC:klTRP1
YSK795	Δbar1::loxP PDS1-9MYC:klTRP1 Δndc80::ndc80Δaa1-116/T248A T252A S255A-3HA-KanMX6
YSK796	Δbar1::loxP PDS1-9MYC:klTRP1 Δndc80::ndc80Δaa1-116/T248A T252A S255A T685A T690A-3HA-KanMX6
YSK802	Δbar1::loxP PDS1-9MYC:klTRP1 Δndc80::ndc80Δaa1-116/T248A T252A S255A T685A T690A-3HA-KanMX6 ade2::tetR-GFP:ADE2 1.4kb left of CEN5-tetO2x112::URA3
YSK818	Δbar1::loxP PDS1-9MYC:klTRP1 Δndc80::NDC80-3HA-KanMX6 TUB1-GFP:URA3
YSK819	Δbar1::loxP PDS1-9MYC:klTRP1 Δndc80::ndc80Δaa1-116/T248A T252A S255A T685A T690A-3HA-KanMX6 TUB1-GFP:URA3
YSK828	Δbar1::loxP PDS1-9MYC:klTRP1 Δndc80::NDC80-3HA-KanMX6 ura3-1:pGal-Mps1-myc:URA3
YSK788	Δbar1::loxP PDS1-9MYC:klTRP1 Δndc80::NDC80-3HA-KanMX6 pSK950
YSK796	Δbar1::loxP PDS1-9MYC:klTRP1 Δndc80::ndc80Δaa1-116/T248A T252A S255A T685A T690A-3HA-KanMX6 pSK950
YSK853	Δbar1::loxP PDS1-9MYC:klTRP1 Δndc80::ndc80Δaa1-116/T248A T252A S255A T685A T690A T145A S150A-3HA-KanMX6
YSK854	Δbar1::loxP PDS1-9MYC:klTRP1 Δndc80::ndc80Δaa1-116/T248A T252A S255A T685A T690A T145A S150A S205A-3HA-KanMX6 pSK953
YSK855	Δbar1::loxP PDS1-9MYC:klTRP1 Δndc80::ndc80Δaa1-116/T248A T252A S255A T685A T690A T145A S150A S205A T180A-3HA-KanMX6 pSK953
YSK856	Δbar1::loxP PDS1-9MYC:klTRP1 Δndc80::ndc80Δaa1-116/T248A T252A S255A T685A T690A T145A S150A S205A T180A S126A-3HA-KanMX6 pSK953
YSK857	Δbar1::loxP PDS1-9MYC:klTRP1 Δndc80::NDC80/ S4D T5D S6D-3HA-KanMX6
YSK858	Δbar1::loxP PDS1-9MYC:klTRP1 Δndc80::NDC80/ S4D T5D S6D T248D T252D-3HA-KanMX6
YSK860	Δbar1::loxP PDS1-9MYC:klTRP1 Δndc80::NDC80/ S4D T5D S6D T248D T252D S205D-3HA-KanMX6
YSK867	Δbar1::loxP PDS1-9MYC:klTRP1 Δndc80::NDC80/ S4D T5D S6D T248D T252D S205D T21D S22D-3HA-KanMX6

YSK868	Δbar1::loxP PDS1-9MYC:klTRP1 Δndc80::NDC80/S4D T5D S6D T248D T252D S205D T21D S22D S37D T38D T43D-3HA-KanMX6
YSK869	Δbar1::loxP PDS1-9MYC:klTRP1 Δndc80::NDC80/S4D T5D S6D T248D T252D S205D T21D S22D S37D T38D T43D T74D T79D T82D-3HA-KanMX6 pSK953
YSK870	Δbar1::loxP PDS1-9MYC:klTRP1 Δndc80::ndc80 Δaa1-116/ T145A S150A S205A-3HA-KanMX6
YSK871	Δbar1::loxP PDS1-9MYC:klTRP1 Δndc80::ndc80 Δaa1-116/ S205A-3HA-KanMX6
YSK875	Δbar1::loxP PDS1-9MYC:klTRP1 Δndc80::NDC80/S4D T5D S6D T248D T252D S205D T21D S22D S37D T38D T43D T74D T79D T82D S97D S100D S106D pSK953
YSK876	Δbar1::loxP PDS1-9MYC:klTRP1 Δndc80::NDC80/S205D
YSK877	Δbar1::loxP PDS1-9MYC:klTRP1 Δndc80::NDC80/S205A
YSK878	Δbar1::loxP PDS1-9MYC:klTRP1 Δndc80::NDC80-3HA-KanMX6 Δmad2::HIS3
YSK884	Δbar1::loxP PDS1-9MYC:klTRP1 Δndc80::ndc80Δaa1-116/ T145A S150A S205A-3HA-KanMX6 TUB1-GFP:URA3
YSK885	Δbar1::loxP PDS1-9MYC:klTRP1 Δndc80::NDC80/ S4D T5D S6D T248D T252D S205D-3HA-KanMX6 TUB1-GFP:URA3
YSK886	Δbar1::loxP PDS1-9MYC:klTRP1 Δndc80::NDC80/ S4D T5D S6D T248D T252D S205D T21D S22D-3HA-KanMX6 TUB1-GFP:URA3
YSK887	Δbar1::loxP PDS1-9MYC:klTRP1 Δndc80::NDC80/S4D T5D S6D T248D T252D S205D T21D S22D S37D T38D T43D-3HA-KanMX6 TUB1-GFP:URA3
YSK891	Δbar1::loxP PDS1-9MYC:klTRP1 Δndc80::NDC80/T145A S150A S205A T248A T252A T255A T685A T690A-3HA-KanMX6
YSK893	Δbar1::loxP PDS1-9MYC:klTRP1 Δndc80::NDC80/T74D T79D T82D-3HA-KanMX6
YSK894	Δbar1::loxP PDS1-9MYC:klTRP1 Δndc80::NDC80/T74D T79D T82D S37D T38D T43D T21D S22D S4D T5D S6D-3HA-KanMX6
YSK895	Δbar1::loxP PDS1-9MYC:klTRP1 Δndc80::NDC80/S205D S248D T252D-3HA-KanMX6
YSK896	Δbar1::loxP PDS1-9MYC:klTRP1 Δndc80::NDC80/S205D S4D T5D S6D-3HA-KanMX6
YSK898	Δbar1::loxP PDS1-9MYC:klTRP1 Δndc80::NDC80/T145A S150A S205A-3HA-KanMX6
YSK904	Δbar1::loxP PDS1-9MYC:klTRP1 Δndc80::NDC80/S205A T248A T252A T255A-3HA-KanMX6
YSK905	Δbar1::loxP PDS1-9MYC:klTRP1 Δndc80::ndc80Δaa1-116/ S205A T248A T252A T255A T685A T690A-3HA-KanMX6 pSK953
YSK906	Δbar1::loxP PDS1-9MYC:klTRP1 Δndc80::NDC80/S205A T248A T252A T255A T685A T690A-3HA-KanMX6
YSK907	Δbar1::loxP PDS1-9MYC:klTRP1 Δndc80::NDC80/T145D S150D S205D-3HA-KanMX6
YSK908	Δbar1::loxP PDS1-9MYC:klTRP1 Δndc80::NDC80/T145A S150A S205A T248A T252A T255A-3HA-KanMX6
YSK912	Δbar1::loxP PDS1-9MYC:klTRP1 Δndc80::NDC80/S4D T5D S6D T248D T252D S205D T21D S22D S37D T38D T43D-3HA-KanMX6 Δmad2::HIS3
YSK913	Δbar1::loxP Δndc80::HIS3 Δmad2::TRP1 pSK953
YSK917	Δbar1::loxP PDS1-9MYC:klTRP1 Δndc80::NDC80-3HA-KanMX6 ade2::tetR-GFP::ADE2 1.4kb left of CEN5-tetO2x112::URA3
YSK922	Δbar1::loxP PDS1-9MYC:klTRP1 Δndc80::ndc80Δaa1-116/ S205A T248A T252A T255A -3HA-KanMX6
YSK923	Δbar1::loxP PDS1-9MYC:klTRP1 Δndc80::NDC80/S205D S248D T252D S37D T38D T43D-3HA-KanMX6
YSK925	Δbar1::loxP PDS1-9MYC:klTRP1 Δndc80::NDC80/ S4D T5D S6D T21D S22D S37D T38D T43D T54D S56D T58D T74D T79D T82D S97D S100D S106D-3HA-KanMX6
YSK926	Δbar1::loxP PDS1-9MYC:klTRP1 Δndc80::NDC80/S205A T248A T252A T255A S37A T38A T43A-3HA-KanMX6
YSK927	Δbar1::loxP PDS1-9MYC:klTRP1 Δndc80::ndc80Δaa1-116/ S205A T685A T690A-3HA-KanMX6
YSK928	Δbar1::loxP PDS1-9MYC:klTRP1 Δndc80::NDC80/S37D T38D T43D-3HA-KanMX6
YSK929	Δbar1::loxP PDS1-9MYC:klTRP1 Δndc80::NDC80/S37D T38D T43D S205D-3HA-KanMX6 pSK953
YSK930	Δbar1::loxP PDS1-9MYC:klTRP1 Δndc80::NDC80/S37D T38D T43D S145D S205D-3HA-KanMX6 pSK953
YSK931	Δbar1::loxP PDS1-9MYC:klTRP1 Δndc80::ndc80Δaa1-116/ T145A S150A S205A T248A T252A T255A-3HA-KanMX6
YSK934	Δbar1::loxP PDS1-9MYC:klTRP1 Δndc80::NDC80/ S205A T248A T252A T255A S37A T38A T43A T21A S22A-3HA-KanMX6
YSK935	Δbar1::loxP Δmad2::TRP1 Δndc80::NDC80-3HA-KanMX6
YSK936	Δbar1::loxP Δmad2::TRP1 Δndc80::ndc80Δaa1-116/ S205A T248A T252A T255A T685A T690A-3HA-KanMX6 pSK953
YSK937	Δbar1::loxP PDS1-9MYC:klTRP1 Δndc80::ndc80Δaa1-116/ T145A S150A-3HA-KanMX6
YSK939	Δbar1::loxP Δmad2::TRP1 Δndc80::NDC80/ T145A S150A-3HA-KanMX6
YSK940	Δbar1::loxP PDS1-9MYC:klTRP1 Δndc80::NDC80/ S205A T248A T252A T255A S37A T38A T43A T21A S22A S4A T5A S6A-3HA-KanMX6
YSK941	Δbar1::loxP PDS1-9MYC:klTRP1 Δndc80::NDC80/S4D T5D S6D T21D S22D S37D T38D T43D S145D S205D-3HA-KanMX6 pSK953
YSK942	Δbar1::loxP PDS1-9MYC:klTRP1 Δndc80::NDC80/ S37A T38A T43A T21A S22A S4A T5A S6A S205A-3HA-KanMX6
YSK943	Δbar1::loxP PDS1-9MYC:klTRP1 Δndc80::NDC80/ S37A T38A T43A T21A S22A S4A T5A S6A T145A S150A-3HA-KanMX6
YSK944	Δbar1::loxP PDS1-9MYC:klTRP1 Δndc80::NDC80/ S37A T38A T43A T21A S22A S4A T5A S6A T145A S150A S205A-3HA-KanMX6
YSK945	Δbar1::loxP Δmad2::TRP1

	Δndc80::NDC80/S4D T5D S6D T248D T252D S205D T21D S22D S37D T38D T43D T74D T79D T82D-3HA-KanMX6
YSK946	Δbar1::loxP Δmad2::TRP1
	Δndc80::NDC80/S4D T5D S6D T21D S22D S37D T38D T43D T54D S56D T58D T74D T79D T82D S97D S100D S106D-3HA-KanMX6
YSK947	Δbar1::loxP Δmad2::TRP1 Δndc80::NDC80/S205D S248D T252D S37D T38D T43D-3HA-KanMX6
YSK948	Δbar1::loxP PDS1-9MYC:klTRP1 Δndc80::ndc80Δaa1-116/ S205A T248A T252A-3HA-KanMX6 pSK953
YSK949	Δbar1::loxP Δmad2::TRP1 Δndc80::NDC80/S4D T5D S6D T248D T252D T21D S22D S37D T38D T43D-3HA-KanMX6
YSK950	Δbar1::loxP PDS1-9MYC:klTRP1 Δndc80::NDC80/ S205A T248A T252A S37A T38A T43A-3HA-KanMX6 pSK953
YSK880	Δbar1::loxP PDS1-9MYC:klTRP1
	Δndc80::NDC80/S4D T5D S6D T248D T252D S205D T21D S22D S37D T38D T43D T74D T79D T82D-3HA-KanMX6 Δmad2::HIS3
YSK788	Δbar1::loxP PDS1-9MYC:klTRP1 Δndc80::NDC80-3HA-KanMX6 pRS415
YSK869	Δbar1::loxP PDS1-9MYC:klTRP1
	Δndc80::NDC80/S4D T5D S6D T248D T252D S205D T21D S22D S37D T38D T43D T74D T79D T82D-3HA-KanMX6 pSK953 pRS415
YSK880	Δbar1::loxP PDS1-9MYC:klTRP1
	Δndc80::NDC80/S4D T5D S6D T248D T252D S205D T21D S22D S37D T38D T43D T74D T79D T82D-3HA-KanMX6 Δmad2::HIS3 pRS415
YSK880	Δbar1::loxP PDS1-9MYC:klTRP1 Δmad2::HIS3
	Δndc80::NDC80/S4D T5D S6D T248D T252D S205D T21D S22D S37D T38D T43D T74D T79D T82D-3HA-KanMX6 pSK953 pSK1029
YSK868	Δbar1::loxP PDS1-9MYC:klTRP1 Δndc80::NDC80/S4D T5D S6D T248D T252D S205D T21D S22D S37D T38D T43D-3HA-KanMX6 pRS415
YSK912	Δbar1::loxP PDS1-9MYC:klTRP1 Δndc80::NDC80/S4D T5D S6D T248D T252D S205D T21D S22D S37D T38D T43D-3HA-KanMX6 Δmad2::HIS3 pRS415
YSK912	Δbar1::loxP PDS1-9MYC:klTRP1 Δndc80::NDC80/S4D T5D S6D T248D T252D S205D T21D S22D S37D T38D T43D-3HA-KanMX6 Δmad2::HIS3 pSK1029
YSK953	Δbar1::loxP PDS1-9MYC:klTRP1 Δndc80::NDC80/ S205A T248A T252A S37A T38A T43A T21A S22A S4A T5A S6A-3HA-KanMX6 pSK953
YSK954	Δbar1::loxP PDS1-9MYC:klTRP1 Δndc80::NDC80/ T74D T79D T82D S205D S248D T252D-3HA-KanMX6
YSK955	Δbar1::loxP PDS1-9MYC:klTRP1 Δndc80::NDC80/ S205A T248A T252A S37A T38A T43A S4 T5 S6-3HA-KanMX6 pSK953
YSK956	Δbar1::loxP PDS1-9MYC:klTRP1
	Δndc80::NDC80/ S205A T248A T252A S37A T38A T43A T21A S22A S4A T5A S6A T74 T79 T82-3HA-KanMX6 pSK953
YSK958	Δbar1::loxP lys2::pGal-Flag-NDC80-3HA::LYS2
YSK960	Δbar1::loxP PDS1-9MYC:klTRP1 Δndc80::NDC80/ S205D S248D T252D S37D T38D T43D T21D S22D-3HA-KanMX6 pSK953
YSK961	Δbar1::loxP PDS1-9MYC:klTRP1 Δndc80::NDC80/ S205D S248D T252D S37D T38D T43D S4D T5D S6D-3HA-KanMX6 pSK953
YSK962	Δbar1::loxP PDS1-9MYC:klTRP1 Δndc80::NDC80/ S4D T5D S6D S205D T21D S22D S37D T38D T43D-3HA-KanMX6
YSK973	Δbar1::loxP Δndc80::ndc80 Δaa 1-255-3HA-KanMX6 Δmad2::TRP1 pSK953
YSK974	Δbar1::loxP Δmad2::TRP1 Δndc80::NDC80/ S205A T248A T252A S37A T38A T43A T21A S22A S4A T5A S6A T74 T79 T82-3HA-KanMX6 pSK953
YSK945	Δbar1::loxP Δmad2::TRP1
	Δndc80::NDC80/S4D T5D S6D T248D T252D S205D T21D S22D S37D T38D T43D T74D T79D T82D-3HA-KanMX6 pRS415
YSK945	Δbar1::loxP Δmad2::TRP1
	Δndc80::NDC80/S4D T5D S6D T248D T252D S205D T21D S22D S37D T38D T43D T74D T79D T82D-3HA-KanMX6 pSK1029
YSK975	Δbar1::loxP PDS1-9MYC:klTRP1
	Δndc80::NDC80/ S4D T5D S6D T248D T252D S205D T21D S22D S37D T38D T43D T54D S56D T58D-3HA-KanMX6 pSK953
YSK979	Δbar1::loxP Δmad2::TRP1 Δndc80::NDC80/ S37D T38D T43D S205D-3HA-KanMX6
YSK980	Δbar1::loxP Δmad2::TRP1 Δndc80::NDC80/ S37D T38D T43D S145D S205D-3HA-KanMX6
YSK991	Δbar1::loxP leu2::Gal10-Flag-NDC80 S4D T5D S6D T248D T252D S205D T21D S22D S37D T38D T43D T74D T79D T82D::LEU2
YSK992	Δbar1::loxP leu2::Gal10-Flag-NDC80::LEU2
YSK996	Δbar1::loxP
	leu2::pGal110-NDC80 ORF -3HA S4D T5D S6D T248D T252D S205D T21D S22D S37D T38D T43D T74D T79D T82D-TermpYX243::LEU2
YSK998	Δbar1::loxP PDS1-9MYC:klTRP1
	Δndc80::NDC80 S4D T5D S6D T248D T252D T21D S22D S37D T38D T43D T74D T79D T82D-3HA-KanMX6
YSK999	Δbar1::loxP PDS1-9MYC:klTRP1 Δndc80::NDC80 S4D T5D S6D S205D T21D S22D S37D T38D T43D T74D T79D T82D-3HA-KanMX6 pSK953

YSK1000	Δbar1::loxP PDS1-9MYC:klTRP1 Δndc80::NDC80 S37A T38A T43A T21A S22A S4A T5A S6A S205A T248A T252A-3HA-KanMX6 pSK953
YSK1001	Δbar1::loxP PDS1-9MYC:klTRP1 Δndc80::NDC80 S205D S248D T252D S37D T38D T43D S4D T5D S6D T74D T79D T82D-3HA-KanMX6 pSK953
YSK1002	Δbar1::loxP PDS1-9MYC:klTRP1 Δndc80::NDC80 S205D S248D T252D S37D T38D T43D T21D S22D T74D T79D T82D-3HA-KanMX6 pSK953
YSK1003	Δbar1::loxP PDS1-9MYC:klTRP1 Δndc80::NDC80 S4D T5D S6D T248D T252D S205D T21D S22D T74D T79D T82D-3HA-KanMX6 pSK953
YSK1007	Δbar1::loxP PDS1-9MYC:klTRP1 Δndc80::HIS3 leu2::pGal10-Flag-NDC80::LEU2 pSK953
YSK1008	Δbar1::loxP PDS1-9MYC:klTRP1 Δndc80::HIS3 leu2::pGal10-Flag-NDC80 S4D T5D S6D T248D T252D S205D T21D S22D S37D T38D T43D T74D T79D T82D::LEU2 pSK953
YSK1009	Δbar1::loxP PDS1-9MYC:klTRP1 Δndc80::HIS3 lys2::pGal-NDC80 ORF from aa 116-3HA S205A T248A T252A T255A T685A T690A::LYS2 pSK953
YSK1010	Δbar1::loxP Δmad2::TRP1 Δndc80::NDC80/ S205D S248D T252D S37D T38D T43D S4D T5D S6D-3HA-KanMX6 pSK953
YSK1011	Δbar1::loxP Δmad2::TRP1 Δndc80::NDC80/ S4D T5D S6D T248D T252D S205D T21D S22D S37D T38D T43D T54D S56D T58D-3HA-KanMX6 pSK953
YSK1014	Δbar1::loxP PDS1-9MYC:klTRP1 Δndc80::NDC80 T74D T79D T82D S205D S248D T252D S4D T5D S6D-3HA-KanMX6 pSK953
YSK1015	Δbar1::loxP PDS1-9MYC:klTRP1 Δndc80::NDC80 T74D T79D T82D S205D S248D T252D S37D T38D T43D-3HA-KanMX6 pSK953
YSK1016	Δbar1::loxP PDS1-9MYC:klTRP1 Δndc80::NDC80 T74D T79D T82D S205D S248D T252D T21D S22D-3HA-KanMX6 pSK953
YSK1023	Δbar1::loxP Δmad2::TRP1 Δndc80::NDC80/ S205D S248D T252D S37D T38D T43D S4D T5D S6D T74D T79D T82D-3HA-KanMX6 pSK953
YSK1024	Δbar1::loxP Δmad2::TRP1 Δndc80::NDC80/ S205D S248D T252D S37D T38D T43D T21D S22D T74D T79D T82D-3HA-KanMX6 pSK953
YSK1025	Δbar1::loxP Δmad2::TRP1 Δndc80::NDC80/ S205D S248D T252D S37D T38D T43D T21D S22D-3HA-KanMX6 pSK953
YSK788	Δbar1::loxP PDS1-9MYC:klTRP1 Δndc80::NDC80-3HA-KanMX6 pSK953
YSK1031	Δbar1::loxP Δmad2::TRP1 Δndc80::NDC80/ T74D T79D T82D S205D S248D T252D S37D T38D T43D-3HA-KanMX6 pSK953
YSK1032	Δbar1::loxP Δmad2::TRP1 Δndc80::NDC80/ T74D T79D T82D S205D S248D T252D T21D S22D-3HA-KanMX6 pSK953
YSK1035	Δbar1::loxP Δmad2::TRP1 Δndc80::NDC80/S37D T38D T43D S145D S205D-3HA-KanMX6 pSK953
YSK1037	Δbar1::loxP Δmad2::TRP1 Δndc80::NDC80/S4D T5D S6D T248D T252D S205D T21D S22D S37D T38D T43D T74D T79D T82D S97D S100D S106D-3HA-KanMX6 pSK953
YSK1039	Δbar1::loxP Δmad2::TRP1 Δndc80::NDC80/S4D T5D S6D T248D T252D S205D T21D S22D T74D T79D T82D-3HA-KanMX6 pSK953
YSK1045	Δbar1::loxP leu2::pGal1-MPS1-TAP::LEU2
YSK1047	Δbar1::loxP PDS1-9MYC:klTRP1 Δndc80::NDC80-3HA-KanMX6 Δmad2::HIS3 leu2::pGal1-MAD2::LEU2
YSK1048	Δbar1::loxP PDS1-9MYC:klTRP1 Δmad2::HIS3 leu2::pGal1-MAD2::LEU2 Δndc80::NDC80/S4D T5D S6D T248D T252D S205D T21D S22D S37D T38D T43D T74D T79D T82D-3HA-KanMX6
YSK1058	Δbar1::loxP PDS1-9MYC:klTRP1 Δmad2::HIS3 ade2::tetR-GFP::ADE2 1.4kb left of CEN5-tetO2x112::URA3 Δndc80::NDC80/S4D T5D S6D T248D T252D S205D T21D S22D S37D T38D T43D T74D T79D T82D-3HA-KanMX6
YSK1059	Δbar1::loxP Δndc80::NDC80-3HA-KanMX6 PDS1-9MYC:klTRP1 Δmad2::HIS3 leu2::pGal1-MAD2::LEU2 TUB1-GFP:URA3
YSK1060	Δbar1::loxP PDS1-9MYC:klTRP1 Δmad2::HIS3 leu2::pGal1-MAD2::LEU2 TUB1-GFP:URA3 Δndc80::NDC80/S4D T5D S6D T248D T252D S205D T21D S22D S37D T38D T43D T74D T79D T82D-3HA-KanMX6
YSK1066	Δbar1::loxP Δndc80::HIS3 Δbub1::TRP1-KL pSK953
YSK1070	Δbar1::loxP Δbub1::TRP1-KL Δndc80::NDC80/S4D T5D S6D T248D T252D S205D T21D S22D S37D T38D T43D T74D T79D T82D-3HA-KanMX6 pSK953
YSK1070	Δbar1::loxP Δbub1::TRP1-KL Δndc80::NDC80/S4D T5D S6D T248D T252D S205D T21D S22D S37D T38D T43D T74D T79D T82D-3HA-KanMX6 pSK953 pRS415
YSK1070	Δbar1::loxP Δbub1::TRP1-KL Δndc80::NDC80/S4D T5D S6D T248D T252D S205D T21D S22D S37D T38D T43D T74D T79D T82D-3HA-KanMX6 pSK953 pSK1082
YSK1082	Δbar1::loxP TETr-GFP::ADE2 ura3::1.4kb left of CEN5::tetO2x112::URA3 NDC80-9MYC::TRP1 ndc80::KanMX6-pGal-UbiR-NDC80
YSK913	Δbar1::loxP Δndc80::HIS3 Δmad2::TRP1 pSK953 pRS415
YSK1083	Δbar1::loxP TETr-GFP::ADE2 ura3::1.4kb left of CEN5::tetO2x112::URA3 NDC80-9MYC::TRP1 ndc80::KanMX6-pGal-UbiR-NDC80 leu2::P-NDC80-3HA-T::LEU2
YSK1084	Δbar1::loxP TETr-GFP::ADE2 ura3::1.4kb left of CEN5::tetO2x112::URA3 NDC80-9MYC::TRP1 ndc80::KanMX6-pGal-UbiR-NDC80

	leu2::P-NDC80 S4D T5D S6D T248D T252D S205D T21D S22D S37D T38D T43D T74D T79D T82D-3HA-T::LEU2
YSK1086	Δbar1::loxP PDS1-9MYC:klTRP1 Δndc80::NDC80/ T248A T252A-3HA-KanMX6 pSK953
YSK1088	Δbar1::loxP Ndc80-RedStar2::natNT2
YSK787	Δbar1::loxP Δndc80::HIS3 PDS1-9MYC:klTRP1 pSK953 pRS415
YSK1093	Δbar1::loxP TETr-GFP::ADE2 ura3::1.4kb left of CEN5::tetO2x112::URA3 NDC80-9MYC::TRP1 ndc80::KanMX6-pGal-UbiR-NDC80 leu2::P-NDC80-3HA-T::LEU2 natNT2pCUP1-1-UBR1
YSK880	Δbar1::loxP PDS1-9MYC:klTRP1 Δndc80::NDC80/S4D T5D S6D T248D T252D S205D T21D S22D S37D T38D T43D T74D T79D T82D-3HA-KanMX6 Δmad2::HIS3
YSK1105	Δbar1::loxP Ndc80-eGFP::LEU2
YSK1106	Δbar1::loxP Ndc80-RedStar2::natNT2 Ndc80-eGFP::LEU2
YSK1107	Δbar1::loxP NDC80-eGFP S4D T5D S6D T248D T252D S205D T21D S22D S37D T38D T43D T74D T79D T82D::LEU2
YSK1108	Δbar1::loxP Ndc80-RedStar2::natNT2 NDC80-eGFP S4D T5D S6D T248D T252D S205D T21D S22D S37D T38D T43D T74D T79D T82D::LEU2
YSK1111	Δbar1::loxP leu2::Ndc80-eGFP S4D T5D S6D T248D T252D S205D T21D S22D S37D T38D T43D::LEU2
YSK1112	Δbar1::loxP Ndc80-RedStar2::natNT2 leu2::Ndc80-eGFP S4D T5D S6D T248D T252D S205D T21D S22D S37D T38D T43D::LEU2
YSK1118	Δbar1::loxP TETr-GFP::ADE2 ura3::1.4kb left of CEN5::tetO2x112::URA3 NDC80-9MYC::TRP1 ndc80::KanMX6-pGal-UbiR-NDC80 leu2::P-NDC80-3HA-T::LEU2 natNT2pCUP1-1-UBR1 Δmad2::HIS3
YSK1119	Δbar1::loxP TETr-GFP::ADE2 ura3::1.4kb left of CEN5::tetO2x112::URA3 NDC80-9MYC::TRP1 ndc80::KanMX6-pGal-UbiR-NDC80 Δmad2::HIS3 leu2::P-NDC80 S4D T5D S6D T248D T252D S205D T21D S22D S37D T38D T43D T74D T79D T82D-3HA-T::LEU2 natNT2pCUP1-1-UBR1
YSK956	Δbar1::loxP PDS1-9MYC:klTRP1 Δndc80::NDC80/ S205A T248A T252A S37A T38A T43A T21A S22A S4A T5A S6A T74 T79 T82-3HA-KanMX6 pRS415
YSK1066	Δbar1::loxP Δndc80::HIS3 Δbub1::TRP1-KL pSK953 pRS415
YSK1120	Δbar1::loxP TETr-GFP::ADE2 ura3::1.4kb left of CEN5::tetO2x112::URA3 NDC80-9MYC::TRP1 ndc80::KanMX6-pGal-UbiR-NDC80 leu2::P-NDC80-3HA-T::LEU2 natNT2pCUP1-1-UBR1 lys2::CFP-TUB1::LYS2
YSK1121	Δbar1::loxP TETr-GFP::ADE2 ura3::1.4kb left of CEN5::tetO2x112::URA3 NDC80-9MYC::TRP1 ndc80::KanMX6-pGal-UbiR-NDC80 leu2::P-NDC80 S4D T5D S6D T248D T252D S205D T21D S22D S37D T38D T43D T74D T79D T82D-3HA-T::LEU2 natNT2pCUP1-1-UBR1 lys2::CFP-TUB1::LYS2
YSK1122	Δbar1::loxP PDS1-9MYC:klTRP1 Δndc80::NDC80/ S205A T248A T252A S37A T38A T43A T21A S22A S4A T5A S6A T74 T79 T82-3HA-KanMX6 Δmad2::HIS3
YSK1123	Δbar1::loxP leu2::Ndc80-eGFP S205A T248A T252A S37A T38A T43A T21A S22A S4A T5A S6A T74A T79A T82A ::LEU2
YSK1124	Δbar1::loxP Ndc80-RedStar2::natNT2 leu2::Ndc80-eGFP S205A T248A T252A S37A T38A T43A T21A S22A S4A T5A S6A T74A T79A T82A ::LEU2
YSK1125	Δbar1::loxP Ndc80-CFP::klTRP1 leu2::Ndc80-eGFP S205A T248A T252A S37A T38A T43A T21A S22A S4A T5A S6A T74A T79A T82A ::LEU2
YSK1128	Δbar1::loxP TETr-GFP::ADE2 ura3::1.4kb left of CEN5::tetO2x112::URA3 NDC80-9MYC::TRP1 ndc80::KanMX6-pGal-UbiR-NDC80 leu2::P-NDC80-3HA-T::LEU2 natNT2pCUP1-1-UBR1 PDS1-9MYC::HISMX6
YSK1129	Δbar1::loxP TETr-GFP::ADE2 ura3::1.4kb left of CEN5::tetO2x112::URA3 NDC80-9MYC::TRP1 ndc80::KanMX6-pGal-UbiR-NDC80 leu2::P-NDC80 S4D T5D S6D T248D T252D S205D T21D S22D S37D T38D T43D T74D T79D T82D-3HA-T::LEU2 natNT2pCUP1-1-UBR1 PDS1-9MYC::HISMX6
YSK1130	Δbar1::loxP Δbub1::TRP1-KL Δmad2::LYS2 pSK953 pRS415 Δndc80::NDC80/S4D T5D S6D T248D T252D S205D T21D S22D S37D T38D T43D T74D T79D T82D-3HA-KanMX6
YSK1131	Δbar1::loxP PDS1-9MYC:klTRP1 ura3-1:pGal-Mps1-myc:URA3 Δndc80::NDC80/ S205A T248A T252A S37A T38A T43A T21A S22A S4A T5A S6A T74 T79 T82-3HA-KanMX6
YSK1136	Δbar1::loxP TETr-GFP::ADE2 ura3::1.4kb left of CEN5::tetO2x112::URA3 NDC80-9MYC::TRP1 ndc80::KanMX6-pGal-UbiR-NDC80 leu2::P-NDC80 S4D T5D S6D T248D T252D S205D T21D S22D S37D T38D T43D-3HA-T::LEU2
YSK1137	Δbar1::loxP TETr-GFP::ADE2 ura3::1.4kb left of CEN5::tetO2x112::URA3 NDC80-9MYC::TRP1 ndc80::KanMX6-pGal-UbiR-NDC80 leu2::P-NDC80 S205A T248A T252A S37A T38A T43A T21A S22A S4A T5A S6A T74A T79A T82A-3HA-T::LEU2
YSK1122	Δbar1::loxP PDS1-9MYC:klTRP1 Δmad2::HIS3 pRS415 Δndc80::NDC80/ S205A T248A T252A S37A T38A T43A T21A S22A S4A T5A S6A T74 T79 T82-3HA-KanMX6
YSK1142	Δbar1::loxP TETr-GFP::ADE2 ura3::1.4kb left of CEN5::tetO2x112::URA3 NDC80-9MYC::TRP1 ndc80::KanMX6-pGal-UbiR-NDC80 leu2::P-NDC80-3HA-T::LEU2 natNT2pCUP1-1-UBR1 lys2::CFP-TUB1::LYS2 Δmad2::HIS3

YSK1143	Δbar1::loxP TETr-GFP::ADE2 ura3::1.4kb left of CEN5::tetO2x112::URA3 NDC80-9MYC::TRP1 ndc80::KanMX6-pGal-UbiR-NDC80 leu2::P-NDC80 S4D T5D S6D T248D T252D S205D T21D S22D S37D T38D T43D T74D T79D T82D-3HA-T::LEU2 natNT2pCUP1-1-UBR1 lys2::CFP-TUB1::LYS2 Δmad2::HIS3
YSK1144	Δbar1::loxP TETr-GFP::ADE2 ura3::1.4kb left of CEN5::tetO2x112::URA3 NDC80-9MYC::TRP1 ndc80::KanMX6-pGal-UbiR-NDC80 leu2::P-NDC80-3HA-T::LEU2 natNT2pCUP1-1-UBR1 PDS1-9MYC::HISMX6 Δmad2::LYS2
YSK1145	Δbar1::loxP tetR-GFP:ADE2 CEN5-tetO2x112:URA3 LEU2 cdc20::HIS3:pGal1-3HA-CDC20 trp1::mCherry-TUB1::TRP1
YSK1152	Δbar1::loxP PDS1-9MYC:klTRP1 Δndc80::NDC80/S4D T5D S6D T248D T252D S205D T21D S22D S37D T38D T43D T74D T79D T82D-3HA-KanMX6 Δbub2::HIS3 pSK953
YSK1152	Δbar1::loxP PDS1-9MYC:klTRP1 Δbub2::HIS3 Δndc80::NDC80/S4D T5D S6D T248D T252D S205D T21D S22D S37D T38D T43D T74D T79D T82D-3HA-KanMX6 pSK953 pRS415
YSK1154	Δbar1::loxP TETr-GFP::ADE2 ura3::1.4kb left of CEN5::tetO2x112::URA3 NDC80-9MYC::TRP1 ndc80::KanMX6-pGal-UbiR-NDC80 leu2::P-NDC80-3HA-T::LEU2 natNT2pCUP1-1-UBR1 his3::mCherry-TUB1::HIS3
YSK1155	Δbar1::loxP TETr-GFP::ADE2 ura3::1.4kb left of CEN5::tetO2x112::URA3 NDC80-9MYC::TRP1 ndc80::KanMX6-pGal-UbiR-NDC80 leu2::P-NDC80 S4D T5D S6D T248D T252D S205D T21D S22D S37D T38D T43D T74D T79D T82D-3HA-T::LEU2 natNT2pCUP1-1-UBR1 his3::mCherry-TUB1::HIS3
YSK1156	Δbar1::loxP TETr-GFP::ADE2 ura3::1.4kb left of CEN5::tetO2x112::URA3 ndc80::KanMX6-pGal-UbiR-NDC80 his3::mCherry-TUB1::HIS3 leu2::P-NDC80 S205A T248A T252A S37A T38A T43A T21A S22A S4A T5A S6A T74A T79A T82A-3HA-T::LEU2 NDC80-9MYC::TRP1
YSK1157	Δbar1::loxP NDC80-3mcherry::natNT2
YSK1158	Δbar1::loxP TETr-GFP::ADE2 ura3::1.4kb left of CEN5::tetO2x112::URA3 NDC80-9MYC::TRP1 ndc80::KanMX6-pGal-UbiR-NDC80 leu2::P-NDC80-3HA-T::LEU2 natNT2pCUP1-1-UBR1 mps1::HIS3MX6-pGal1-3HA-MPS1
YSK1159	Δbar1::loxP ndc80::KanMX6-pGal-Ubi-R-NDC80
YSK1162	Δbar1::loxP TETr-GFP::ADE2 ura3::1.4kb left of CEN5::tetO2x112::URA3 NDC80-9MYC::TRP1 ndc80::KanMX6-pGal-UbiR-NDC80 leu2::P-NDC80 S205A T248A T252A S37A T38A T43A T21A S22A S4A T5A S6A T74A T79A T82A-3HA-T::LEU2 Δmad2::HIS3
YSK1165	Δbar1::loxP TETr-GFP::ADE2 ura3::1.4kb left of CEN5::tetO2x112::URA3 NDC80-9MYC::TRP1 ndc80::KanMX6-pGal-UbiR-NDC80 leu2::P-NDC80 S205A T248A T252A S37A T38A T43A T21A S22A S4A T5A S6A T74A T79A T82A-3HA-T::LEU2 PDS1-9MYC::HISMX6
YSK1167	Δbar1::loxP ndc80::KanMX6-pGal-Ubi-R-NDC80 leu2::P-NDC80-3HA-T::LEU2
YSK1168	Δbar1::loxP ndc80::KanMX6-pGal-Ubi-R-NDC80 leu2::P-NDC80 S4D T5D S6D T248D T252D S205D T21D S22D S37D T38D T43D T74D T79D T82D-3HA-T::LEU2
YSK1169	Δbar1::loxP ndc80::KanMX6-pGal-Ubi-R-NDC80 leu2::P-NDC80 S205A T248A T252A S37A T38A T43A T21A S22A S4A T5A S6A T74A T79A T82A-3HA-T::LEU2
YSK1170	Δbar1::loxP TETr-GFP::ADE2 ura3::1.4kb left of CEN5::tetO2x112::URA3 NDC80-9MYC::TRP1 ndc80::KanMX6-pGal-UbiR-NDC80 leu2::P-NDC80 S4D T5D S6D T248D T252D S205D T21D S22D S37D T38D T43D T74D T79D T82D-3HA-T::LEU2
YSK1171	Δbar1::loxP Δbub1::TRP1-KL Δndc80::NDC80/ S205A T248A T252A S37A T38A T43A T21A S22A S4A T5A S6A T74 T79 T82-3HA-KanMX6 pSK953 pRS415
YSK1172	Δbar1::loxP TETr-GFP::ADE2 ura3::1.4kb left of CEN5::tetO2x112::URA3 NDC80-9MYC::TRP1 ndc80::KanMX6-pGal-UbiR-NDC80 leu2::P-NDC80 S4D T5D S6D T248D T252D S205D T21D S22D S37D T38D T43D T74D T79D T82D-3HA-T::LEU2 Δmad2::HIS3
YSK1173	Δbar1::loxP TETr-GFP::ADE2 ura3::1.4kb left of CEN5::tetO2x112::URA3 ndc80::KanMX6-pGal-UbiR-NDC80 his3::mCherry-TUB1::HIS3 leu2::P-NDC80 S4D T5D S6D T248D T252D S205D T21D S22D S37D T38D T43D T74D T79D T82D-3HA-T::LEU2 NDC80-9MYC::TRP1
YSK1174	Δbar1::loxP TETr-GFP::ADE2 ura3::1.4kb left of CEN5::tetO2x112::URA3 NDC80-9MYC::TRP1 ndc80::KanMX6-pGal-UbiR-NDC80 leu2::P-NDC80 S4D T5D S6D T248D T252D S205D T21D S22D S37D T38D T43D T74D T79D T82D-3HA-T::LEU2 PDS1-9MYC::HISMX6
YSK1175	Δbar1::loxP NDC80-3mcherry::natNT2 NSL1-yeGFP::HIS3MX6
YSK1176	Δbar1::loxP TETr-GFP::ADE2 ura3::1.4kb left of CEN5::tetO2x112::URA3 NDC80-9MYC::TRP1 ndc80::KanMX6-pGal-UbiR-NDC80 leu2::P-NDC80 S4D T5D S6D T248D T252D S205D T21D S22D S37D T38D T43D T74D T79D T82D-3HA-T::LEU2 mps1::HIS3MX6-pGal1-3HA-MPS1
YSK1179	Δbar1::loxPTETr-GFP::ADE2 ura3::1.4kb left of CEN5::tetO2x112::URA3 NDC80-9MYC::TRP1 ndc80::KanMX6-pGal-UbiR-NDC80 leu2::P-NDC80 S4D T5D S6D T248D T252D S205D T21D S22D S37D T38D T43D T74D T79D T82D-3HA-T::LEU2 his3::mCherry-TUB1::HIS3 Δmad2::LYS2
YSK1180	Δbar1::loxP TETr-GFP::ADE2 ura3::1.4kb left of CEN5::tetO2x112::URA3 NDC80-9MYC::TRP1 ndc80::KanMX6-pGal-UbiR-NDC80 leu2::P-NDC80 S4D T5D S6D T248D T252D S205D T21D S22D S37D T38D T43D T74D T79D T82D-3HA-T::LEU2 PDS1-9MYC::HISMX6 Δmad2::LYS2
YBL761	Δbar1::loxP Δndc80::ndc80 Δaa 1-255-3HA-KanMX6

YBL762	Δbar1::loxP Δndc80::ndc80 Δaa 1-116-3HA-KanMX6
YBL763	Δbar1::loxP Δndc80::ndc80 Δaa 1-43-3HA-KanMX6
YMS398	Δbar1::loxP-HIS3-loxP TUB1-GFP:URA3 LEU2 NDC80-9MYC:klTRP
YAW427	Δbar1::loxP SPC25-TAP:: URA3 NUF2-6HA::klTRP1

3.4 Culturing conditions & Media

E. coli

E. coli strains were grown in LB_{Amp} liquid medium or on LB_{Amp} plates at 37°C.

LB:
10 g/l Tryptone
5 g/l Yeast extract
10 g/l NaCl
pH 7.0

SOB:
20 g/l Tryptone
5 g/l Yeast extract
0.5 g/l NaCl
pH 7.0
25 mM KCl
10 mM $MgCl_2$

Solid media contained 2% (w/v) agar.

Ampicillin was added to a final concentration of 100 µg/ml.

S. cerevisiae

Yeast strains were cultured at 25°C.

YPD:
10 g/l Yeast extract
20 g/l Peptone from casein
20 g/l Glucose

YPG:
10 g/l Yeast extract
20 g/l Peptone from casein
20 g/l Galactose

YPR:
10 g/l Yeast extract
20 g/l Peptone from casein
20 g/l Raffinose

YPGR:
10 g/l Yeast extract
20 g/l Peptone from casein
1 g/l Galactose
20 g/l Raffinose

SD (synthetic dropout):
6.7 g/l Yeast Nitrogen Base w/o amino acids
20 g/l Glucose
0.8 g/l Complete Supplement Mixture –Ade/His/Trp/Leu/Ura

supplement:[1]	final concentration:
Adenine	30 mg/l
Histidine	20 mg/l
Leucine	20 mg/l
Tryptophan	30 mg/l
Uracil	20 mg/l

[1]omit the respective compound for SD-Trp, SD-His, SD-Leu ...

Solid media contained 2% (w/v) agar.

FOA plates: SD plates containing all amino acids and 0.1% 5´-FOA.

YPD plates with kanamycin: YPD plates with the addition of 200 mg/l G418.

Media for microscopy contained 0.01% adenine and were filter sterilized instead of autoclaving.

3.5 Oligonucleotides

All sequences are given in 5´ to 3´direction.

Name	Sequence
NDC80-1	ATATTACCATGGGACTACAAGGACGACGATGACAAGCATATGCAAAGCTCAACAAGTACTGA
NDC80-2	TAATGGTACCTTGGTTTCATTGTCACCTTCCTAT
NDC80-3	TATTTTCCATGGTCAGCAGATTATCAATAAATCAA
NDC80-4	CAATCGTCATTGGAAAACTCTG
NDC80-5	TGGAATACTTGAGAAGGGGAGT
NDC80-6	CCCGTTTCTACATATGCAAAGCTCAACAA
NDC80-7	ATTTGATAGATCTAATTCTCGATAGACTTA
NDC80-8	ATTTGGATCCTTAATTTGTTACGTTATGTTCAG
NDC80-9	CCACTAAGACATATGAACTTCCAAAGC
NDC80-10	ATGATCAATCATATGATTGCCAGGAATAC
NDC80-11	TTCTCCGCGGAACAACTTCTTCGACAG
NDC80-12	CAAGGATCCTTAAGGCTGGCTCAGA
NDC80-13	TGTTGGCGGCCGCATATGTAGAAACGGGTATC
NDC80-14	GAAATAACACATATGAGCCAGCC
NDC80-15	GAATGGGCCCGGTTTCATTGTCACC
NDC80-16	CTGCGAGATCAAACTAGCGTG
NDC80-17	CAGTTTCTCCACCATTAGCTCATA
NDC80-58	ACCCGTGGATCCAAATGCAAAGCTCAACAAGTACTGA
NDC80-59	ACCCGTGGATCCAAATGCAAAGCGATGATGATACTGA
NDC80-60	ATATTACCATGGGACTACAAGGACGACGATGACAAGCATATGCCAAAGCGCAGCAGCTACTGA
NDC80-61	CCCGTTTCTACATATGCAAAGCGCAGCAGCT
NDC80-64	GAATTGTCCGAAGCGAATTCCAAATTTG
NDC80-65	TAAGCGAATTCCTTATGATTTATG
NDC80-fUbiR-62	CCTTTCTTTAAACGTTAGGGTGTACTATAATATATTCCATAAGAGATACCCGTTTGCGCGCGTAATACGACTCAC
NDC80-rUbiR-63	ACCGATGAGGGTCCATGTGATGTAGCACATGTTGATCAGTACTTGTTGAGCTTTGGGATCCGTGCCTACCACCT
KAN-HIS	TGGGCCTCCATGTCGCTGG
PDS1-1	TGGAGTTAGTGTACAGCGAAG
PDS1-2	CCCGCAGCACATTAGTAGAAA
S2-NSL1	TTATCATTTACCACGAGGTTGACTGTCTTATATGTTATTTATTCAATCGATGAATTCGAGCTCG
S3-NSL1	AACGTTGAAAAGGTCAAGCGCTTAATGGACTTCCTGGAGGAGGATCGTACGCTGCAGGTCGAC
MPS1-7-fTAP	GATGTGGTAGACACTGTTTTAAGGAAATTTGCAGATTACAAAATTTCCATGGAAAAGAGAAG
MPS1-8-rTAP	TTATGTTCATAACTGGCACATGCTTTTCTTCCTTATGCGGCTCTTTACGACTCACTATAGGG
MPS1-S3-1	AAAATTTAGAAGAGCCGCATAAGGAAGAAAAGCATGTGCCAGTTACGTACGCTGCAGGTCGAC
MPS1-S2-2	AAATAAATCAGTACATGCATGGCAAACTCTAAATGTATTTATGTAZCGATGAATTCGAGCTCG
SPC25-fTAP-5	CGCGGCATTTTTAGTCGTGGCCCGCGATATGCTTCTGGCATCTTTATCCATGGAAAAGAGAAG
SPC25-rTAP-6	TAAATCATAGGCCCAGAATAAACTGAACAGATGCGTATAAAGGCGTACGACTCACTATAGGG
NDC80-S2	GGGGCTGAGCTTTGCTGTAGATTGCTCGGGTATTATATATCATTTATTTTAATCGATGAATTCGAGCTCG
NDC80-S3	TGAAGAGTTACGAAATTTGGAGTTTGAAACTGAACATAACGTAACAAATCGTACGCTGCAGGTCGAC

NDC80 mutagenesis primers (Ser/Thr To Ala)

NDC80-18	CATTAATTAATCAAAATGCACAAGAAATCGCGATTCTGGCCCAGCCTTTAAAG
NDC80-19	CTTTAAAGGCTGGGCCAGAATCGCGATTTCTTGTGCATTTTGATTAATTAATG
NDC80-20	GGAGTTTGAAGCTGAACATAACGTCGCGAATCGTACGCTGCAGGTCGAC
NDC80-21	GTCGACCTGCAGCGTACGATTCGCGACGTTATGTTCAGCTTCAAACTCC
NDC80-22	GACAAAAACTTCCAAGCCGCTATTCAAGAGG

NDC80-23	CCTCTTGAATAGCGGCTTGGAAGTTTTTGTC
NDC80-24	AAATTTGATATCGAAGCAAATCATCCCATTGCAATAAAATTTC
NDC80-25	GAAATTTTATTGCAATGGGATGATTTGCTTCGATATCAAATTT
NDC80-26	GGTTACGGCTTTGCTAAGTCGATCGAGAATGAG
NDC80-27	CTCATTCTCGATCGACTTAGCAAAGCCGTAACC
NDC80-28	GTCAATAAATAATGCGCAAATTTCGGCTG
NDC80-29	CAGCCGAAATTTGCGCATTATTTATTGAC
NDC80-48	GAGGAGAAGAAACGCCGCGAATCAAGGCCTAGCCGACATGATCAATAAG
NDC80-49	CTTATTGATCATGTCGGCTAGGCCTTGATTCGCGGCGTTTCTTCTCCTC
NDC80-50	GGACCCTCACCGGTTTGCGGCCCAAATACCAACTGCAAC
NDC80-51	GTTGCAGTTGGTATTTGGGCCGCAAACCGGTGAGGGTCC
NDC80-52	CGTTTCTATAAATGCAAAGCGCAGCAGCTACTGATCAACATGTGCTAC
NDC80-53	GTAGCACATGTTGATCAGTAGCTGCTGCGCTTTGCATTTATAGAAACG
NDC80-54	CATTAATTAATCAAAATGCACAAGAAATCGCGATTCTGAGCCAGCC
NDC80-55	GGCTGGCTCAGAATCGCGATTTCTTGTGCATTTTGATTAATTAATG
NDC80-56	GGACAAGAAGCGCGGTTGCAGGAGGTGCAAATGGCGCCGCATTGGCTC
NDC80-57	GAGCCAATGCGGCGCCATTTGCACCTCCTGCAACCGCGCTTCTTGTCC

NDC80 mutagenesis primers (Ser/Thr To Asp)

NDC80-30	CGTTTCTATAAATGCAAAGCGATGATGATACTGATCAACATGTGCTAC
NDC80-31	GTAGCACATGTTGATCAGTATCATCATCGCTTTGCATTTATAGAAACG
NDC80-32	GGACCCTCATCGGTTTGATGATCAAATACCAACTGCAAC
NDC80-33	GTTGCAGTTGGTATTTGATCATCAAACCGATGAGGGTCC
NDC80-34	GAGGAGAAGAAACGACGATAATCAAGGCCTAGACGACATGATCAATAAG
NDC80-35	CTTATTGATCATGTCGTCTAGGCCTTGATTATCGTCGTTTCTTCTCCTC
NDC80-36	GAGTATTGCCAGGAATGATATCGACGGGGATGGCATTCCCACAGG
NDC80-37	CCTGTGGGAATGCCATCCCCGTCGATATCATTCCTGGCAATACTC
NDC80-38	GGACAAGAAGCGACGTTGCAGGAGGTGACAATGGTGATGCATTGGCTC
NDC80-39	GAGCCAATGCATCACCATTGTCACCTCCTGCAACGTCGCTTCTTGTCC
NDC80-40	GAAACAGCGTCGACAGATTAGACATAAATCAACTTGGCGACCTGCAGCAAC
NDC80-41	GTTGCTGCAGGTCGCCAAGTTGATTTATGTCTAATCTGTCGACGCTGTTTC
NDC80-42	AATTTGATATTGAAGACAATCATCCCATTGATATCAAATTTCTAAAAC
NDC80-43	GTTTTAGAAATTTGATATCAATGGGATGATTGTCTTCAATATCAAATT
NDC80-44	GTCAATAAATAAAGACCAAATTTCAGCTGTAGGTGGC
NDC80-45	GCCACCTACAGCTGAAATTTGGTCTTTATTTATTGAC
NDC80-46	CATTAATTAATCAAAATGATCAAGAAATAGACATTCTGAGCCAGCC
NDC80-47	GGCTGGCTCAGAATGTCTATTTCTTGATCATTTTGATTAATTAATG

ChIP primers

ChrIII-1	ACTTTGGCTTTCCGCTCGTG
ChrIII-2	GAAAGTCTTCTAGAGTTACAGG
ChrIII-3	GACCAGCATGTAGGAAGGTG
ChrIII-4	ACATTGATAAATTGCTCTCACCA
CEN3-12	GATCAGCGCCAAACAATATGG
CEN3-13	AACTTCCACCAGTAAACGTTTC

Oligonucleotides used in this work were synthesised by Thermo (Ulm) or MWG-Biotech (Ebersberg).

3.6 Chemicals, enzymes and other materials

All chemicals were obtained from Applichem (Darmstadt) unless otherwise stated. Plasticware was provided by Sarstedt (Nümbrecht).

Company	**Products**
Amersham (Freiburg)	Protein A Sepharose CL4-B, ECL detection system Calmoduline-Sepharose, [γ-32P]-ATP
Bio-Rad (Hercules) Braun (Melsungen)	PolyPrep chromatography columns, protein standards Glass beads (Ø 0.45-0.5 mm)
Biocat (Heidelberg)	Phusion High-Fidelity DNA Polymerase
Calbiochem (La Jolla)	Alpha factor, G418 sulfate
Difco (Detroit)	Yeast extract, Tryptone, YNB
Fluca (Buchs)	Diethanolamine, Lithiumacetate, TEMED, Formaldehyde
ICN (Mannheim)	Zymolyase
Invitrogen (Karlsruhe)	TEV-protease, 4-12% Nupage gradient gels
Kodak (New Haven)	x-ray films
MBI (St.Leon Roth)	Restriction enzymes, DNA ladders, dNTPs
Millipore (Bedford)	PVDF blotting membranes, sterile filtering devices
Microsynth (Balgach Switzerland)	Sequencing
NEB (Beverly)	Restriction enzymes
Pineda (Berlin)	Custom-ordered anti-Ndc80 antibody
Qiagen (Hilden)	QiaexII glass milk for DNA isolation from agarose gels Qiagen Plasmid Mini Kit
Roche (Mannheim) Roth (Karlsruhe)	α-Myc, α-HA, Expand PCR kit, CDP-Star Colloidal Coomassie, EDTA, Glycine, Phenol, Tris
Serva (Heidelberg)	Coomassie Brilliant blue R250 and G250, PEG 8000 Raffinose, SDS, Tween
Sigma (Deisenhofen)	α-rabbit, α-mouse, α-rat, human IgG agarose
Thermo (Ulm)	Oligonucleotides

3.7 Instruments

Company	Instrument
Bio-Rad	Blotting apparatus Trans blot SD, SDS-PAGE system FluorS-Multi Imager, Power supplies, Gel dryer
Binder	Incubators for plates
Biometra	Power supplies, P25 Rocker WT17 Sonifier B15
Branson	Sonifier B15
Becton Dickinson	FACS Callibur
DuPont	Centrifuges
Eppendorf	Heating blocks, Table top centrifuges
Fritsch	Pulverissette 6
Heraeus	Incubators for plates
Hamamatsu	Orca-ER Camera for fluorescence microscope
Infors	Incubators for liquid cultures
Liebherr	Freezer -20°C, refigerator
Lauda	Waterbath
Merck	Ultrasound waterbath
Microfluidics	Microfluidiser for *E.coli* cell lysis
Millipore	Water deionising facility, MilliQPlus
Olympus	Fluorescence microscope
Pharmacia	Agarose gel electrophoresis system
Sorvall	Centrifuges
Singer Instruments	Micromanipulator for tetrade dissection
Techne	PCR machines
Thermo Electron	Freezer -80°C, Photometer
Zeiss	Light microscope

4 METHODS

4.1 Molecular biology techniques

4.1.1 Restriction analysis

Restriction analyses were performed as described in the data sheets of the respective restriction enzyme. Usually, 1-5 µg of plasmid DNA was digested using 1-10 U of enzyme in a volume of 10-30 µl and incubated for 1 h at 37°C. The resulting fragments were analyzed on 0.7-3% agarose gels.

4.1.2 Polymerase Chain Reaction (PCR)

For gene deletion and genomic tagging of yeast genes, PCR-products generated by Expand long template Taq polymerase were used:

A 50 µl reaction contained:	program:			
1 x PCR buffer	initial denaturation:	94°C	3 min	
1 µM primers	denaturing:	94°C	20 sec	} 10 x
0.5 mM dNTPs	annealing:	54°C	45 sec	} 10 x
300 ng plasmid DNA	extension:	68°C	2.5 min	} 10 x
1.5 U polymerase	denaturing:	94°C	20 sec	} 20x
	annealing:	54°C	45 sec	} 20x
	extension:	68°C	2.5min +20 sec/cycle	} 20x
	final extension:	68°C	7 min	

For colony PCR, the following set-up was used:

A 25 µl reaction contained:	program: 30 cycles		
1 x PCR buffer	initial denaturation:	94°C	3 min
1 µM primers	denaturing:	94°C	45 sec
200 µM dNTPs	annealing:	Tm	45 sec
0.5 µl genomic DNA	extension:	72°C	1 min/kb
3 U Taq polymerase	final extension:	68°C	7 min

For cloning of genes from the *S. cerevisiae* genome, Phusion High-Fidelity DNA Polymerase was used, since it has a very low error rate (4.4×10^{-7}):

A 50 µl reaction contained:	program: 30 cycles		
1 x HF-PCR buffer	initial denaturation:	98°C	3 min
0.5 µM primers	denaturing:	98°C	20 sec
200 µM dNTPs	annealing:	Tm	30 sec
100 ng genomic DNA	extension:	72°C	30 sec/kb
1 U Phusion polymerase	final extension:	72°C	5 min

4.1.3 Cloning of PCR products

PCR products were precipitated with NH_4Ac/isopropanol in order to remove dNTPs and oligonucleotides, treated with T4 polymerase for the removal of oligo-A overhangs, and finally separated by agarose gel electrophoresis and gel extracted. 5' ends were phosphorylated in a polynucleotide kinase (PNK) reaction supplemented with 1.5 mM ATP. After heat inactivation of the PNK (10 min at 65°C), the phosphorylated PCR-product was ligated to an alkaline phosphatase treated vector.

4.1.4 Agarose gel electrophoresis

To all samples, loading dye was added and fragments were separated on 0.7-3% agarose gels in 1x TAE buffer.

TAE buffer:	242 g/l Tris	6x loading dye:	0.25% Bromphenol blue
	57.1 ml/l Glacial acid		0.25% Xylene cyanol
	100 ml/l 0.5 M EDTA		30% Glycerol
	pH 7.2		

4.1.5 Isolation of DNA from agarose gels

All DNA fragments were isolated from agarose gels using the QIAEX II gel extraction kit from Qiagen according to the manufacturer's protocol.

4.1.6 DNA quantification

For quantification of DNA, the absorption of the solution at 260 nm was measured. The OD_{260} of 1 corresponds to a DNA concentration of 50 µg/ml. To determine the purity of the solution, its absorption at 280 nm was determined. The ratio of OD_{260} to OD_{280} gives an information about its contamination with RNA or proteins, respectively.

4.1.7 Klenow reaction

Klenow polymerase was used for the removal of 3´protruding ends. The reaction was performed in the presence of 200 µM dNTPs in 1x Klenow buffer with 10 U/µg DNA. After incubation at 37°C for 10 min, the enzyme was heat inactivated for 10 min at 70°C.

4.1.8 T4 DNA polymerase reaction

T4 polymerase was used for the removal of 5´ protruding ends. The reaction was performed in the presence of 0.5 mM dNTPs in T4 DNA polymerase buffer with 4 U/µg DNA. After incubation at 11°C for 20 min, the enzyme was heat inactivated for 10 min at 75°C.

4.1.9 Treatment with Calf Intestinal Alkaline Phosphatase (CIAP)

In order to prevent religation, vectors were treated with calf intestinal alkaline phosphatase (CIAP). 10 U CIAP were added to 5 µg DNA in a 50 µl reaction and incubated for 2 h at 37°C and subsequently heat inactivated at 85°C for 15 min.

4.1.10 Ligation

Ligations were performed using 100 ng of vector DNA and 2 Weiss units DNA ligase in a volume of 10 µl. The molar ratio of vector to insert was 1:3 for sticky-end ligations and 1:1 for blunt-end ligations. The reaction mixture was incubated o/n at RT.

4.1.11 Phenol/Chloroform extraction

In order to remove proteins from DNA, the sample was mixed with 1 volume of pre-equilibrated phenol (phenol:chloroform:isoamylalcohol 25:24:1), vortexed for 1 min and centrifuged for 10 min at 14 Krpm at RT. The aqueous phase was removed, re-extracted with 1 volume of chloroform and finally EtOH precipitated.

4.1.12 *E. coli* colony PCR

One *E.coli* clone was resuspended in 20 µl H_2O and boiled for 5 min at 95°C. 5 µl were used as template in a 25 µl PCR reaction.

4.1.13 DNA precipitation

LiCl/EtOH

1/10 volume of 10 M LiCl and 2.5 volumes of ice cold EtOH (100%) were added to the sample, incubated for 30 min at –20°C and centrifuged for 30 min at 4°C and 14 Krpm. The pellet was washed with 70% EtOH, dried and resuspended in TE or H_2O.

NH_4Ac/Isopropanol

This precipitation was used for the removal of oligonucleotides from PCR reactions. 1/10 volume of 10 M NH_4Ac and 1 volume of isopropanol were added to the sample, incubated for 30 min at RT and centrifuged for 30 min at RT and 14 Krpm. The pellet was washed with 70% EtOH, dried and resuspended in TE or H_2O.

4.1.14 Competent cells

Chemical competent cells (according to Hanahan, 1983)

DH5α cell were inoculated in 50 ml SOB/10 mM $MgCl_2$ from an o/n culture. The culture was incubated at 37°C and harvested at an OD_{578} of 0.5 (10 min, 4 Krpm, and 4°C). The pellet was resuspended in 15 ml cold Tbf1 and incubated on ice for 10 min. After another centrifugation step, the pellet was carefully resuspended in 1.8 ml cold Tbf2 and 200 µl aliquots were frozen in liquid nitrogen. Competent cells were stored at –80°C.

Tbf1:	30 mM Kac, pH 5.8 50 mM $MgCl_2$ 100 mM KCl 15% Glycerol	Tbf2:	10 mM MOPS/NaOH, pH 7.0 75 mM $CaCl_2$ 10 mM KCl 15% Glycerol

Electro-competent cells

DH5α cell were inoculated in 500 ml SOB/10 mM $MgCl_2$ with 5 ml of an o/n culture. The culture was incubated at 37°C until an OD_{578} of 0.5 was reached, cooled on ice for 30 min and harvested at 4 Krpm and 4°C for 10 min. The cells were washed with 500 ml, 300 ml and 15 ml cold water, respectively and finally with 10 ml 15% glycerol. The pellet was carefully resuspended in 1.5 ml 10% glycerol and 50 µl aliquots were frozen in liquid nitrogen. Competent cells were stored at –80°C.

4.1.15 Transformation of *E. coli*

Transformation by heat shock

3 µl ligation reaction (out of 10 µl) were added to 50 µl competent cells and incubated for 30 min on ice. The cells were heat shocked for 90 sec at 37°C and subsequently cooled on ice for 5 min. 800 µl SOC was added and the transformation reaction was incubated for 1 h at 37°C under vigorous shaking. 150 µl were plated on LB_{Amp} and incubated o/n at 37°C.

SOB: 5 g/l Yeast extract
20 g/l Tryptone
0.5 g/l NaCl
10 ml/l 250 mM KCl
5 ml/L $MgCl_2$
pH 7.5

SOC: SOB supplemented with 4% Glucose

Electroporation

To the electro-competent cells, 3 µl DNA was added and incubated for 5 min on ice. The electroporation was performed in cuvettes with a Gene Pulser (BioRad) at 25 µF, 2.5 kV and 200 Ω. 1 ml SOC was immediately added and the suspension was shaken for 1 h at 37°C. The transformation was plated on LB_{Amp} and incubated o/n at 37°C.

4.1.16 Isolation of plasmid DNA from *E. coli*

Plasmid DNA for restriction analysis, cloning and transformation of *S. cerevisiae* was isolated by the alkaline lysis method (Sambrook et al. 2001). 3 ml o/n culture in LB_{Amp} was centrifuged for 5 min at 4 Krpm at 4°C. The cell pellet was resuspended in 400 µl cold solution I (resuspension buffer). Lysis was performed with 400 µl solution II (lysis buffer) for 5 min at RT. Neutralisation was achieved by adding 400 µl solution III (neutralisation buffer) and centrifugation for 20 min at 14 Krpm at 4°C. The supernatant was precipitated by the addition of 0.7 volumes isopropanol for 20 min at RT and centrifuged for 20 min. The DNA-pellet was washed with 70% EtOH, air dried and resuspended in 40 µl TE. The DNA concentration was determined photometrically.

Solution I: 50 mM Tris-HCl pH 8.0
10 mM EDTA
100 µg/ml RNAse A

Solution II: 0.2 N NaOH
1% SDS

Solution III: 2,8 M Kac pH 5,1

TE: 10 mM Tris-HCl pH 8.0
1 mM EDTA pH 8.0

If plasmid DNA was used as template for site directed mutagenesis, it was purified using the Qiagen Plasmid Mini Kit according to the manufacturers recommendations. The resulting DNA was highly pure and thus suitable for the PCR-reaction.

4.1.17 DNA-sequencing

All sequencing reactions were performed by Microsynth (Balgach, Switzerland) or MWG-Biotech (Ebersberg).

4.1.18 Site directed mutagenesis

To introduce point mutations in the NDC80-ORF, the QuickChange Site-Directed Mutagenesis Kit (Stratagene) which is based on a PCR-reaction was used. The kit was used according to the manufacturers recommendations with the following modifications:

- the extension time of the PCR-reaction was 2 min/kb
- the DpnI digest was performed o/n at 37°C
- the whole PCR-reaction was EtOH precipitated and transformed into XL10Gold ultracompetent cells

4.2 Cellular biology techniques

4.2.1 Yeast transformation (adapted from Schiestl and Gietz, 1989)

50 ng of plasmid DNA or 1-2 µg of PCR product were used for transformation of yeast cells. 50 ml of a logarithmically growing culture were harvested at 3 Krpm for 5 min and 4°C, washed first with 1 volume of water and then with 1 ml of LiSorb. The pellet was resuspended in LiSorb at 10 µl/OD. To 100 µl of competent cells, the DNA, 100 µg single stranded carrier DNA and 600 µl LiPEG were added. After shaking (1400 rpm) for 30 min at RT and the addition of 70 µl DMSO, the cells were heat shocked for 15 min at 42°C (37°C for temperature sensitive strains), washed with water and plated on selective plates. For GFP taggings, galactose promoter integration and transformation on antibiotic containing plates, cells were recovered for 6 h at 25°C in YPD or YPG medium before plating on selective plates. Correct integration or tagging was verified by colony PCR, Western blotting or fluorescence microscopy.

LiSorb: 100 mM LiAc
10 mM Tris/HCl pH 8.0
1 mM EDTA pH 8.0
1 M Sorbitol

LiPEG: 100 mM LiAc
10 mM Tris/HCl pH 8.0
1 mM EDTA pH 8.0
40% PEG 3350

4.2.2 Isolation of genomic DNA from *S. cerevisiae*

100 OD of a logarithmically growing culture were harvested for 10 min at 3 Krpm and the pellet was resuspended in 1 ml NTES buffer supplemented with 1 mg RNAse. The sample was transferred to four 1.5 ml cups and glass beads were added to the meniscus. Cells were lysed for 30 min at 4°C and 1800 rpm. After a phenol/chloroform extraction, the aqueous phase was EtOH precipitated. After a wash step with 70% EtOH, the pellet was dried and resuspended in 50 µl TE.

NTES-buffer: 10 mM Tris/HCl pH 8.0
100 mM NaCl
1 mM EDTA pH 8.0

4.2.3 Yeast colony PCR

One yeast clone was resuspended in 40 µl NTES-buffer and glass beads were added to the meniscus. The sample was shaken for 30 min at 1800 rpm and 4°C and phenol/chlorophorm extracted. 0.5 µl of the aqueous phase was used as template for the PCR.

4.2.4 Mating

An a and an α mating strain were freshly streaked out on YPD-plates and mixed. After 6 hours, zygote formation could be observed microscopically.

4.2.5 Sporulation and tetrad dissection

For sporulation, diploid strains were inoculated in 10 ml of sporulation medium and incubated for 4 to 6 days at 25°C. For tetrad dissection, 1 ml was harvested and resuspended in 50 µl sorbitol buffer with 10 U zymolyase for 20-35 min at 30°C. The reaction was stopped by the addition of 1 ml cold sorbitol buffer. 20 µl were spotted on a selective plate and tetrads were dissected with a micromanipulator.

Sorbitol buffer: 1 M Sorbitol
10 mM Tris/HCl pH 7.5

Zymolyase: 500 U/ml H_2O

4.2.6 Cell synchronisation

α-factor arrest

All strains synchronised by α-factor contained a disrupted BAR1 gene to increase the sensitivity of the yeast strain to the pheromone. 250 ng/ml of α-factor was added to a logarithmically growing culture at an OD_{578} of 0.3-0.5. After a 3 h incubation, more then 95% of the cells had a shmoo indicating a G_1-arrest. Cells were released from the arrest by washing and resuspension in fresh medium.

α-factor: 1 mg/ml in 0.1 M NaAc pH 5.6

Metaphase arrest in the absence of spindles (Nocodazole arrest)

To a logarithmically growing culture, 15 µg/ml nocodazole was added at an OD_{578} of 0.3-0.5. After a 3 h incubation, more then 95% of the cells were arrested in G_2/M with large buds. Cells were released from the arrest by washing and resuspension in fresh medium.

Nocodazole: 10 mg/ml in DMSO

Metaphase arrest in the presence of spindles (Cdc20 depletion)

In order to repress CDC20 gene expression, a galactose inducible promoter was integrated in front of the CDC20-ORF. In order to deplete CDC20-gene-expression, a logarithmically growing

culture was shifted from YPG to YPD medium. After a 3 h incubation at 23 °C, cells were large budded and arrested in metaphase.

Hydroxyurea (HU) arrest

To arrest a yeast culture in S-phase, HU was used at a final concentration of 100 mM. HU was added to a logarithmically growing culture at an OD_{578} of 0.3-0.5. After a 4 h incubation, more then 95% of the cells were arrested in S-phase with a bud. Cells were released from the arrest by washing and resuspension in fresh medium.

4.2.7 Depletion of NDC80-Expression

To deplete the expression of NDC80, the gene was put under the control of the galactose inducible Promotor (pGal1). The respective strain was grown at 25°C in YPGR (0.1% galactose, 2% Raffinose). The protein-levels of Ndc80 under these conditions were comparable to the wild-type situation. The cells were arrested in G_1-phase by the addition of α-factor. At the same time, the expression of NDC80 from the Gal1-promotor was repressed by the addition of 2% glucose. After 3 hours, the cells were pelleted by centrifugation (3000 rpm, 25°C, 3 min) and washed three times with glucose-containing media (YPD, 2% glucose). Finally, the cells were released at an OD of 0.2 in fresh YPD-medium and cultured at 25°C.

4.2.8 Mps1-overexpression

To overexpress Mps1, the gene was put under the control of the galactose inducible Promotor (pGal1). The respective strain was grown in YPR until mid logarithmic phase. The expression of Mps1 was induced by the addition of 2% galactose for 3 hours.

4.2.9 Nocodazole survival assay

Cells were grown to OD_{578}=0.2 in YPD at 25°C. 0.3 OD of the culture was harvested and pelleted (3000rpm/2min/RT). The pellet was resuspended in 1ml of YPD. Four 10-fold serial dilutions were prepared and 160µl of the last dilution was plated onto YPD (3 plates per timepoint) for the zero timepoint. Nocodazole (15µg/ml) was then added to the liquid culture, cells were incubated for an additional 2 h and 5 h at 25°C and 0.3 OD's were plated as described above. The viability

for each strain was determined by dividing the number of colonies formed after treatment with nocodazole for 2 h and 5 h by the number of colonies formed at the 0 h timepoint.

4.2.10 Quantification of Pds1-levels

5 OD_{578} of a yeast strain with 9myc-tagged Pds1 were harvested at different time points, lysed and the protein concentration was determined. For each time point, 40 µg total protein extract was analysed by SDS-PAGE and immunoblotting. Chemoluminescence was detected and quantified using a Fluor-STM-Multi Imager (BioRad) and the software Quantity One.

4.2.11 Dot spots for growth analysis

1 OD_{578} of logarithmically growing cells was harvested and resuspended in 1 ml of media. Four successive 1:10 dilutions were prepared and 4 µl of each dilution was spotted onto plates which were incubated at 23°C or 37°C. For the growth analysis on SDC + 5'-FOA plates, strains were grown in the logarithmic phase for 2 days in uracil containing media to eliminate the selection pressure for the URA3-plasmid.

4.2.12 Microscopy

All microscopy samples were analyzed on a Olympus fluorescence microscope. 1 ml of a logarithmically growing yeast culture was harvested, washed twice with water and resuspended in Non-Fluorescent Media (NFM). The sample was kept on ice until the microscopical evaluation. For a 3 dimensional resolution of spindles, 8 z stacks were acquired and maximal intensity projection was calculated using the CellR-software (Olympus).

Non-fluorescent media (NFM):
0.09% KH_2PO_4
0.023% K_2HPO_4
0.05% $MgSO_4$
0.35% $(NH_4)_2SO_4$
2% glucose
pH 5.5

4.2.13 FACS analysis

For each time point, 2 OD_{578} of cells were harvested and fixed o/n with 10 ml of 70% EtOH. Cells were washed with 50 mM Tris buffer pH 7.5, resuspended in 1 ml TrisHCl pH 7.5 supplemented with 2 mg RNAse and shaken for 4 h at 37 °C. The buffer was exchanged for 500 µl pepsin solution and the incubation continued for another 3 hours. For DNA staining, the sample was washed with 1 ml staining buffer and resuspended in 400 µl propidium iodide solution. The sample was diluted 1:50, so that 300 counts/sec were achieved and analysed with a FACS Calibur (Becton Dickinson). For a measurement, 30 000 events were counted at low flow rate. Data were evaluated with the CellQuestPro software. In the histograms, the x-axis is the relative DNA content determined by propidium iodide fluorescence, and the y-axis is the relative number of cells.

10 x RNAse:	10 mg/ml in 10 mM Tris/HCl pH 7.5 15 mM NaCl	Pepsin solution:	50 mg Pepsin 550 µl 1 N HCl in 9.5 ml H_2O pH 2-4
Staining solution:	180 mM Tris/HCl pH 7.5 180 mM NaCl 70 mM $MgCl_2$	Propidium iodide:	5 mg/ml (100 x) in staining solution

4.2.14 Chromatin immunoprecipitation - ChIP (adapted from Hecht et al. 1999)

At an OD_{578} of 0.5, 50 ml culture were harvested at 3 Krpm for 5 min, washed with 1 volume of water and fixed in 45 ml H_2O with 1.25 ml 37% formaldehyde. After shaking for 45 min at RT, cells were washed twice with 1 volume of PBS, resuspended in 1 ml PBS and transferred to a 2 ml tube. After one further centrifugation step, the pellet was resuspended in 200 ml lysis buffer, glass beads added to the meniscus and lysis was performed for 30 min at 4°C and 1800 rpm. The efficiency of the lysis was controlled by light microscopy. The tube was punctuated with a hot needle and set on top of a 15 ml tube. Glass beads were removed by centrifugation for 2 min at 1000 rpm/ 4°C and the lysate was sonicated (90 sec, 50 %, interval, 60 % output) in an ice/water bath in order to shear the genomic DNA. After transfer into a 1.5 ml tube, the sample was clarified for 30 min at 14 Krpm and 4°C. 20 µl of the supernatant representing the input were stored o/n at 4°C. The remaining supernatant was added to 10 µl of Protein A Sepharose CL-4B matrix and incubated o/n at 4°C with the respective antibody. The next day, beads were washed

3x with 200 µl lysis buffer, 2x with 200 µl WI and WII buffers respectively and once with 200 µl TE. In between each washing step, the beads were pelleted by centrifugation for 1 min at 1000 rpm. Elution was performed with 130 µl elution buffer for 10 min at 65°C. Beads were pelleted for 2 min at 14 Krpm and 120 µl of the supernatant decrosslinked for 6 h at 65°C. 100 µl elution buffer was added to the input from the previous day and also incubated for 6 h at 65°C. Proteins were digested in 120 µl TE with 15 µl proteinase K and 1 µg carrier DNA. After phenol extraction, the DNA was precipitated with 25 µl 5 M LiCl in 50 mM Tris/HCl pH 8 and 600 µl EtOH. The pellet was dried and resuspended in TE at a ratio of 1 OD/µl for the input and 0.2 OD/µl for the IP. 5 µl of a 1:40 dilution of the input and a 1:5 dilution of the IP were used as template for a triplex PCR with 3 different primer sets: ChrIII-1/2 (4 kb from CEN, 213 bp product), CEN3-12/13 (at the centromere, 243 bp product) and ChRIII-3/4 (1.9 kb from CEN, 321 bp product). dNTPs were added at a final concentration of 200 µM and the ratio of the primers varied from 0.3 µM to 1.2 µM, so that an equimolar amplification of all 3 products was achieved. 1.5 U polymerase (peqLab) was used for a 50 µl reaction. PCR products were separated on an 3% agarose gel with 1 x TAE as running buffer.

PBS:	140 mM NaCl 2.5 mM KCl 8.1 mM Na_2HPO_4 x $2H_2O$ 1.5 mM KH_2PO_4
Lysis buffer:	50 mM Hepes/KOH pH 7.5 140 mM NaCl 1 mM EDTA pH 8.0 1% Triton X100 0.1% NaDOC
Wash I (WI):	50 mM Hepes/KOH pH 7.5 500 mM NaCl 1 mM EDTA pH 8.0 1% Triton X100 0.1% NaDOC
Wash II (WII):	10 mM Tris/HCl pH 8.0 250 mM LiCl 1 mM EDTA pH 8.0 0.5% NaDOC 0.5% NP-40
TE:	10 mM Tris-HCl pH 8.0 1 mM EDTA pH 8.0
Elution buffer:	1% SDS in TE
Proteinase K:	10 mg/ml in 1 mM $CaCl_2$ 5 mM Tris/HCl pH 8.0
TAE -buffer:	242 g/l Tris 57.1 ml/l Glacial acid 100 ml/l 0.5 M EDTA pH 7.2

4.2.15 Epitopal tagging of genes

For epitopal tagging of endogenous yeast genes and for gene deletions, the PCR based method of Knop et al. (1999) was used. Integration cassettes were amplified by PCR with oligonucleotides containing an additional 50 bp adapter sequence required for genomic integration. Most of the tags used in this work were introduced at the C-terminus of the respective gene. PCR reactions and yeast transformations were performed as previously described. Integrations were verified by colony PCR, fluorescence microscopy or immunoblotting.

4.2.16 CEN5-GFP tagging (Michaelis et al. 1997)

For the visualisation of the yeast-kinetochore region, a GFP-tagged version of the tet-repressor (tetR-GFP) was transformed into the respective strain. In a second step, the tet-operater sequence (tetO) was integrated 1.4kb left of the centromere of chromosome V (CEN5). Since tetR-GFP binds to the tetO-sequence, the clustered kinetochores of *S. cerevisiae* can be detected by fluorescence microscopy as a distinct green signal.

4.2.17 Recycling of HIS3-marker (modified after Güldener et al. 1996)

In order to recycle the HIS3-marker flanked by loxP-sites, the yeast strain was transformed with a URA3-plasmid containing the GAL-inducible CRE-Recombinase (pSH47). For the expression of CRE, the strain was grown in SRC-URA at 30°C. At an OD_{578} of 0.5, galactose was added to the culture at a final concentration of 2% for 12 hours. 200 µl of a 1:100 dilution of the culture was plated onto a YPD-plate. After 3 days at 30°C, clones were checked for no growth on SDC-HIS. A positive clone was plated onto SDC + 5'-FOA to counterselect against the URA3-plasmid. The resulting strain was HIS^-.

4.2.18 Yeast glycerol stocks

For long time storage of *S. cerevisiae*, the respective strain was grown on a plate at the desired temperature. The cells were then scraped off the plate and resuspended in 15% glycerol, shock frozen in liquid nitrogen and finally stored at –80°C.

4.2.19 URA3/5'-FOA system

This positive/negative selection method is useful in the identification and selection of *Saccharomyces cerevisiae* strains that contain the mutant ura3-gene. URA3 encodes orotidine-5'phosphate decarboxylase, an enzyme which is required for the biosynthesis of uracil. $Ura3^-$ cells can be selected on media containing 5'-FOA. The $URA3^+$ cells are not viable because 5'-FOA is converted to the toxic compound 5-fluorouracil by the action of decarboxylase, whereas $ura3^-$ cells are resistant to the drug. The negative selection on 5'-FOA media is highly discriminating. Therefore, the URA3/FOA selection procedure can be used for expelling URA3-containing plasmids.

4.2.20 A system for the integration of an ndc80-mutant into the endogenous DNA-locus

In the first step, the endogenous NDC80-ORF was replaced by the HIS3-marker. The HIS3-marker is flanked by the NDC80-Promotor and NDC80-Terminator sequences which are needed for the integration by homologous recombination. Since NDC80 is essential, the strain contained a second NDC80 wild-type copy on a URA3-plasmid for viability (shuffle strain). The transformants were selected on SDC His^- plates. In the second step, the integration cassette containing the 3HA-tagged ndc80-mutant and the KANMX6-marker was transformed. This cassette recombines with the endogenous NDC80-Promotor and NDC80-Terminator, respectively. As a consequence, the HIS3-marker pops out of the NDC80-locus. Therefore, the cells were selected on YPD + KAN plates. Subsequently, the positive clones (KAN^+) were screened for "no growth" on SDC His^- plates. The resulting strain was grown on non-selective media for 3 days at 23°C to allow for the loss of the URA3-plasmid. Finally, cell which have spontaneously lost the URA3-plasmid were selected on SDC + 5'FOA plates (for details see 4.2.19). The correct integration of the ndc80-mutant was verified by α-HA Western-Blot and by colony-PCR using NDC80-specific primers (NDC80-16 & NDC80-13). The individual steps of this method are outlined in Figure 10.

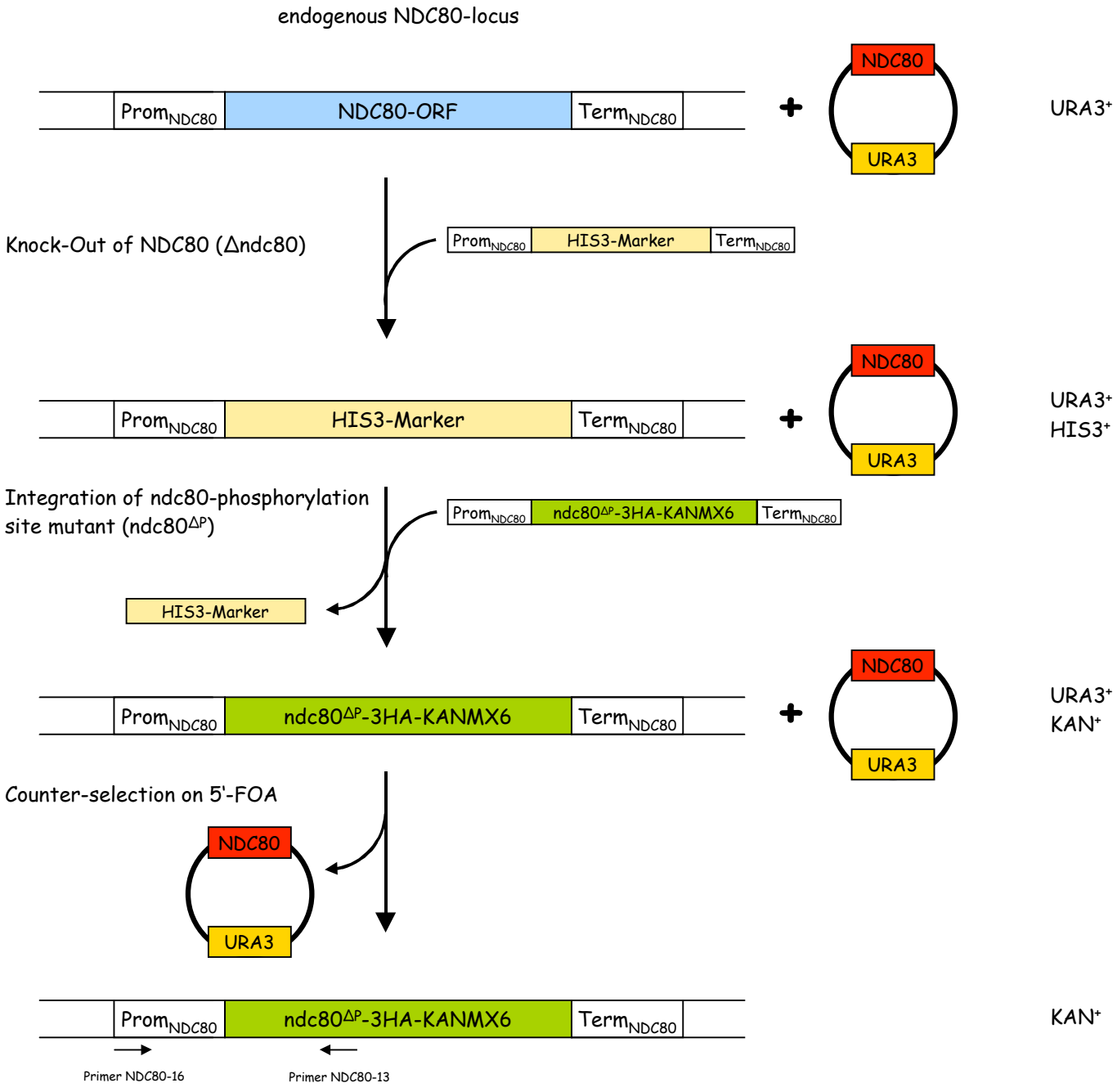

Figure 10: A system for the integration of an ndc80-mutant into the endogenous DNA-locus.

To integrate an ndc80-mutant into the endogenous NDC80-locus, the NDC80-gene was first knocked out by the insertion of the HIS3-marker in a strain which contained a second NDC80-copy on a URA3-plasmid. The resulting strain was transformed with the ndc80$^{\Delta P}$-integration cassette which included the KANMX6-marker. Both steps require the NDC80-Promotor and NDC80-Terminator sequences for the integration by homologous recombination. Positive clones were URA3^{+} HIS3^{-} and KAN^{+}. Finally, cells which spontaniously lost the URA3-plasmid were selected on SDC + 5'-FOA-plates and the correct integration of the ndc80$^{\Delta P}$-mutant was verified by α-HA Western-Blot and by colony-PCR using the indicated primers.

4.2.21 Expression and purification of HIS_{10}-tagged proteins from *E.coli*

For the recombinant expression of His_{10}-tagged yeast proteins, the respective plasmid was transformed into *E.coli*. 500 ml LB (+ 100 µg/ml Carbenicillin) were inoculated with 20 of the resulting colonies and grown to an OD_{578} of 0.3 at 37°C. After cooling the culture to the desired temperature, the expression of the protein was induced by the addition of 1mM IPTG for 3 hours at 18- 25°C depending on the expressed protein. After centrifugation at 5000 rpm for 20 min at 4°C, the cell pellet was resuspendet in 30 ml of binding buffer and lysed using a Microfluidizer. The lysate was clarified at 20 Krpm for 30 min at 4°C and the supernatant was incubated with 1 ml of pre-equilibrated NiNTA-agarose o/n at 4°C on a rotating wheel. The suspension was applied to a chromatography column (BioRad). After two subsequent wash steps (10 ml WashI, 10 ml WashII), the protein was eluted with 10 x 1 ml Elution buffer.

For the coexpression of two proteins (e.g. His_{10}-$Ndc80^{1-257}$ and Flag-Mps1), the respective plasmids (pBL941 and pSK1070) were co-transformed into *E.coli* and selected on $LB_{Amp/KAN}$ plates. The LB-culture was supplemented with 100 µg/ml Carbenicillin and 30 µg/ml Kanamycin.

Binding buffer:	20 mM TrisHCl pH 8.0 500 mM NaCl 5 mM Imidazole
WashI:	20 mM TrisHCl pH 8.0 60 mM Imidazole 500 mM NaCl
Elution buffer:	20 mM TrisHCl pH 8.0 500 mM NaCl 1 M Imidazole
WashII:	20 mM Tris/HCl pH 8.0 100 mM Imidazole 500 mM NaCl

4.3 Biochemical techniques

4.3.1 Yeast protein extracts

10-20 OD_{578} were harvested for 5 min at 3 Krpm and 4°C and washed with 1 ml ESB buffer. The pellet was resuspended in ESB-buffer at a concentration of 2 µl/OD and heated for 3 min at 95°C to denature the proteins and inactivate proteases and phosphatases. In order to lyse the cells, glass beads were added to the meniscus and shaken for 30 min at 4°C and 1800 rpm. After lysis, the tube was punctured with a hot needle and placed on top of a 15 ml tube and a centrifugation step for 3 min at 2.5 Krpm and 4°C followed. The lysate was transferred to a new 1.5 ml tube and clarified for 30 min at 14 Krpm and 4°C. The protein concentration of the supernatant was determined with the Bradford assay.

ESB buffer: 80 mM Tris/HCl pH6.8
2% SDS
10% Glycerol
1.5% DTT

4.3.2 Bradford

Protein concentration was determined after the method of Bradford (1976). To 1 µl sample and 99 µl of water, 900 µl of Bradford solution was added and incubated for 5 min at RT. The absorption of the sample was measured at 595 nm. To determine the concentration of the sample a standard curve with rabbit IgG ranging from 0 – 40 mg/ml was used.

5 x Bradford solution: 500 mg/l Coomassies Brilliant Blue G250
250 ml/l EtOH
500 ml/l H_3PO_4

4.3.3 SDS-PAGE

Separation of proteins by SDS polyacrylamide gel electrophoresis was performed according to the method of Laemmli (1970). 8-15% SDS-polyacrylamide gels were used depending on the size of the analysed protein.

Running buffer: 3 g/l Tris Base
14.2 g/l Glycin
1 g/l SDS

4.3.4 Coomassie staining

Coomassie staining of SDS-PAGE gels was performed as described in Cooper et al (1981). For staining of gels that were expected to contain weak bands (< 50 ng protein/band), the colloidal Coomassie solution RotiBlue (Roth) was used.

4.3.5 Western blotting

Proteins that were separated on a SDS polyacrylamid gel were transferred onto a PVDF membrane with a blotting apparatus from BioRad. The semi dry method of Kyshe-Andersen (1984) was used. The transfer took place at 15 V for 1 h. To check for equal protein loading, the membrane was stained with Ponceau S solution for 10 min at RT. The dye was removed by 2 wash steps with PBS for 5 min. The membrane was then blocked for 1 h at RT with blocking buffer and incubated 1 h with the primary antibody. After 3 washes with blocking buffer for 10 min, the secondary antibody was applied for another hour. The membrane was washed again 3 times for 10 min with blocking buffer and 2 x 5 min with assay buffer in order to adjust the pH for the following enzymatic reaction. For the visualization of the formed antibody complexes, the reaction of the alkaline phosphatase with the substrate CDP-Star was used. After 5 min incubation with the CDP-Star solution, the chemoluminescence could be detected on a film. After the Western Blot, the PVDF-membrane was stained with PVDF-Coomassie for a loading control.

primary antibodies: (in blocking buffer)	α-HA	1:1000
	α-myc	1: 500
	α-Flag	1:1000
	α-ProteinA	1:2500
	α-His	1:1000

secondary antibodies: (in blocking buffer)	α-mouse	1:5000
	α-rat	1:5000
	α-rabbit	1:5000

Blotting buffer:	5.8 g/l Tris Base 2.9 g/l Glycin 0.38 g/l SDS
5 x PBS:	51.5 g/l Na_2HPO_4 x $2H_2O$ 11.75 g/l NaH_2PO_4 x H_2O 20 g/l NaCl pH 7.4
Blocking buffer:	0.2% Casein 0.1% Tweeen-20 in 1 x PBS
Assay buffer:	0.1 M Diethanolamine 1 mM $MgCl_2$ pH 10

Ponceau S solution:	Ponceau S	1g
	glacial acetic acid	50ml
	H_2O	ad 1l

PVDF-Coomassie:	0.1% CoomassieBlueR250 10% glacial acetic acid 50% Methanol

4.3.6 TAP purification (adapted from Puig et al. 2001)

For isolation of TAP-tagged proteins with associated binding partners, the tandem affinity purification method was used. The TAP tag containes a Protein A domain and a Calmoduline Binding Peptide (CBP) separated by a TEV cleavage site. For one TAP purification, 1-4 l of yeast culture (OD_{587} of 1) were harvested for 15 min at 5 Krpm and 4°C. The pellet was washed with 50 ml of cold water and 25 ml of lysis buffer. At this step, the dry pellet could be frozen in liquid nitrogen and stored at –80°C. The next day, the pellet was thawed on ice and resuspended in lysis buffer including inhibitors at a concentration of 100 OD/ml. Cells were lysed with glass beads for 12 min at 4°C and 1800 rpm (using Pulverissette 6). The lysate was clarified at 20 Krpm and 4°C for 30 min and preequilibrated huIgG beads were added (10 µl of 50% slurry to 100 OD). After a 3 h to o/n rotation at 4°C, the beads were collected in a chromatography column (BioRad) and washed with 10 ml of Lysis buffer and TEV cleavage buffer, respectively. At this step, the complex was eluted from the beads by incubation with TEV protease. The TEV cleavage reaction (2.5 U TEV/1000 ODs) was performed in a Mobicol column in 200 µl buffer supplemented with 0.5 mM DTT for 4 h at 16°C on a turning wheel. The sample was eluted with a syringe into a new cup and incubated with preequilibrated Calmoduline-Sepharose for 1 hour at 4°C in 10 ml Lysis buffer + 2 mM $CaCl_2$. The column was washed twice with Lysis buffer + 2 mM $CaCl_2$ and finally eluted twice with elution buffer for 10 min at 30°C. All steps of the purification were performed in the presence of Protease- and Phosphatase-inhibitors.

Lysis buffer:	50 mM Tris/HCL pH 7.5 100 mM NaCl 1.5 mM $MgCl_2$ 0.075% NP40		TEV buffer:	50 mM Tris/HCl pH 7.5 100 mM NaCl 1.5 mM $MgCl_2$ 0.075% NP-40 0.5 mM DTT
Protease inhibitors: (final conc.)	E-64 Phenantroline Pepstatin Leupeptin PMSF	10 µM 1 mM 10 µg/ml 10 µM 2 mM	Elution buffer:	10 mM Tris/HCl pH 8 5 mM EGTA 50 mM NaCl
Phosphatase inhibitors: (final conc.)	Vanadate 5 mM Microcystin 50 nM NaF 10 mM β-glycerophosphate 100 mM			

4.3.7 TCA protein precipitation

To precipitate proteins, TCA was added to the solution at a final concentration of 10% and incubated on ice for 20 min. If the protein concentration was low (< 50 ng/ml), the sample was preincubated on ice with Na-deoxycholate at a final concentration of 0.015% before TCA addition. After a centrifugation step (30 min/ 4°C/ 14 Krpm), the protein pellet was resuspendet in 1x sample buffer and neutralised with NH_3 if necessary.

4.3.8 Kinase Assays

For the Mps1-kinase assays, either recombinant Ndc80 (approx. 50-150 ng of His_{10}-Ndc80 or His_{10}-$Ndc80^{1-257}$) or the whole Ndc80-complex (approx. 150 ng of protein) purified from yeast (via Spc25-TAP) were used as substrates. Mps1 was either affinity purified from yeast using the TAP-method or expressed and isolated from *E.coli* (His_{10}-Mps1). To demonstrate that Ndc80 is a direct substrate of Mps1 *in vitro*, the respective proteins were incubated together in kinase assay buffer, along with control reactions containing only substrate or only Mps1-kinase. The reactions were performed in a 50-100µl volume in the presence of 10 µCi [γ-^{32}P]-ATP (specific activity: 3000 Ci/mmol) and 10 µM cold ATP and incubated at 30°C for 60 min. Reactions were terminated by the addition of 10% TCA (final concentration) on ice. After a centrifugation step (30 min/ 4°C/ 14 Krpm), the precipitated proteins were resuspended in 1x sample buffer, boiled for 10 min at 70°C, and separated on a SDS-PAGE gel. The Coomassie stained gel was dried and exposed to a phosphorimager screen. The incorporation of ^{32}P was visualised using a phosphorimager and the QuantityOne software from Biorad.

For the identification of phorphorylation sites by mass spectrometry, kinase assays were performed in the absence of [γ-^{32}P]-ATP. Instead, 10 mM cold ATP was used. In addition, more substrate (approx. 2 µg of protein) was used and the reaction was incubated at 30°C for 3 hours.

kinase assay buffer: 50 mM TrisHCl 7.5
10 mM MgCl2
100 mM NaCl
0.5 mM DTT
1 mM PMSF

4.3.9 Sample preparation for the identification of phospho-sites by mass spectrometry

To identify the phosphorylated residues of Ndc80, the protein was cut out from the Coomassie-stained SDS-PAGE gel. The gel slice was treated according to the following protocol in order to produce a tryptic digest of the protein:

Wash: dH_2O (10 min /RT), shake
Shrink: acetonitrile (15 min /RT), shake
Reduce: 10 mM DTT in 100 mM NH_4HCO_3 (30 min /56°C), shake
Shrink: acetonitrile (15 min /RT), shake
Alkylate: 55 mM jodacetamide (20 min /RT), shake in the dark
Wash: 100 mM NH_4HCO_3 (15 min /RT), shake
Shrink: acetonitrile (15 min /RT), shake
Trypsin-digest: add 20 ng/µl TrypsinGold (on/37°C)

For the analysis by LC-ESI-Quadrupol-TOF, the pH of the tryptic digest was ajusted to pH 3 using formic acid and subsequently applied to the HPLC-system.
For the analysis by MALDI-TOF, the sample was adjusted to 5% formic acid and subsequently loaded onto a Poros Oligo R3-column. After two wash steps (20 µl 0.1% TFA) the sample was eluted directly onto the target using 0.8 µl DHB/PA-matrix (2,5- di-hydroxyl benzoic acid/phosphoric acid).

4.3.10 *in vitro* binding assay

In order to test for the physical interaction between His_{10}-$NDC80^{1-257}$ and Flag-MPS1, the two proteins were coexpressed in *E.coli* and metal-affinity-purified using NiNTA matrix as described (4.2.21).

5 RESULTS

In the past, several independent observations implicated that phosphorylation of the kinetochore may act as a signal regulating the activity of the spindle checkpoint.

Andreassen et al. (1992) showed, that cells treated with 2-aminopurine, a nonspecific kinase inhibitor, could escape mitotic arrest induced by microtubule inhibitors indicating that phosphorylation events are essential for the proper activation of the spindle assembly checkpoint. Using the so called "3F3/2-antibody" it was shown, that a phospho-epitop is present at the mammalian kinetochore and that kinetochore phosphorylation is dependent on the absence of tension across the mitotic spindle. This finding indicated that phosphorylation of a so far unidentified kinetochore substrate positively regulates the activity of the checkpoint control pathway (Cyert et al. 1988; Gorbsky and Ricketts 1993). One of the kinases which have been implicated in spindle checkpoint signalling is Mps1. Overexpression of Mps1 leads to a cell cycle arrest in mitosis (Hartwick et al. 1996) and Mps1-depleted cells do not undergo checkpoint arrest in response to microtubule depolymerisation by nocodazole (Stucke et al. 2002). It was shown that Mps1 transiently binds to the kinetochore in mammalian cells during mitosis (Stucke et al. 2002). This association is mediated by its amino-terminal, non-catalytic domain and specifically requires the presence of the Ndc80-complex (Stucke et al. 2004). In addition, Mps1 was found as a faint Coomassie-stained protein band in a Spc24-ProA pull down of yeast cells arrested in mitosis (C. Jaeger, unpublished results).

As mentioned in the introduction, the Ndc80-complex has been shown to take part in checkpoint control (Janke et al. 2001) and is required for the recruitment of the checkpoint proteins Mad1 and Mad2 to the kinetochore in mammalian cells (Martin-Lluesma et al. 2002).

Taken together, these data suggested that phosphorylation of the Ndc80-complex might regulate spindle checkpoint activity and that Mps1 is a candidate kinase which could be involved in this process. Therefore, the goal of the present work was to elucidate whether components of the *S. cerevisiae* Ndc80-complex are phosphorylated by Mps1 and if this phosphorylation has an influence on the regulation of the spindle checkpoint.

5.1 General characterisation of the Ndc80-complex

In the present work, the influence of Ndc80-complex phosphorylation on the activity of the spindle checkpoint in *S. cerevisiae* was investigated. The functional characterisation of Ndc80-phosphorylation depended strongly on the following biochemical and cell biological techniques.

5.1.1 TAP-purification of the Ndc80-complex

The efficient isolation of the Ndc80-complex by affinity chromatography was important to test the physical interaction between the Ndc80-complex and Mps1. Furthermore, the purified Ndc80-complex was used for *in vitro* kinase assays and for the identification of phosphorylation sites by mass spectrometry. The Ndc80-complex was shown to contain four proteins: Ndc80, Nuf2, Spc24 and Spc25 (Wigge et al. 2001; Janke et al. 2001). To confirm this finding and to isolate the Ndc80-complex for subsequent analyses, a wild-type strain containing SPC25-TAP was used to purify the Ndc80-complex by the Tandem-Affinity Purification (TAP) method (Figure 11, left panel). After the first purification step on IgG-agarose beads, the Ndc80-complex is present together with some contaminants and the TEV-protease which is used to elute the complex from the beads. After the second affinity step, only the members of the Ndc80-complex are eluted from the Calmoduline-matrix as a stable tetrameric complex. The right panel in Figure 11 shows a Coomassie stained SDS-Gel with the eluates from the two subsequent affinity purification steps.

5.1.2 Kinetochore localisation of the Ndc80-complex

Beside the biochemical isolation of the Ndc80-complex, the detection of the Ndc80-complex at the kinetochore *in vivo* was of major importance for the functional characterisation of its phosphorylation. As described in the introduction, the Ndc80-complex was shown to be part of the *S. ceresisiae* kinetochore (Wigge et al. 2001; Janke et al. 2001). In the present thesis, two methods were used to detect the Ndc80-complex at the kinetochore: fluorescence microscopy and ChIP-analysis.

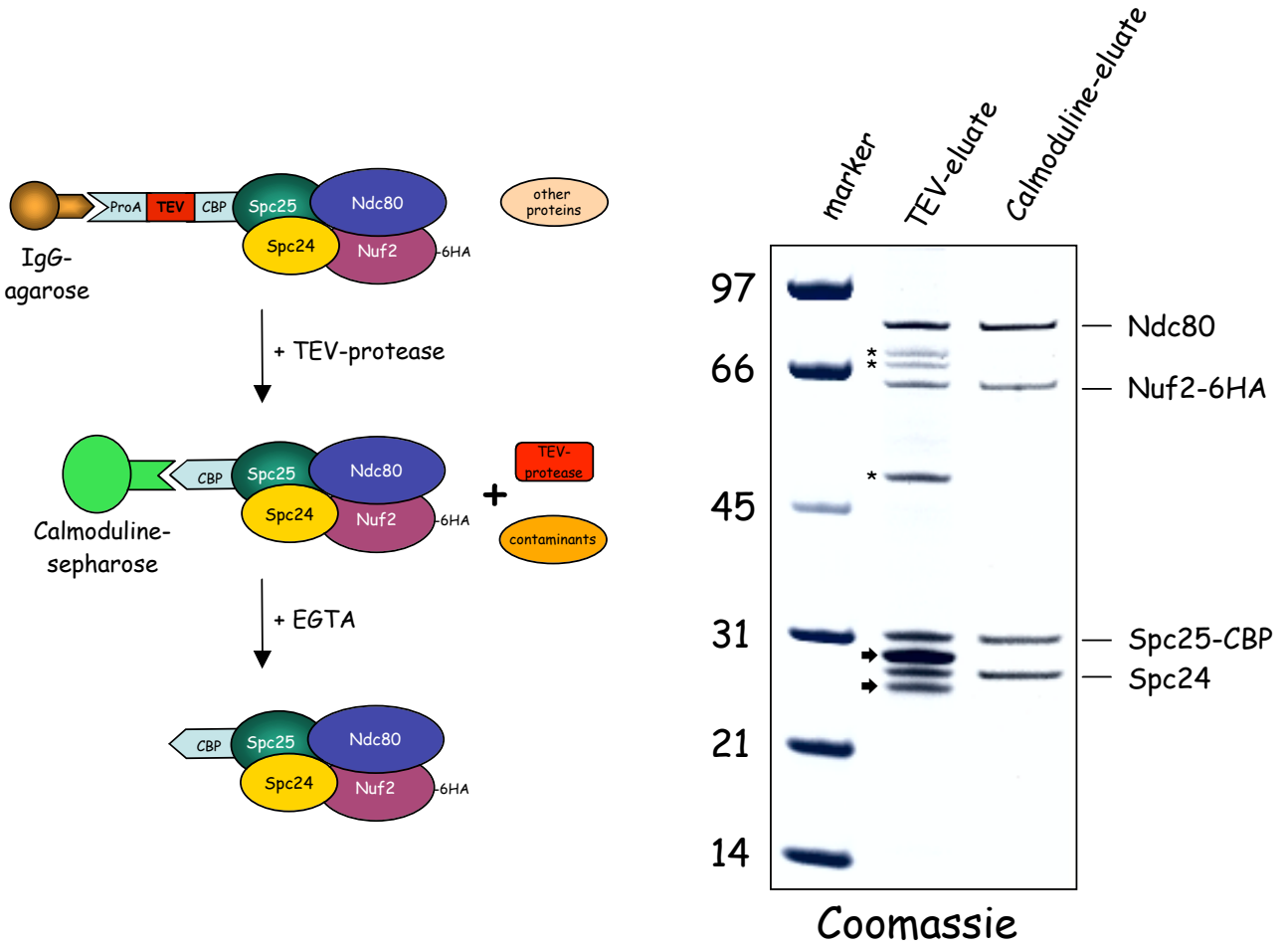

Figure 11. Ndc80 forms a tetrameric complex with Nuf2 and Spc24/Spc25 (Ndc80 complex).

The Ndc80-complex was purified from the yeast strain YAW427 (SPC25-TAP NUF2-3HA) using the Tandem Affinity Purification (TAP) method in two subsequent affinity steps with Spc25-TAP as a bait (left panel). A Coomassie stained SDS-Gel of the separated complex is shown (right panel). The individual proteins were cut out and identified by mass spectrometry. The sizes of the molecular weight markers are indicated on the left. Contaminants are marked with a star, TEV protease runs in two bands and is indicated by ➡.

To visualise the Ndc80-complex at the kinetochore by fluorescence microscopy, a strain containing Ndc80-Cherry was grown to mid-logarithmic phase and subsequently analysed. As shown in Figure 12A, Ndc80-Cherry specifically co-localises with the kinetochore protein Nsl1 throughout the different phases of the cell cycle.

A second method which was used to analyse the kinetochore localisation of the Ndc80-complex is the ChIP assay. In this assay, proteins that bind to chromatin directly or indirectly are

covalently crosslinked to DNA using formaldehyde. The genomic DNA is then sheared by sonication and the particular protein of interest is immuno-precipitated using a specific antibody. If the analysed protein is associated with the DNA, this particular region can be detected by PCR using specific primers. In this case, the association of Ndc80 with centromeric DNA was analysed. Two regions flanking the centromere were used as negative controls in a triplex PCR-reaction. The kinetochore localisation of the Ndc80-complex was analysed using a wild-type strain expressing Ndc80-9myc. The α-Ndc80 ChIP shows that Ndc80 is associated with CEN-DNA (Figure 12B, lanes 1 and 2). The control ChIP (α-myc) indicates that this interaction is specific (Figure 12B, lanes 3 and 4). In both cases, the centromeric DNA was enriched in the triplex DNA which confirms the kinetochore association of Ndc80. The two DNA regions flanking the centromere were not amplified in the immunoprecipitates indicating efficient shearing of the chromatin and the specificity of the observed interaction.

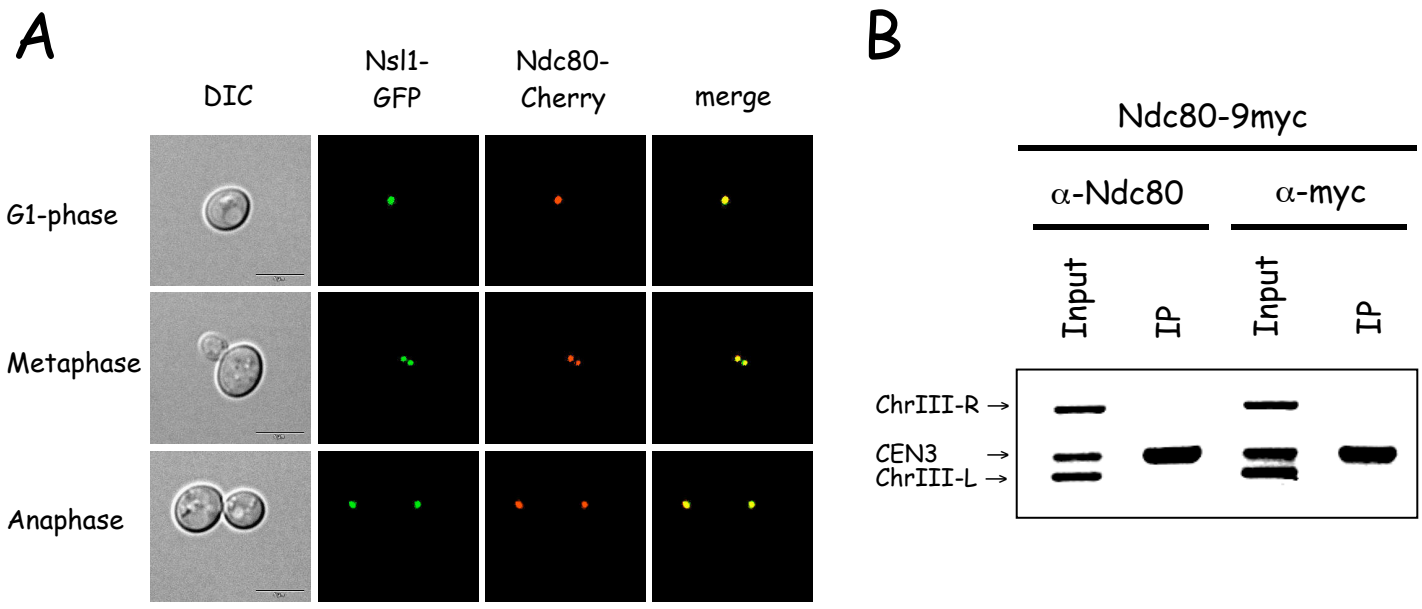

Figure 12. The Ndc80-complex is part of the *S. cerevisiae* kinetochore.

(A) *Ndc80 localises to the kinetochore.* The subcellular localisation of Ndc80 was analyzed by fluorescence microscopy in YSK1175 (Ndc80-Cherry Nsl1-GFP). Nsl1-GFP serves as a kinetochore marker. Scale bar, 5 µm.

(B) *Ndc80 specifically associates with centromeric DNA.* Wild-type cells containing Ndc80-9myc were analysed by Chromatin immunoprecipitation (CHIP). Ndc80-9myc was precipitated using two different antibodies. The first one was a polyclonal antibody directed against full length Ndc80 (α-Ndc80). As a control, Ndc80-9myc was immunopreciptated using the monoclonal α-myc antibody. The presence of CEN3 DNA and two flanking sequences (ChrIII-R and ChrIII-L) was analysed by triplex PCR.

5.2 Interaction between the Ndc80-complex and Mps1

5.2.1 Mps1 physically interacts with the Ndc80-complex *in vivo*

As described above, there is evidence that the Ndc80-complex is involved in spindle checkpoint control and that Mps1-overexpression leads to mitotic arrest most likely through checkpoint activation (see Introduction 1.4.2). In addition, endogenous Mps1 has been shown to interact weakly with the Ndc80-complex (C. Jaeger, unpublished results). To test whether Mps1 interacts with the Ndc80-complex in response to checkpoint activation by Mps1-overexpression (Figure 13A), the Ndc80-complex was affinity purified via Spc24-ProA after transient overexpression of Mps1 from the Gal-promoter (pGal-MPS1-myc). After acid elution of the complex, the proteins were subjected to SDS-PAGE and visualised by Coomassie staining (Figure 13B, right panel). The resulting protein bands were analysed by mass spectrometry. A band migrating around 90 kDa was identified as Mps1-myc which shows that Mps1 co-precipitates with the Ndc80-complex when the spindle checkpoint is activated by Mps1-overexpression. These data are consistent with the detection of small amounts of endogenous Mps1 in a Spc24-ProA pull down (C. Jaeger, unpublished results). However, they do not indicate whether Mps1 associates with the kinetochore bound Ndc80-complex or with the soluble Ndc80-complex.

5.2.2 The Mps1 kinase weakly associates with the *S. cerevisiae* kinetochore *in vivo*

It was shown that Mps1 transiently localises to the kinetochore in mammalian cells (Stucke et al. 2002; Howell et al. 2004). In yeast however, the kinetochore localisation of Mps1 could not be shown so far. The first attempt to investigate the subcellular Mps1-localisation was the analysis of Mps1-GFP by fluorescence microscopy. This way, no clear localisation pattern could be observed. To increase the strength of the fluorescent signal, Mps1 was tagged with 3xGFP at the C-terminus which did not improve the situation significantly. Only background staining could be observed. The fact that Mps1 could not be detected at the kinetochore by fluorescence microscopy can be explained by its extremely low protein-levels. In addition, bleaching of the fluorescent GFP-fusion protein and the transient nature of the interaction of kinases with their

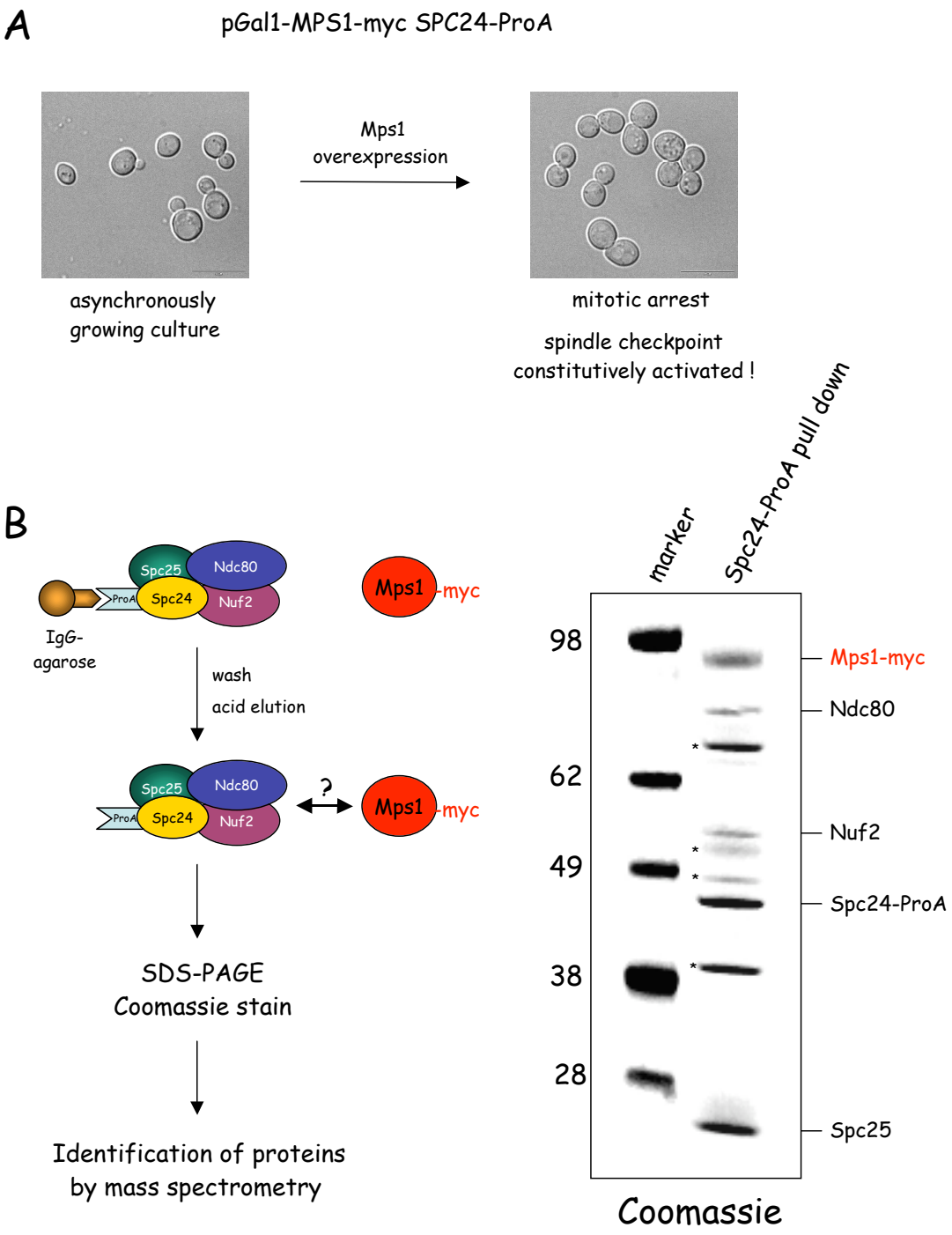

Figure 13. Mps1 physically interacts with the Ndc80-complex *in vivo*.

(A) Mps1-myc was overexpressed from the Gal1-promoter in a strain containing pGal1-MPS1-myc and SPC24-ProA. Cells arrested in mitosis with a large bud and a permanently active spindle checkpoint (DIC, Scale bar, 10 µm).

(B) Cells were treated as described in (A), the Ndc80-complex was isolated via Spc24-ProA by a single affinity purification step and separated by SDS-PAGE (left). The bands were excised from the Coomassie stained gel (right) and the proteins were identified by mass spectrometry. Contaminants are marked with a star.

substrates makes the analysis even more difficult. Furthermore, microscopical studies are focused on individual cells. In order to investigate the potential kinetochore-localisation of Mps1 with a more sensitive method, a ChIP assay was performed. In contrast to microscopical studies, the kinetochore-association of Mps1 is analysed starting from 50 ODs of cells and thus from a higher amount of protein. Another advantage of the ChIP-assay over microscopical analyses is the fact that protein-protein and protein-DNA interactions are covalently crosslinked using formaldehyde. Therefore, a potential transient association of Mps1 with the kinetochore is frozen at a particular point in time. This association can then be studied without having the problem of continuous association and dissociation of Mps1 from the kinetochore. In addition, the detection of CEN-DNA by PCR adds another amplification step to the analysis. Therefore, a ChIP-assay is more sensitive than fluorescent detection systems.

The kinetochore association of Mps1 in yeast was analysed by ChIP in a strain containing Mps1-9myc. Ndc80-9myc served as a positive control. As shown in Figure 14, the kinase Mps1 weakly associates with centromeric DNA. Together with the data from the Spc24-ProA pull down experiment (Figure 13), this finding shows that Mps1 is physically linked to the kinetochore via the Ndc80-complex. This result is consistent with the observations made in the mammalian system.

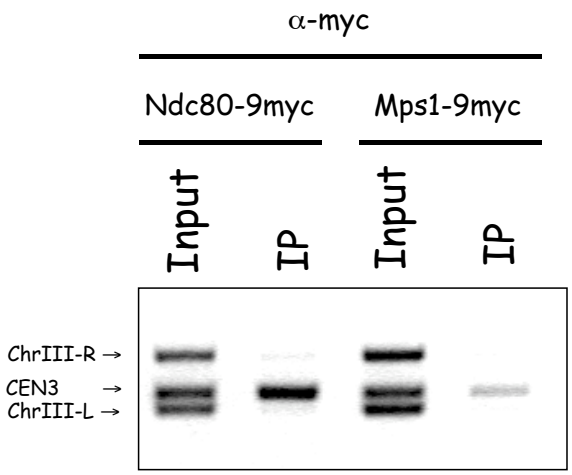

Figure 14. Mps1 weakly associates with centromeric DNA *in vivo.*

CHIP assay. Wild-type cells containing NDC80-9myc or MPS1-9myc were analysed by Chromatin immunoprecipitation (CHIP). α-myc antibody was used for immunoprecipitation. The presence of CEN3 DNA and two flanking sequences (ChrIII-R and ChrIII-L) was analysed by triplex PCR.

5.3 Phosphorylation of Ndc80 by Mps1

5.3.1 Mps1 directly phosphorylates Ndc80 *in vitro*

To examine whether one of the members of the Ndc80-complex is a direct substrate of Mps1, *in vitro* kinase assays were performed. Mps1-TAP was expressed in yeast and affinity purified by the Tandem-Affinity Purification (TAP) method. The Coomassie stained gel shows that Mps1 could be efficiently isolated to a high degree of purity after the second affinity step (Figure 15A). The yeast Ndc80-complex was purified with Spc25-TAP as a bait (Figure 11) and used as a substrate. The respective autoradiograph (10 min exposure) in Figure 15B shows that Ndc80 is directly phosphorylated by Mps1. After over night exposure to the phosphorimager screen, weak signals could also be observed for the other members of the complex (Nuf2, Spc24 and Spc25; data not shown). This result clearly shows that Ndc80 is the main target for Mps1. Furthermore, Mps1 autophosphorylation indicates that the isolated kinase is highly active.

To confirm the specificity of Ndc80-phosphorylation by Mps1 and to exclude that co-purifying factors from yeast contribute to the phosphorylation of Ndc80, Mps1-kinase assays were performed using recombinant Ndc80 as substrate. As described previously, the Ndc80 protein contains coiled-coil regions in the C-terminal part of the protein and a globular domain at the N-terminus (Figure 8). The coiled-coil stretch is known to promote the physical interaction between Ndc80 and Nuf2. In contrast, the function of the N-terminus is poorly understood. It was therefore tempting to speculate whether the N-terminus is the main target for phosphorylation by Mps1. Beside the His_{10}-tagged Ndc80-full length protein (His_{10}-Ndc80), a fragment containing the N-terminal tail and the HEC-domain (His_{10}-$Ndc80^{1-257}$) was expressed in *E.coli* and purified using metal-affinity purification (NiNTA-matrix). The respective autoradiograph shown in Figure 15C confirms that Ndc80 is a direct substrate of Mps1 *in vitro*. Mps1 phosphorylates both the full length protein and the N-terminal globular fragment of Ndc80 (His_{10}-$Ndc80^{1-257}$). The phosphorylation of His_{10}-$Ndc80^{1-257}$ can also be observed on the Coomassie level since the respective protein band shifts up in response to Mps1-CBP addition. Besides His_{10}-$Ndc80^{1-257}$, two more N-terminal Ndc80 fragments (His_{10}-$Ndc80^{1-116}$ and His_{10}-$Ndc80^{47-257}$) were tested. Both fragments are phosphorylated by Mps1 *in vitro* (data not shown).

A second potential source of impurities is the Mps1-kinase preparation (Figure 15A). Although it is highly pure on the Coomassie level, it could still contain a regulatory factor or activating kinase which co-purifies together with Mps1 in sub-stoichiometric amounts and contribute to Ndc80-phosphorylation. To exclude this possibility, kinase assays were performed using His_{10}-Mps1 expressed in *E.coli* and metal-affinity purified via its His_{10}-tag. Recombinant His_{10}-Mps1 strongly autophosphorylates itself in *E. coli* demonstrating that it is highly active. When Ndc80-complex (from yeast) or recombinant Ndc80 (His_{10}-Ndc80, His_{10}-$Ndc80^{1-257}$, His_{10}-$Ndc80^{1-116}$ and His_{10}-$Ndc80^{47-257}$) were used as substrates in an *in vitro* His_{10}-Mps1-kinase reaction, Ndc80 was phosphorylated in the same way as when Mps1-CBP from yeast was used (data not shown). This result confirms that the phosphorylation of Ndc80 by Mps1 is specific and direct.

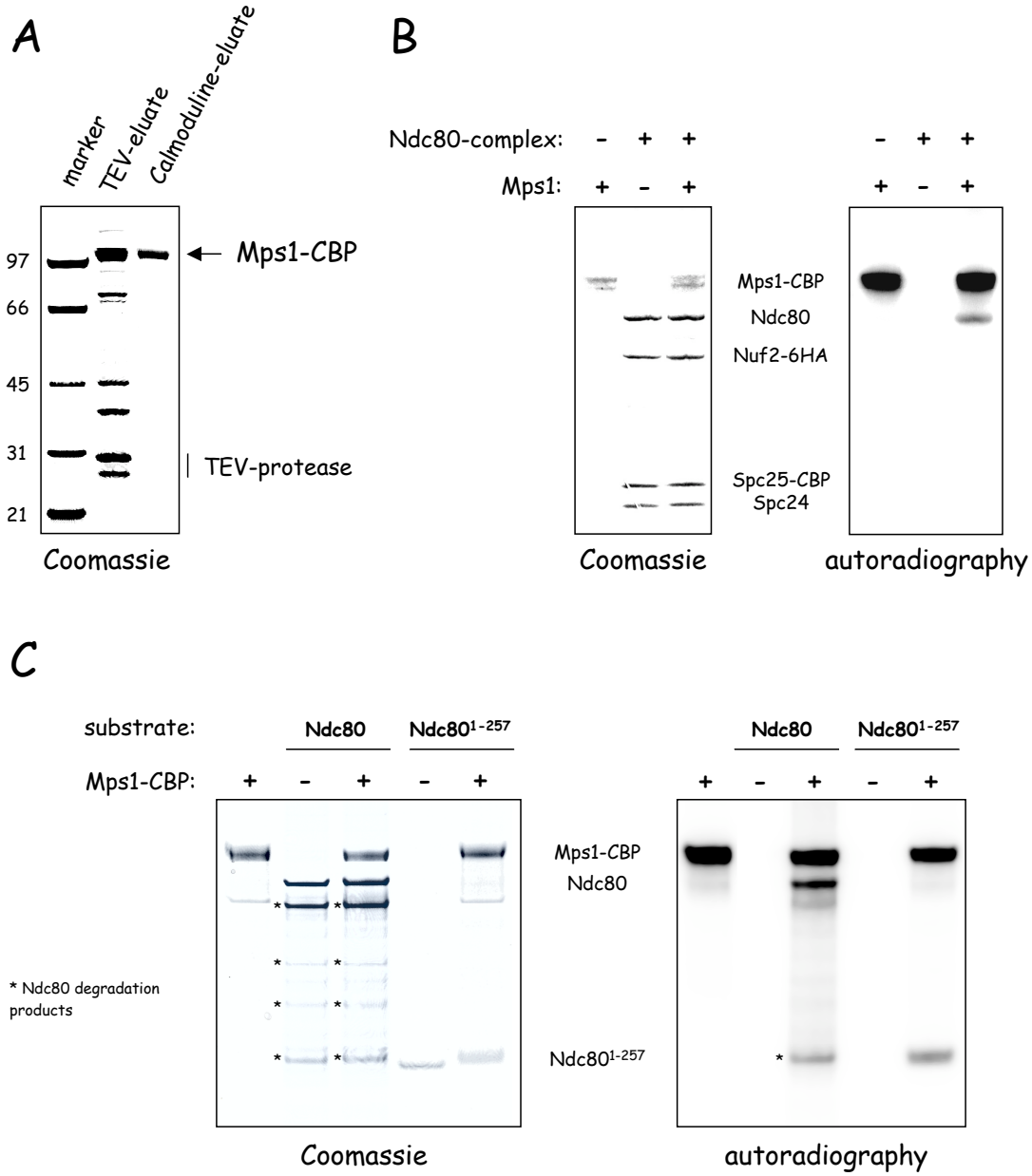

Figure 15. Mps1 specifically phosphorylates Ndc80 *in vitro.*

(A) *TAP-purification of Mps1 from S. cerevisiae.* To isolate sufficient amounts of Mps1 from yeast, a strain containing Gal1-Mps1-TAP on a high copy 2µ-plasmid was grown in raffinose containing media to mid-log phase. Overexpression of Mps1-TAP was subsequently induced by the addition of 2% galactose for 4.5 hours. Mps1-TAP was then affinity purified in two subsequent steps via its TAP-tag and the eluates were analysed by SDS-PAGE. The Coomassie stained proteins were isolated from the gel and identified by mass spectrometry. Highly pure Mps1-CBP was used in the kinase assays (B and C).

(B) *Mps1 specifically phosphorylates Ndc80 but not the other members of the Ndc80-complex.* The indicated combinations of purified proteins were incubated for 60 min at 30°C in the presence of [γ-^{32}P]-ATP and phosphorylation events were assayed by autoradiography after SDS-PAGE.

(C) *Mps1 specifically phosphorylates recombinant His_{10}-Ndc80 and His_{10}-Ndc80$^{1-257}$.* The indicated combinations of purified proteins were incubated for 60 min at 30°C in the presence of [γ-^{32}P]-ATP and phosphorylation events were assayed by autoradiography after SDS-PAGE.

5.3.2 Mps1 physically interacts with Ndc80$^{1-257}$ *in vitro*

Since Mps1 interacts with the Ndc80-complex *in vivo* and directly phosphorylates the N-terminus of Ndc80, the physical interaction of Mps1 and Ndc80$^{1-257}$ was analysed in an *in vitro* binding assay using recombinant proteins. Flag-Mps1 and His$_{10}$-Ndc80$^{1-257}$ were co-expressed in *E. coli* and purified on a NiNTA matrix. The association of Flag-Mps1 with His$_{10}$-Ndc80$^{1-257}$ was then tested by immunoblotting. As shown in Figure 16 (lane 3 and 4), Flag-Mps1 specifically co-precipitates with the N-terminus of Ndc80 (His$_{10}$-Ndc80$^{1-257}$). Only background binding of Flag-Mps1 to the beads could be detected (lanes 1 and 2) which shows that the interaction between Flag-Mps1 and His$_{10}$-Ndc80$^{1-257}$ is specific. In addition, the association of Flag-Mps1 with the Ndc80/Nuf2- or Spc24/Spc25-dimer was tested. Flag-Mps1 was found to bind to Ndc80/Nuf2 but not to Spc24/Spc25 (data not shown) confirming the high specificity of the interaction.

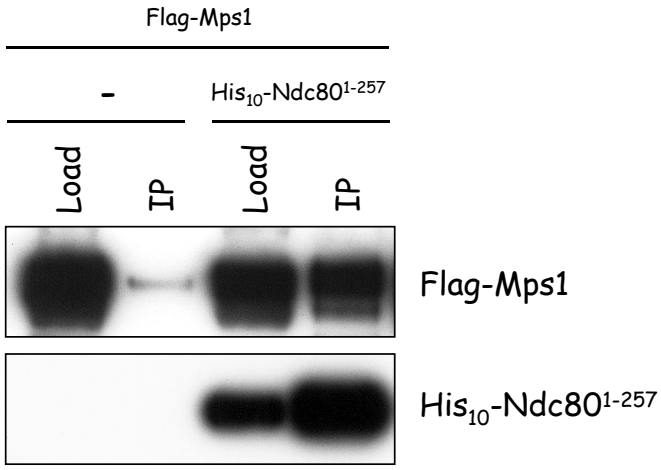

Figure 16. Mps1 physically interacts with Ndc80$^{1-257}$ *in vitro*.

His$_{10}$-Ndc80$^{1-257}$ and Flag-Mps1 were co-expressed in *E. coli* and purified using metal-affinity chromatography (NiNTA-matrix). As a control, Flag-Mps1 alone was expressed and tested for unspecific binding to the NiNTA-beads. Lysates and eluates were separated by SDS-PAGE and immunoblotted using monoclonal α-His antibody (His$_{10}$-Ndc80$^{1-257}$) and α-flag (Flag-Mps1).

5.3.3 Phosphorylation of Ndc80 depends on Mps1 *in vivo*

The phosphorylation of Ndc80 by Mps1 and their physical interaction were observed *in vitro*. To check the *in vivo* relevance of these findings, the phosphorylation pattern of Ndc80 in a yeast strain overexpressing Mps1 was analysed. A strain containing NDC80-3myc and pGal1-MPS1-

TAP was grown in raffinose containing media to mid-log phase. After the induction of Mps1-overexpression from the Gal1-promoter, whole cell extracts were prepared and Ndc80-3myc (α-myc) and Mps1-TAP (α-ProteinA) were detected by immunoblotting. As shown in Figure 17, Ndc80-3myc can be detected in a slower and in a faster migrating form when Mps1 is overexpressed. The slower migrating species was sensitive to treatment with calf intestinal phosphatase (Figure 17, lane 3) indicating that the post-translational modification of Ndc80 in response to Mps1-overexpression is due to phosphorylation.

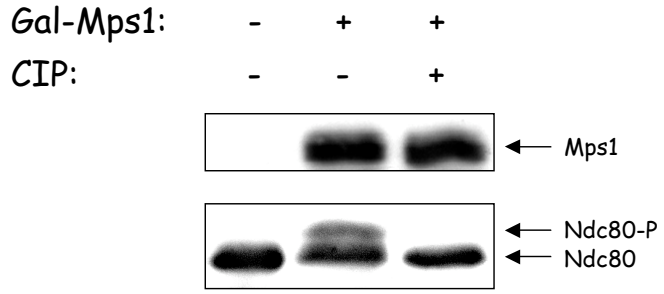

Figure 17. Phosphorylation of Ndc80 is dependent on Mps1 *in vivo*.

The yeast strain YSK658/pSK950 (NDC80-3myc pGal1-MPS1-TAP) was grown in YPR to mid log phase. Expression of Mps1-TAP from the Gal1-promoter was induced by the addition of galactose. Crude protein extracts were prepared and incubated with buffer only (lane 1 + 2), or with calf intestinal phosphatase (CIP, lane 3) for 1 hour at 30°C. Samples were analysed by immunoblotting using α-ProteinA to monitor Mps1-TAP expression and α-myc antibody for the detection of Ndc80-3myc.

5.4 Identification of Ndc80-phosphorylation sites by mass spectrometry

5.4.1 Strategy

As the previous experiments show, phosphorylation of Ndc80 depends on Mps1 *in vivo*. To analyse the influence of Ndc80-phosphorylation on the regulation of the spindle checkpoint, phosphorylation sites within Ndc80 should be identified and mutated either to Alanine (Ala, A) to abolish phosphorylation or to Aspartic Acid (Asp, D) to mimic the negative charge which is created by phosphorylation. Using these phosphorylation site mutants as an experimental tool, the phenotypic effects of non-phosphorylated or constitutively phosphorylated Ndc80 should be examined *in vivo*.

The first approach to identify Ndc80-phosphorylation sites were *in vitro* kinase assays using Mps1-kinase purified from *S. cerevisiae* (Mps1-CBP) and either the whole Ndc80-complex purified from *S. cerevisiae* (Figure 11) or recombinantly expressed Ndc80 (His_{10}-Ndc80 or His_{10}-$Ndc80^{1-257}$) as substrates (Figure 18, left). An example of a Coomassie stained gel is shown in Figure 18. The protein bands were isolated from the gel and subsequently analysed by mass spectrometry to identify the phosphorylated residues within Ndc80 (Figures 19-21).

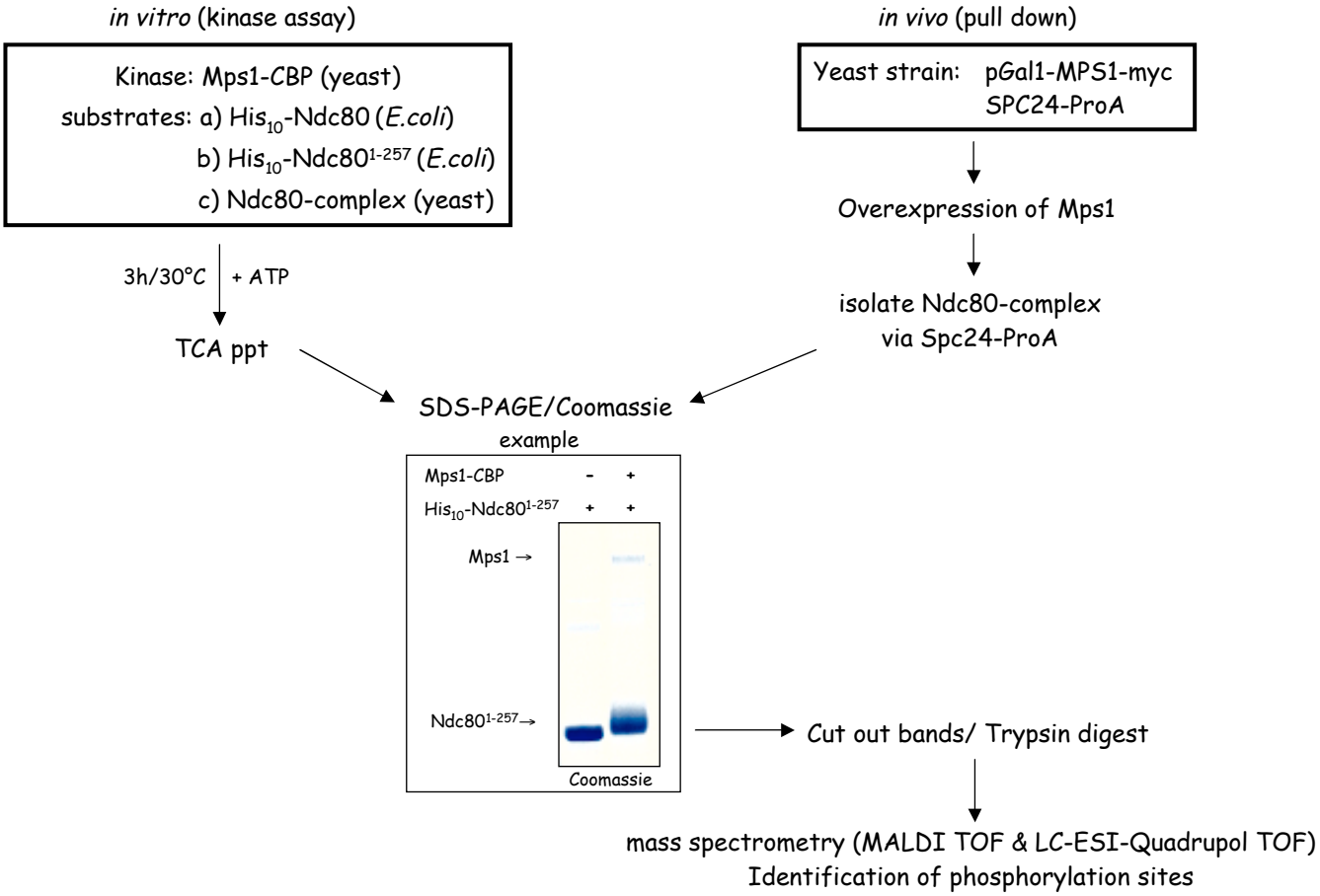

Figure 18. Mapping the *in vitro* and *in vivo* phosphorylation sites of Ndc80 by mass spectrometry.

To identify the Mps1-dependent phosphorylation sites of Ndc80 *in vitro*, kinase assays with Mps1 and either recombinant substrates (His_{10}-Ndc80 or His_{10}-$Ndc80^{1-257}$) or the whole Ndc80-complex purified from yeast were performed (left). The indicated substrates were incubated with purified Mps1-CBP in the presence of 10 mM ATP for 3 hours at 30°C. The kinase reactions were terminated by the addition of 10% TCA and the proteins were resolved by SDS-PAGE. The Coomassie stained bands were cut out and analysed by mass spectrometry for the identification of phosphorylation sites. An example of a Coomassie stained SDS-PAGE gel with His_{10}-$Ndc80^{1-257}$ as a substrate is shown. To identify the *in vivo* phosphorylation sites of Ndc80 in yeast, Mps1 was overexpressed from the Gal1-promoter and the Ndc80-complex was isolated using Spc24-ProA as a bait (right). The complex was separated by SDS-PAGE and subsequently analysed by mass spectrometry.

In total, 35 sites were identified of which 31 are located in the globular N-terminus of Ndc80. Four additional sites are placed in the coiled-coil regions in the C-terminal part of the protein (Figure 19). The identified *in vitro* phosphorylation sites are indicated in Table 2. To confirm the

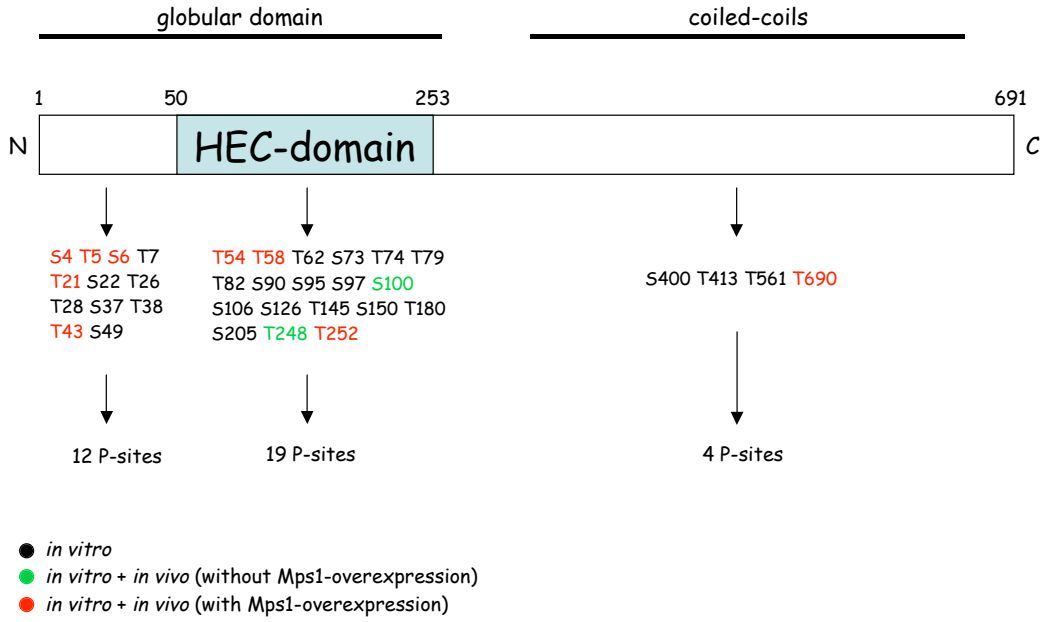

Figure 19. Distribution of the identified *in vitro* and *in vivo* Ndc80-phosphorylation sites.

Ndc80 is predominantly phosphorylated in the N-terminal, globular part of the protein. Numbers of phosphorylated residues refer to their position in the protein.

identified phosphorylation sites *in vivo*, the Ndc80-complex was purified from yeast via Spc24-ProA after transient overexpression of Mps1 (Figure 13). As a control, the Ndc80-complex was purified without Mps1-overexpression. The proteins were separated by SDS-PAGE and the gel was Coomassie stained. The bands were isolated from the gel and analysed by mass spectrometry. From this analysis, 11 phosphorylation sites which were initially identified *in vitro* could be confirmed *in vivo* (Figure 19 & Table 2).

Two of them were present independent of Mps1-overexpression. Whether these two sites are phosphorylated by endogenous Mps1 or by another kinase is not known. The remaining 9 *in vivo* sites could only be identified after Mps1-overexpression and are therefore clearly dependent on Mps1-kinase activity. Table 2 summarises the results from the analyses.

	in vitro (kinase assays)			*in vivo* (pull down)
Substrate:	His_{10}-Ndc80 (*E.coli*)	His_{10}-$Ndc80^{1-257}$ (*E.coli*)	Ndc80 complex (yeast)	Ndc80 complex (yeast)
Kinase:	Mps1-CBP (yeast)	Mps1-CBP (yeast)	Mps1-CBP (yeast)	Mps1-myc (overexpressed, yeast)
S4	P or T5 S6 T7	P or T5 S6 T7	P or T5 S6 T7	P or T5 S6 T7
T5	P or S4 S6 T7	P or S4 S6 T7	P or S4 S6 T7	P or S4 S6 T7
S6	P or S4 T5 T7	P or S4 T5 T7	P or S4 T5 T7	P or S4 T5 T7
T7	P or S4 T5 S6	P or S4 T5 S6	P or S6	
T21	P	P	P	P
S22	P or T21	P or T21		
T26	P	P		
T28	P	P		
S37	P or T38	P or T38	P or T38	
T38	P	P	P or S37	
T43	P	P	P	P
S49	P	P		
T54	P	P	P	P
T58	P	P	P	P
T62	P	P		
S73	P or T74	P or T74		
T74	P or S73	P or S73		
T79	P	P		
T82	P	P		
S90	P	P		
S95	P	P		
S97	P or S95	P or S95		
S100	P	P	P	P
S106	P	P		
S126	P	P		
T145	P	P		
S150	P	P		
T180	P	P		
S205	P	P		
T248	P	P	P	P
T252	P	P	P	P
S400	P			
T413	P			
T561	P			
T690	P		P	P

Table 2. *In vitro* and *in vivo* phosphorylation sites of Ndc80.

In total, 35 phosphorylation sites were identified *in vitro* (black). 11 of these sites were confirmed *in vivo* out of which 9 depended on Mps1-overexpression (red). Two of the *in vivo* sites were present before Mps1-overexpression (green). The numbers of phosphorylated residues refer to their position in the protein. (P = phosphorylated).

All identified sites are either Serine (Ser, S) or Threonine (Thr, T) residues. It was described that Mps1 is a dual specific kinase (Lauze et al. 1995) meaning that it can also phosphorylate Tyrosine (Tyr, Y) residues. However, for Mps1-dependent phosphorylation of Ndc80, phospho-Tyrosine residues were not identified. It should be noted that in some instances, the phosphate group could not be asigned to a specific residue. For the phospho-peptide including the residues S73, T74, T79 and T82 for example, not all sites could be unambiguously identified as phospho-residues. The phosphorylation of the residues T79 and T82 was confirmed by fragmentation. These sites are therefore clearly phosphorylated. In the case of the remaining residues S73 and T74, it was not possible to specify which of the two residues carries the phosphate group. Furthermore, it is not possible to tell if only one residue is phosphorylated or if both of the residues carry a phosphate group on alternative molecules. Therefore, the number of phosphorylated residues might actually be lower than 35. The minimum number of identified sites is 29. These sites could unambiguously be detected. The identified Ndc80-phosphorylation sites are indicated in Table 2. Furthermore, a given phosphorylated peptide did not necessarily carry all the identified phosphate groups on one single molecule. Some of the phospho-peptides could be detected in their mono-phosphorylated form (peptide containing S100 and S106), others also in their di-phosphorylated (peptide containing S37, T38 and T43) or tri-phosphorylated state (peptide containing S4, T5, S6 and T7). Consequently, a given Ndc80-molecule is not necessarily phosphorylated on all of the 35 identified Serine- and Threonine-residues.

5.4.2 Identification of Ndc80-phosphorylation sites by MALDI-TOF

To identify a phosphorylated Ndc80-peptide, the respective protein band was isolated from the Coomassie-stained SDS-PAGE gel and digested with the protease trypsin which cleaves the polypeptide chain after Arginine and Lysine residues. This proteolytic digest results in a mixture of Ndc80-peptides which is subsequently desalted by a C18-ZipTip and applied to a target carrying a particular matrix (α-Cyano-4-hydroxy-cinnamic acid, CCA). The peptides are then ionised by a laser and move through the mass analyser (TOF). Finally, the mass of the peptides is meassured by a detector (Figure 20A). In the resulting peptide mass spectrum, the masses of potential Ndc80-phosphopeptides can be observed. The example in Figure 20B shows the identification of the masses of a particular Ndc80-peptide (SLINQNTQEITILSQPLK) in its non-

phosphorylated and phosphorylated form. If the intensity of a particular peak was high enough, the corresponding Ndc80-phosphopeptide was directly fragmented and thus confirmed.

In many cases however, the intensity was too low. However, from the presence of a particular mass alone one cannot finally conclude that it indeed correspond to the expected Ndc80-peptide. To aquire sequence information and identify the phosphorylated residue, the phophopeptide was fragmented by a LC-ESI-Quadrupole-TOF system.

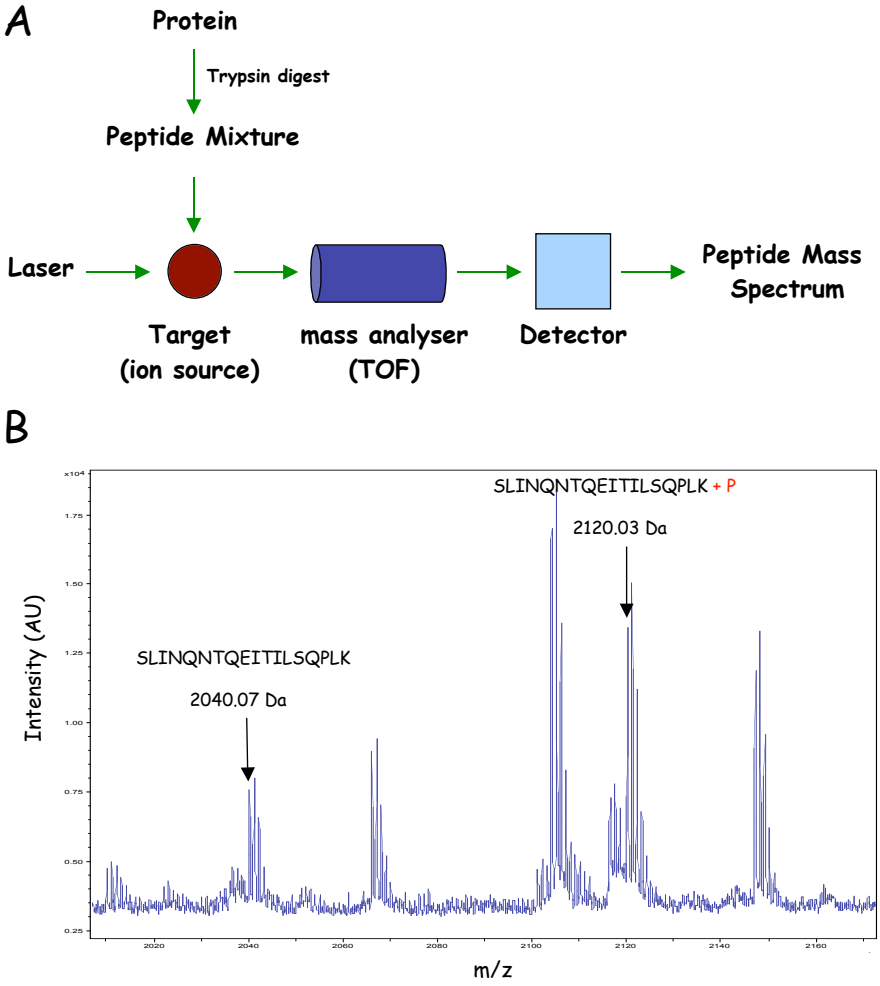

Figure 20. Identification of Ndc80-Phosphorylation sites by MALDI-TOF.

(A) *MALDI-TOF setup.* To identify phosphorylated peptides, the respective protein band is cut out from the Coomassie stained gel. The protein is proteolytically digested with trypsin which cleaves the polypeptide chain after Arginine and Lysine residues. The resulting peptide mixture (including the matrix) is subsequently applied onto the target in order to immobilise it. The peptides are ionised by a laser beam under vacuum in an electric field and move through the TOF-analyser with a velocity that depends on their mass and charge. The time each individual peptide needs to pass through the TOF-analyser is finally meassured by the detector which results in a peptide mass fingerprint (PMF) of the analysed protein.

(B) *Peptide mass spectrum.* A section of the spectrum of a sample containing phosphorylated Ndc80 is shown. The masses which correspond to a particular Ndc80 peptide (SLINQNTQEITILSQPLK) in its non-phosphorylated and phosphorylated state could be identified. AU = arbitrary units.

5.4.3 Confirmation of Ndc80-phosphorylation sites by LC-ESI-Quadrupole-TOF

To confirm the presence of a particular Ndc80-phosphopeptide and to identify its phosphorylated residue, the peptide mixture from a tryptic digest was analysed by LC-ESI-Quadrupole-TOF (Figure 21A). After separation by HPLC, the peptides were directly ionised by electro-spray (ESI, electro-spray ionisation). A given peptide is selected in the Quadrupole and enters the fragmentation chamber where it is fragmented by collision with nitrogen gas. The masses of the peptide-fragments are finally detected by a TOF-analyser. From the masses of the resulting peptide-fragments, one can conclude the sequence of the original peptide and identify the phosphorylated residue (Figure 21B). During the ionisation of a phosphorylated peptide, H_3PO_4 is eliminated from the phosphorylated residue (Figure 21C). This results in Methyl-dehydro-Alanine (MdA) in case of phospho-Threonine and in Dehydro-Alanine (dA) in the case of phospho-Serine. The presence of MdA or dA thus indicates the phosphorylated site within the peptide chain. Figure 22 shows the result of such analysis. In Figure 22A, the profile of the HPLC-run is shown. Every 2 seconds, a peptide mass fingerprint (PMF) is acquired. Usually, a given peptide and its phosphorylated counterpart elute at different times. Therefore, the peptide mass fingerprint at a particular time point may contain mainly one species whereas the other species is underrepresented. Figure 22B shows the PMF at 38.5 minutes elution-time which includes the masses of a particular Ndc80-peptide (SLINQNTQEITILSQPLK) in its non-phosphorylated and phosphorylated form. In order to gain sequence information, this potential phosphopeptide is fragmented. The fragmentation spectrum of this peptide in its phosphorylated state is shown in Figure 22C. The masses of its peptide-fragments were identified which confirms that the corresponding mass of the original peptide indeed belongs to the assumed Ndc80-peptide. In place of a particular Threonine (T252), the mass of Methyl-dehydro-Alanine could be identified indicating that this Threonine residue was phosphorylated.

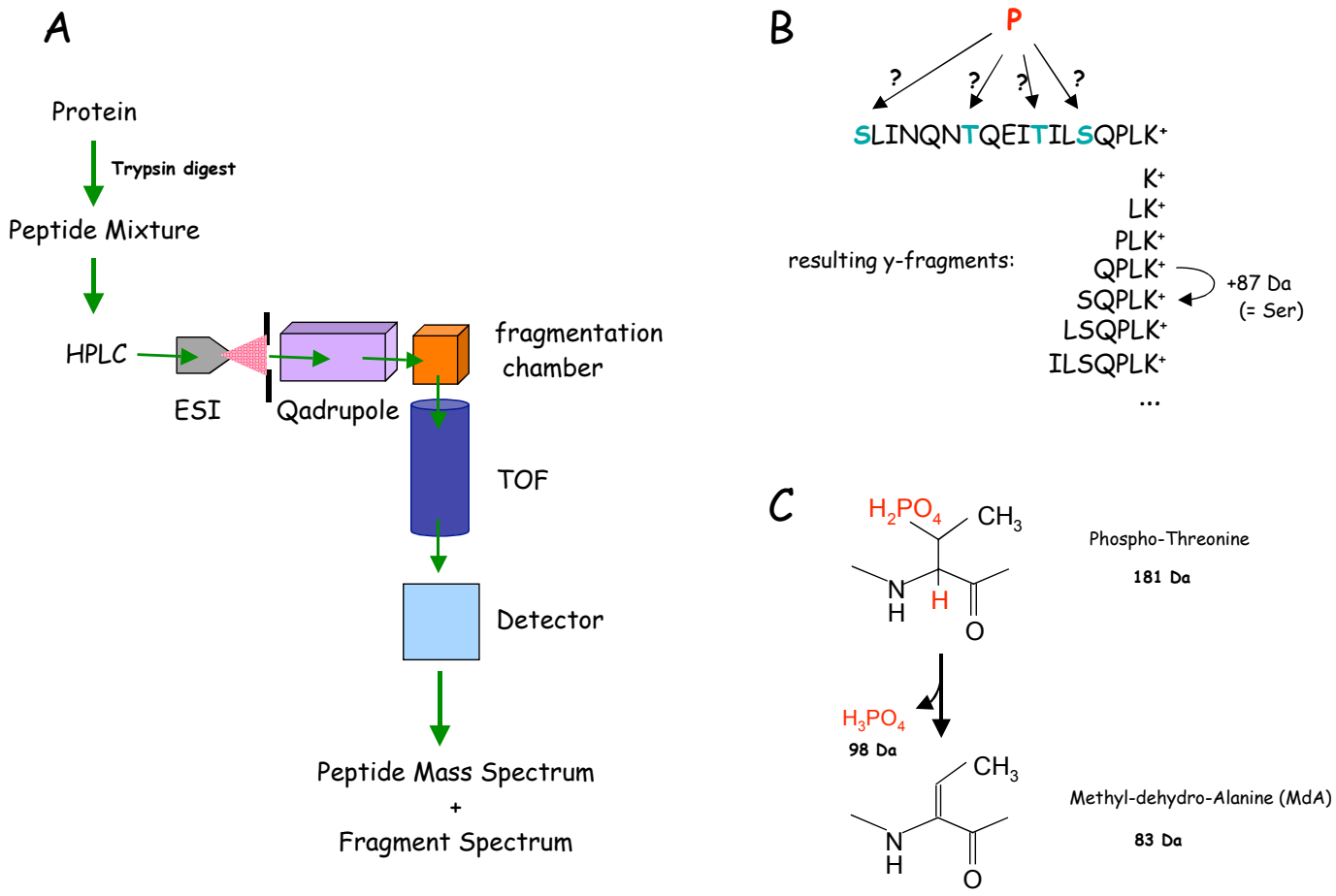

Figure 21. Identification of Ndc80-Phosphorylation sites by LC-ESI-Quadrupole TOF.

(A) *Setup of the LC-ESI-Quadrupole TOF.* To determine the sequence of a given phospho-peptide and identify the phosphorylated residue, the respective protein band is cut out from the Coomassie stained gel and the protein is proteolytically digested using trypsin. The resulting peptide mixture is separated by an HPLC and subsequently ionised by electro-spray (ESI, electro-spray ionisation). A particular peptide with a defined mass to charge ratio (m/z) is selected in the Quadrupole and enters the fragmentation chamber where it is fragmented by collision with nitrogen. The masses of the peptide-fragments are finally detected by a TOF-analyser.

(B) *Determination of a peptide sequence.* The LC-ESI-Quadrupole TOF analysis of a given Ndc80-peptide results in a complex mixture of many fragments. Among those fragments are the outlined y-fragments which carry a positive charge at their C-terminus. The mass difference between two y-fragments allows the identification of the next amino acid in the peptide chain and therefore the identification of the peptide-sequence. Furthermore the phosphorylated residue can be identified.

(C) *Identification of the phosphorylated residue.* During the ionisation of a phosphorylated peptide, H_3PO_4 is eliminated from the phosphorylated residue. In case of phospho-Threonine e.g., this results in Methyl-dehydro-alanine (MdA). The presence of MdA thus indicates the phosphorylated site within the peptide chain.

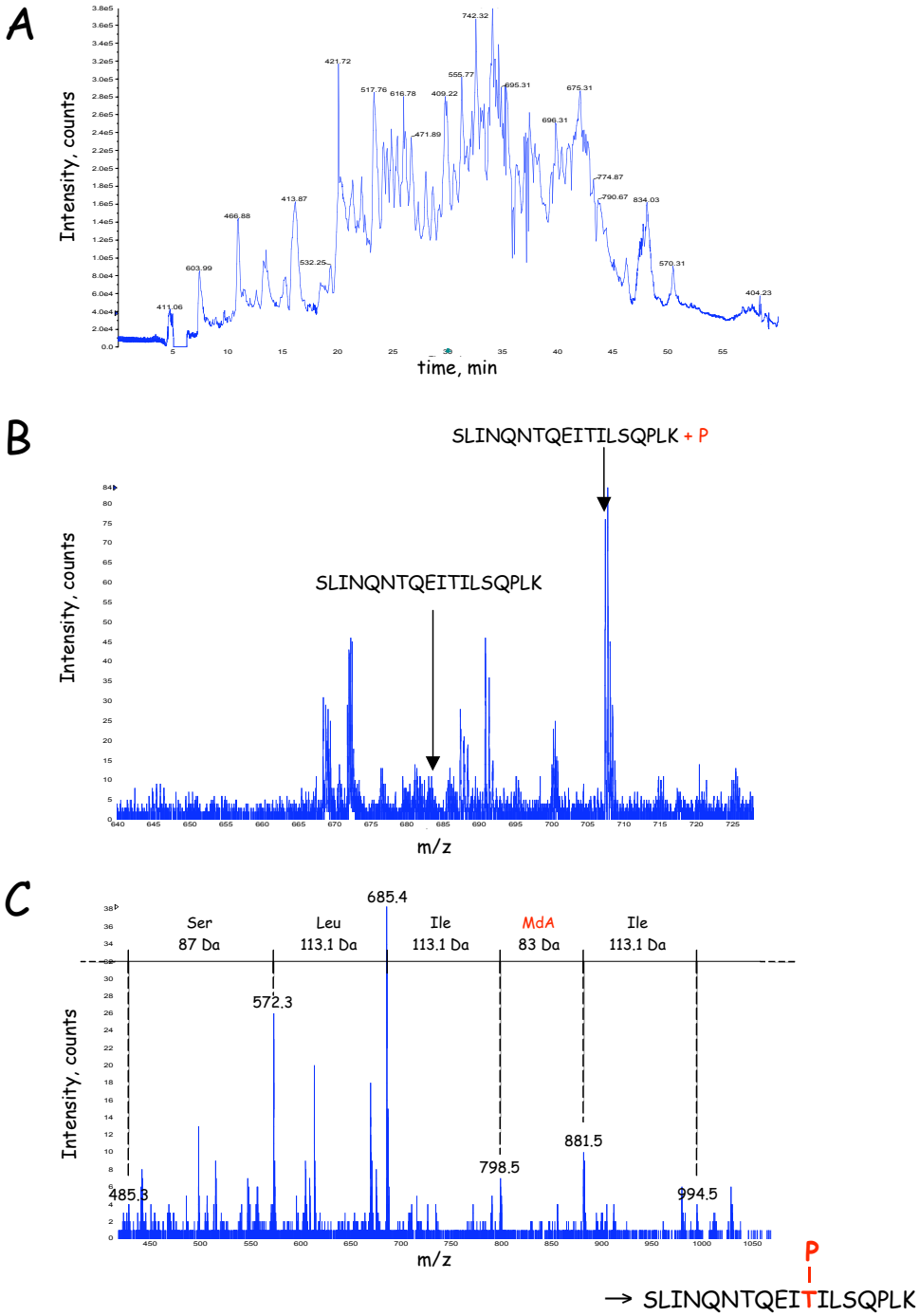

Figure 22. Identification of a particular Ndc80-phosphorylation site (T252).

(A) *HPLC-Chromatogram.* The tryptic digest of Ndc80 results in a complex peptide mixture which is separated by HPLC. The corresponding elution profile is shown. Every 2 seconds, a peptide mass fingerprint (PMF) is acquired by a ESI-TOF system.

(B) *Peptide mass fingerprint.* The PMF at 38.5 min elution time is shown which contains the masses of the Ndc80-peptide SLINQNTQEITILSQPLK in its non-phosphorylated and phosphorylated state.

(C) *Fragment spectrum*. The phosphorylated Ndc80-peptide SLINQNTQEITILSQPLK is fragmented which provides sequence information and allows the identification of the phosphorylated residue within the peptide chain.

5.5 Functional analysis of Ndc80-phosphorylation

5.5.1 Analysis of ndc80 deletion mutants

Since a high number of phosphorylated Serine and Threonine residues could be identified (Figure 19), the initial approach to study Ndc80-phosphorylation was to generate NDC80-deletion strains in which a part of the N-terminus is missing. Such preliminary analysis should eliminate several phosphorylation sites at once and give a first indication which stretch of the heavily phosphorylated N-terminus might be most important in regard to phosphorylation and whether the N-terminus is at all required for spindle checkpoint regulation.

Three NDC80-constructs were generated which contain NDC80 that is truncated from the N-terminus to eliminate an increasing number of Serine and Threonine residues shown to be phosphorylated (Figure 23A). The respective full length NDC80 was used as control. In the first mutant, only the N-terminal tail containing the first 43 amino acids was deleted (ndc80Δ1-43) which eliminated 11 of the identified phosphorylation sites. In the second mutant, the N-terminal tail and approximately one third of the HEC-domain was deleted (ndc80Δ1-116). This stretch contained 24 of the phosphorylation sites which were identified by mass spectrometry. The third mutant was truncated up to amino acid 255, eliminating the N-terminal tail and the entire conserved HEC-domain (ndc80Δ1-255). This region contained almost all (31 out of 35) identified Ndc80-phosphorylation sites.

These constructs were integrated into the NDC80-locus in the yeast genome of the NDC80-shuffle strain (YSK787) in which the endogenous NDC80-gene is deleted. Since NDC80 is an essential gene, this strain requires an episomal NDC80-copy for example on a URA3-plasmid for survival. The URA3 marker encodes orotidine-5'phosphate decarboxylase, an enzyme which is required for the biosynthesis of uracil. One can counterselect against this plasmid on plates containing 5'-FOA. 5'-FOA is converted to the toxic compound 5-fluorouracil by the action of decarboxylase. Therefore, ura3$^-$ cells can be selected on media containing 5'-FOA whereas URA3$^+$ cells are inviable. Yeast strains generally lose plasmids at a certain rate. If the integrated deletion mutant can complement for the wild-type NDC80 present on the URA3-plasmid, cells which lost the plasmid will survive on 5'-FOA containing plates. On the other hand, if the deletion of the N-terminal part of NDC80 cannot complement for the wild-type protein, the cells

will die either because they spontaneously lost the essential plasmid or due to the accumulation of 5-fluorouracil generated by orotidine-5'phosphate decarboxylase on 5'-FOA containing plates.

To test the viability of the NDC80-deletion mutants, the respective strains were grown in YPD at mid-logarithmic phase for 2 days. During this period, the strain was given time to lose the [NDC80-URA3]-plasmid. 10-fold serial dilutions of the respective strains were then spotted onto YPD as a growth control and on SDC + 5'-FOA plates to test for viability. The result is shown in Figure 23B. Whereas the two mutants ndc80Δ1-43 and ndc80Δ1-116 are viable on plates containing 5'-FOA, the mutant lacking the N-terminal tail and the entire HEC-domain (ndc80Δ1-255) is lethal indicating an essential function of the conserved HEC-domain.

To analyse whether the viable Ndc80-deletion mutants are temperature sensitive, the strains were spotted on YPD plates and incubated at 37°C for four days. As shown in Figure 23B, both viable Ndc80-deletion strains grow at 37°C comparable to wild-type cells indicating that they do not possess a temperature sensitive phenotype due to misfolding of the protein at elevated temperatures.

To check whether the deletion of the N-terminus had an impact on expression or degradation rate of the protein, whole cell extracts were prepared from the viable deletion mutants (ndc80Δ1-43 and ndc80Δ1-116) and Ndc80 was detected by immunoblotting. Figure 23C shows the result of this analysis. Both mutants show comparable expression levels as the wild-type control strain indicating equal expression and stability of the respective proteins.

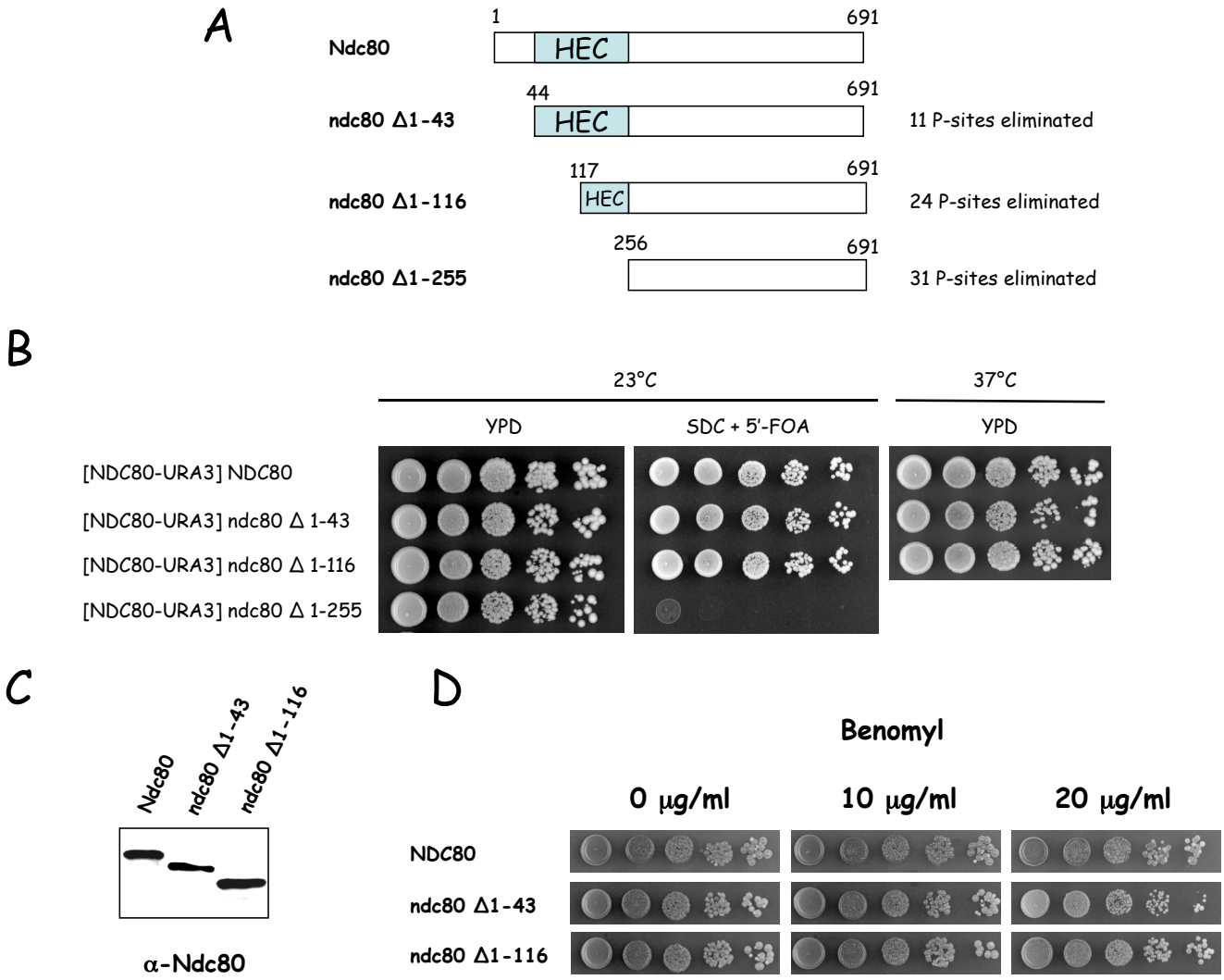

Figure 23. Analysis of ndc80 deletion mutants.

(A) *The constructed ndc80 deletion strains are shown.* Ndc80 was truncated from the N-terminus to eliminate an increasing number of phosphorylation sites (P-sites).

(B) *Deletion of the HEC-domain is lethal.* The ability of the indicated strains to grow in the absence of the NDC80-plasmid was tested. 10-fold serial dilutions of cells growing exponentially in YPD for 2 days were plated on SDC + 5'-FOA (for counterselection against the [NDC80-URA3] plasmid). As a control, cells were plated onto YPD. The plates were incubated at 23°C or 37°C for 4 days.

(C) *Protein-expression levels of ndc80Δ1-43 and ndc80Δ1-116.* Logarithmically growing YPD-cultures containing Ndc80, ndc80Δ1-43 or ndc80Δ1-116 were harvested and crude cell extracts were prepared. The Ndc80-protein levels were analysed by immunoblotting using α-Ndc80 antibody. Equal protein loading was confirmed by Ponceau staining.

(D) *Ndc80 deletion mutants are insensitive to benomyl.* Serial dilutions of the indicated strains were spotted onto YPD plates supplemented with increasing concentrations of benomyl and incubated for 4 days at 23°C.

5.5.2 Spindle checkpoint analysis of ndc80Δ1-43 and ndc80Δ1-116

As described above (1.3), the spindle checkpoint monitors proper attachment of the kinetochores to microtubules as well as the tension which is created once all kinetochores are bipolarly attached. To test whether a mutant of interest is defective in sensing tension, its growth characteristics on YPD-plates containing the microtubule depolymerising drug benomyl can be analysed. In the past, this method was extensively used to identify many spindle checkpoint mutants such as *mad1* (mitotic arrest deficient 1), *mad2* (mitotic arrest deficient 2), or *bub1* (budding uninhibited by benomyl 1). High concentrations of benomyl lead to the complete depolymerisation of the microtubule polymers. At low concentrations however, benomyl slows down microtubule assembly which interferes with kinetochore-microtubule connections which in turn activates the spindle checkpoint. When the mitotic spindle assembly is impaired, spindle checkpoint mutants fail to delay their cell cycle progression and quickly die because of chromosome loss. In wild-type cells however, the defects of the mitotic spindle apparatus are monitored by the intact spindle checkpoint which delays cell cycle progression until the spindle is correctly assembled. Therefore, wild-type cells grow in the presence of low benomyl concentrations whereas checkpoint mutants show increased sensitivity to the drug. The analysis of spindle checkpoint function of the viable deletion mutants ndc80Δ1-43 and ndc80Δ1-116 is shown in Figure 23D. Both strains grow like wild-type on plates supplemented with increasing concentrations of benomyl indicating an intact spindle checkpoint of these mutants.

To analyse the integrity of the spindle checkpoint in more detail, the Pds1-protein levels of ndc80Δ1-116 were analysed in the absence or in the presence of the microtubule depolymerising drug nocodazole. As described before (1.3), the meta-to-anaphase transition is controlled by the spindle checkpoint. Once all kinetochores are properly attached to microtubules emanating from the opposing poles in metaphase, the spindle checkpoint is inactivated. This leads to the initiation of anaphase in which the cohesin complex is cleaved by the action of the protease Esp1 and sister chromatids are segregated. The protein levels of Pds1, the Esp1-inhibitor, are a marker for the activity of the spindle checkpoint since Pds1 is degraded upon spindle checkpoint inactivation at the meta-to-anaphase transition. Pds1-levels are high in metaphase when the checkpoint is active and start to decrease at the onset of anaphase after the checkpoint has been inactivated. The checkpoint can be artificially activated by the microtubule depolymerising drug nocodazole. In

wild-type cells, nocodazole leads to the activation of the checkpoint since unattached kinetochores are present in the cell and tension across the mitotic spindle cannot be built up. As a consequence, cells arrest in metaphase with high Pds1 protein levels and a DNA content of 2N.
Pds1 protein levels were analysed in the ndc80Δ1-116 mutant by immunoblotting. Cells were arrested in G_1-phase with α-factor and subsequently released into the cell cycle in the presence or absence of nocodazole. The progression through the cell cycle was monitored by FACS-analysis. In both cases, the cells behaved like the respective wild-type control strain (data not shown). In the presence of nocodazole, the Pds1-levels stayed high due to the activated checkpoint. In the absence of nocodazole, the Pds1-levels increased when cells entered mitosis and dropped at the meta-to-anaphase transition indicating an intact checkpoint of the ndc80Δ1-116 mutant.

5.5.3 The spindle checkpoint of ndc80^{11A} is impaired

The analysis of the ndc80 deletion mutants showed no significant effect regarding the activity of the spindle checkpoint. In the ndc80Δ1-116 mutant, 24 phosphorylation sites were eliminated by the deletion of the N-terminus. Using this mutant as a starting point, single mutations were introduced by site-directed mutagenesis changing Serine and Threonine residues to Alanine to abolish phosphorylation. The resulting strains were analysed on YPD-plates containing benomyl for the identification of checkpoint deficient ndc80 mutants.
The positions of the mutated sites are indicated in Figure 24A. The Serine residue at position 205 was mutated first which did not change the growth characteristics of the corresponding yeast strain (ndc80Δ1-116 S205A) on benomyl-containing plates. Next, T248 and T252 were mutated. The growth of the resulting strain (ndc80Δ1-116 S205A T248A T252A) was analysed. As shown in Figure 24B, this mutant showed significantly increased sensitivity to benomyl compared to the wild-type strain indicating an impaired spindle checkpoint. This phenotype could theoretically be caused by the three introduced point mutations or a combination of the mutations and the elimination of the N-terminus. To check the first possibility, the mutations were introduced into the NDC80 full length construct and the resulting strain (ndc80 S205A T248A T252A) was analysed for growth on benomyl. No benomyl sensitivity could be observed, indicating that a combination of the three point mutations and a function in the N-terminus is required for the benomyl sensitivity observed in this mutant (ndc80Δ1-116 S205A T248A T252A). To check if

the function in the N-terminus which contributes to the benomyl sensitivity is connected to the identified Ndc80-phosphorylation sites, more Serine and Threonine residues were replaced by Alanine in the ndc80 S205A T248A T252A mutant. The substitution of S37, T38 and T43 by Alanine had no effect on benomyl sensitivity of the respective strain (ndc80 S205A T248A T252A S37A T38A T43A). Next, T21 and S22 were mutated which also did not change the growth properties of the strain (ndc80 S205A T248A T252A S37A T38A T43A T21A S22A). When S4, T5 and S6 were additionally replaced by Alanine, the benomyl sensitivity of the ndc80Δ1-116 S205A T248A T252A mutant was restored clearly demonstrating that this phenotype is exclusively caused by the elimination of phosphorylation of the Ndc80 N-terminus. In total, 11 sites are required for the benomyl sensitive phenotype of the respective Alanine mutant (ndc80 S205A T248A T252A S37A T38A T43A T21A S22A S4A T5A S6A or $ndc80^{11A}$).

5.5.4 $ndc80^{11D}$ positively regulates the spindle checkpoint

If non-phosphorylatable Ndc80 ($ndc80^{11A}$) leads to a defective spindle checkpoint, the phosphorylated form of Ndc80 should have the opposite phenotype and positively influence the checkpoint. To check this hypothesis, the 11 phosphorylation sites responsible for the described phenotype of the $ndc80^{11A}$ mutant were now mutated to Aspartic Acid (D) to generate the corresponding $ndc80^{11D}$ mutant. The negative charge of Aspartic Acid is thought to mimic the phosphorylated form of Ndc80. When this mutant was spotted onto YPD plates containing up to 20 µg/ml benomyl, it grew comparable to the wild-type control strain. However, when higher concentrations of benomyl (up to 40 µg/ml) were used, the $ndc80^{11D}$ mutant was still able to form colonies whereas the wild-type cells were not (Figure 24C). This observation indicates that upon benomyl-treatment, the $ndc80^{11D}$ mutant activates the spindle checkpoint longer than in the wild-type situation and thus provides enough time to cope with spindle defects that are lethal to wild-type cells.

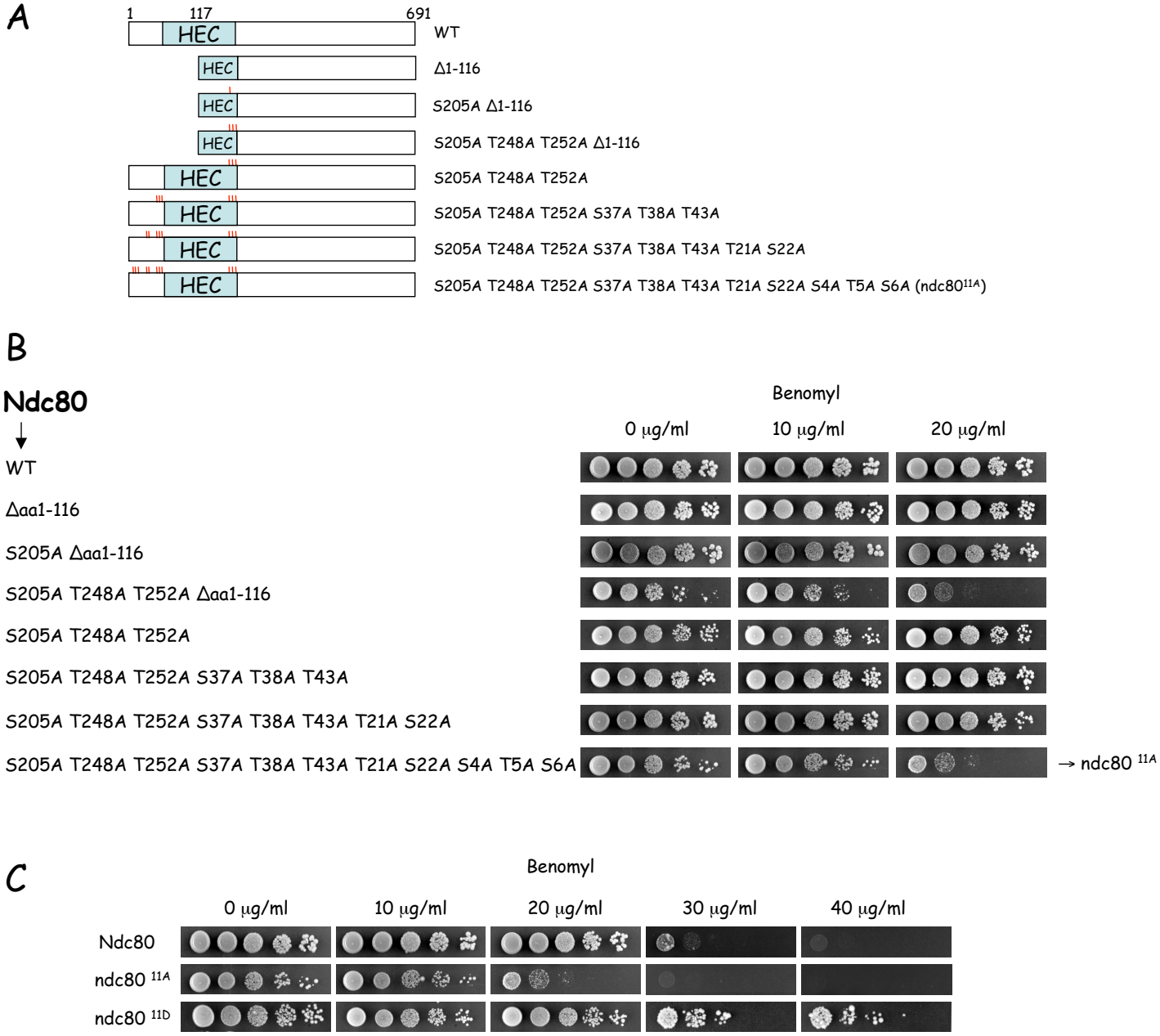

Figure 24. ndc80^{14A} and ndc80^{14D} show opposite growth characteristics in the presence of benomyl.

(A) The ndc80 mutants analysed in (B) are shown. The positions of the mutated Serine and Threonine residues within the Ndc80-protein are indicated.

(B) *ndc80^{11A} is benomyl sensitive.* Serial dilutions of the indicated Ndc80 strains were spotted onto YPD plates supplemented with increasing concentrations of benomyl and incubated for 4 days at 23°C.

(C) *ndc80^{11D} (S205D T248D T252D S37D T38D T43D T21D S22D S4D T5D S6D) is benomyl resistant.* Serial dilutions of the indicated Ndc80 strains were spotted onto YPD plates supplemented with increasing concentrations of benomyl and incubated for 4 days (0-20 μg/ml) or 11 days (30-40 μg/ml) at 23°C. Wild-type cells (Ndc80) and the ndc80^{11A} mutant were spotted as controls.

5.5.5 The lethality of the ndc80^{14D} mutant depends on the spindle checkpoint

If a negatively charged surface of the Ndc80 N-terminus leads to an enhanced spindle checkpoint signal in comparison to wild-type cells, the introduction of more negative charges could potentially lead to an even stronger activation of the checkpoint. If the checkpoint activation is strong enough, it should permanently arrest the cells in metaphase and eventually lead to a lethal phenotype. To test this hypothesis, three more Threonine residues (T74, T79 and T82) of the ndc80^{11D} mutant were replaced by Aspartic Acid. The resulting mutant ndc80^{14D} (ndc80 S205D T248D T252D S37D T38A T43D T21D S22D S4D T5D S6D T74D T79D T82D) was inviable (Figure 25, compare line 1 and 2; Table 3). The reason for the lethality of the ndc80^{14D} mutant could be either a defective kinetochore or a constitutive activation of the checkpoint which would lead to a permanent cell cycle arrest in mitosis. If the lethality of the ndc80^{14D} mutant is due to permanent checkpoint activation, then the elimination of the spindle checkpoint should rescue the cells. As described above (1.3.1.1), the major players of the spindle checkpoint pathway are the Mad- and Bub-proteins, respectively. To test whether the activation of the spindle checkpoint in ndc80^{14D} is dependent on these proteins, MAD2 was knocked out in the lethal ndc80^{14D}-background. As shown in Figure 25 line 3, the elimination of MAD2 (Δmad2) is able to rescue the lethal phenotype of the ndc80^{14D} mutant. As a control, a wild-type copy of MAD2 was re-introduced into ndc80^{14D} Δmad2 on a CEN-plasmid. The resulting strain (ndc80^{14D} Δmad2 MAD2) is inviable again (Figure 25, line 4), which confirms the specificity of the genetic interaction between NDC80 and MAD2. This observation is also supported by the fact that the lethality of another ndc80^{D} mutant (S4D T5D S6D T21D S22D S37D T38D T43D T54D S56D T58D T74D T79D T82D S97D S100D S106D; ndc80^{17D}; Table 3) can also be rescued by the elimination of MAD2. To further strengthen this finding, a second checkpoint protein of the same pathway, Bub1, was knocked out (Δbub1) in the lethal ndc80^{14D} mutant. The deletion of BUB1 is also able to rescue the lethal phenotype of ndc80^{14D} (Figure 25, line 5). As with MAD2, the introduction of BUB1 on a plasmid restores the lethality of ndc80^{14D} (Figure 25, line 6) confirming that the observed effect is indeed due to BUB1.

To check the specificity of the observed data, the corresponding Alanine mutant (ndc80^{14A}) was analysed. As shown in Figure 25 line 7, this mutant is viable. The elimination of MAD2 or BUB1 has no significant impact on the growth characteristics of the respective strains (Figure 25, line 8

and 9). This observation confirms the specificity of the effects which are seen for ndc80^{14D}.

At this stage, one could argue that the ndc80^{14D}-protein is completely nonfunctional (e.g. misfolded, unstable) and that the elimination of MAD2 or BUB1 *per se* rescues lethality in the Δndc80 background. To show that the presence of the constitutively phosphorylated form of Ndc80 (ndc80^{14D}) causes the observed lethal phenotype, it was tested whether the deletion of the spindle assembly checkpoint itself can rescue the lethality in the absence of any Ndc80-protein (Δndc80). As shown in Figure 25 line 10-12, the respective strains are not viable. This result again demonstrates that the rescue of ndc80^{14D} by Δmad2 or Δbub1 is highly specific and depends on the presence of the ndc80^{14D} protein.

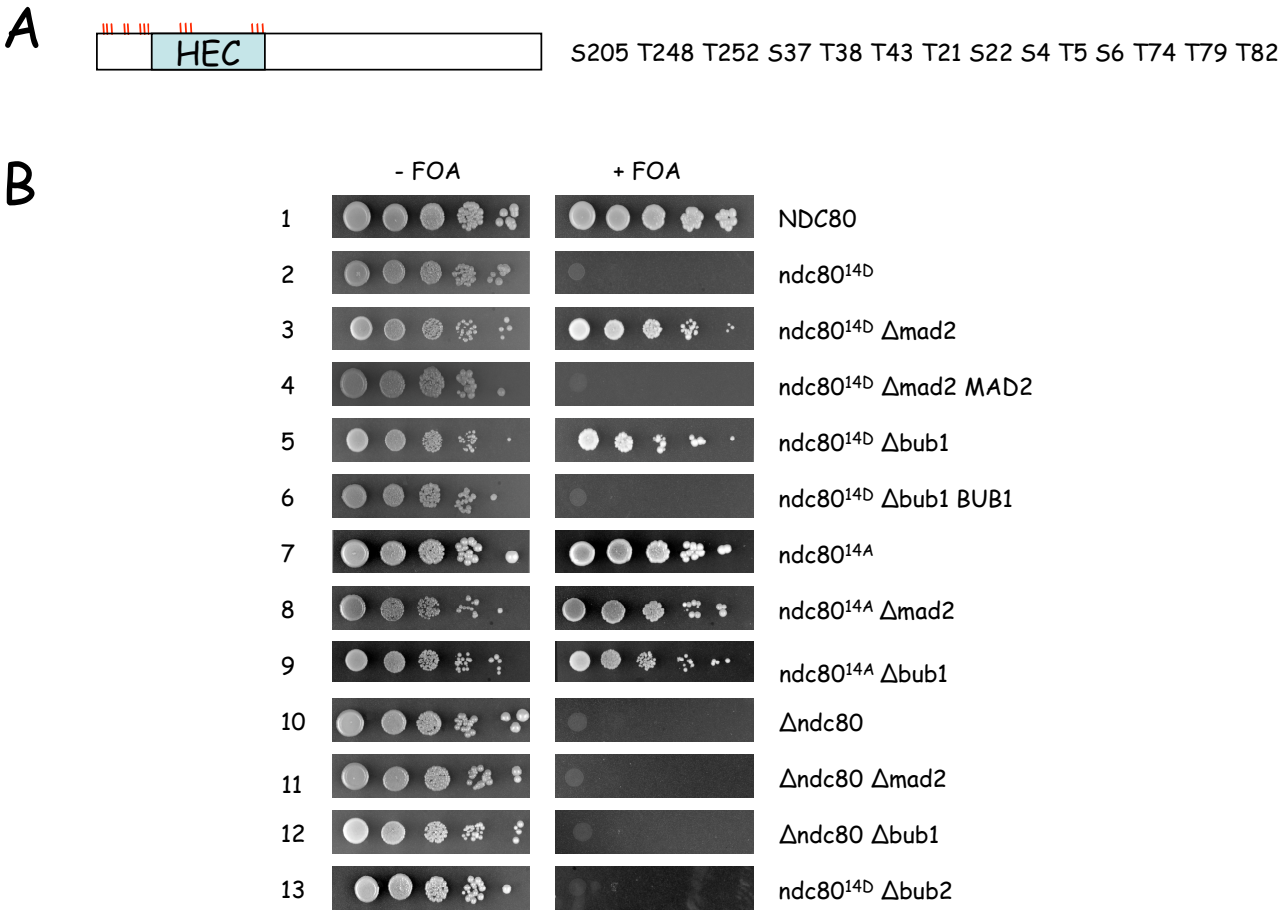

Figure 25. The lethal ndc80^{14D} phenotype is rescued by the elimination of the spindle assembly checkpoint.

(A) The mutated NDC80-phosphorylation sites are indicated. The sites were mutated either to Alanine to abolish phosphorylation or to Aspartic acid to mimic the negative charge created by phosphorylation. The viability of the corresponding yeast strains (ndc80^{14A} and ndc80^{14D}) was analysed in (B).

(B) Cultures of the indicated strains (all containing the [NDC80-URA3] plasmid) were grown logarithmically in YPD for 2 days. Serial dilutions were spotted onto SDC-LEU (control) or SDC-LEU + 5'-FOA (for counterselection against the [NDC80-URA3] plasmid) and grown for 7 days at 23°C.

The checkpoint controlled by MAD2 and BUB1 monitors the correct assembly of the mitotic spindle. However, there is another surveillance mechanism in mitosis, the so called spindle positioning checkpoint (1.3.2) which controls the right orientation of the spindle in respect to the mother-bud axis. One of the major players in this pathway is BUB2, which monitors the correct position of the SPBs. To test whether Ndc80-phosphorylation has an impact on the spindle positioning pathway, BUB2 was deleted in the ndc80^{14D} mutant. The resulting strain (ndc80^{14D} Δbub2) was tested for viability. As shown in Figure 25 line 13, the elimination of BUB2 cannot rescue the lethal phenotype of ndc80^{14D}. This finding clearly demonstrates that Ndc80-phosphorylation is involved in the regulation of the spindle assembly checkpoint but not in the spindle positioning pathway. The working hypothesis which proposes that the phosphorylation of Ndc80 leads to the activation of the spindle checkpoint should be extensively tested in the following experiments.

Strain	Ser/Thr to Asp-mutantions	viability
YSK857	S4D T5D S6D	+
YSK858	S4D T5D S6D T248D T252D	+
YSK860	S4D T5D S6D S205D T248D T252D	+
YSK867	S4D T5D S6D T21D S22D S205D T248D T252D	+
YSK868	S4D T5D S6D T21D S22D S37D T38D T43D S205D T248D T252D (= ndc8011D)	+
YSK869	S4D T5D S6D T21D S22D S37D T38D T43D T74D T79D T82D S205D T248D T252D (= ndc80^{14D})	-
YSK875	S4D T5D S6D T21D S22D S37D T38D T43D T74D T79D S97D S100D S106D T82D S205D T248D T252D	-
YSK897	S4D T5D S6D T21D S22D S37D T38D T43D T74D T79D S97D S100D S106D T82D T145D S150D S205D T248D T252D	-
YSK893	T74D T79D T82D	+
YSK876	S205D	+
YSK894	S4D T5D S6D T21D S22D S37D T38D T43D T74D T79D T82D	+
YSK895	S205D S248D T252D	+
YSK896	S4D T5D S6D S205D	+
YSK907	T145D S150D S205D	+
YSK925	S4D T5D S6D T21D S22D S37D T38D T43D T54D S56D T58D T74D T79D T82D S97D S100D S106D (= ndc80^{17D})	-
YSK928	S37D T38D T43D	+
YSK941	S4D T5D S6D T21D S22D S37D T38DT43D S145D S205D	+
YSK949	S4D T5D S6D T21D S22D S37D T38D T43D T248D T252D	+
YSK954	T74D T79D T82D S205D S248D T252D	+
YSK962	S4D T5D S6D T21D S22D S37D T38D T43D S205D	+
YSK975	S4D T5D S6D T21D S22D S37D T38D T43D T54D S56D T58D T248D T252D S205D	+
YSK998	S4D T5D S6D T21D S22D S37D T38D T43D T74D T79D T82D T248D T252D	+
YSK999	S4D T5D S6D T21D S22D S37D T38D T43D T74D T79D T82D S205D	+
YSK1014	S4D T5D S6D T74D T79D T82D S205D S248D T252D	+

Table 3: Viability of NDC80 Ser/Thr to Asp point mutants.

5.6 Functionality of the ndc80^{14D} protein

The fact that the lethality of the ndc80^{14D} mutant can be rescued by the elimination of Mad2 or Bub1 indicates that the corresponding ndc80^{14D} protein is functional. In order to confirm that the lethality of this mutant is indeed due to the permanent activation of the spindle assembly checkpoint and therefore a specific effect of Ndc80-phosphorylation, the expression of the protein and its subcellular localisation were analysed (Figure 26). A strain containing ndc80^{14D}-3HA was grown asynchronously and its protein levels were determined by immunoblotting (α-HA). As a control, a wild-type strain containing Ndc80-3HA was analysed. The ndc80^{14D}-3HA protein is present in equal amounts as the corresponding wild-type protein indicating that expression and stability of the ndc80^{14D}-3HA protein are not influenced by the Ser/Thr to Asp mutations (Figure 26A). The Blot further shows that the ndc80^{14D}-3HA protein migrates slightly slower then the wild-type protein in the SDS-PAGE gel due to the introduced point mutations. The increase in mass of the mutated protein cannot be the only reason for this altered running behavior since the difference in mass between Aspartic Acid (115.1 Da) and Threonine (101.1 Da) or Serine (87.1 Da) is not sufficient to explain this shift. This effect is rather due to the additional negative charges introduced in ndc80^{14D} which prevents also negatively charged SDS-molecules from binding to the denatured protein. This in turn leads to the retention of the protein during the electrophoresis comparable to the phosphorylated Ndc80 protein (Figure 15C, Figure 17 and Figure 18).

In order to analyse the kinetochore localisation of the ndc80^{14D} protein, a ChIP assay was performed. Since the ndc80^{14D} mutant is inviable, it was transiently expressed from the inducible Gal10-promoter in the NDC80 wild-type background. To distinguish the two forms of Ndc80, the mutant was Flag-tagged whereas the wild-type protein was left untagged (NDC80 Gal10-Flag-ndc80^{14D}). The corresponding wild-type strain (NDC80 Gal10-Flag-NDC80) was used as control. The result of the ChIP-analysis is shown in Figure 26B. Flag-ndc80^{14D} as well as Flag-NDC80 are able to specifically co-precipitate centromeric DNA. To confirm the kinetochore localisation of the ndc80^{14D} protein, it was fused with RedStar2, a red fluorescent protein tag and its kinetochore association in different cell cycle phases was analysed by fluorescence microscopy. As an internal positive control, the GFP-tagged Ndc80 wild-type protein was expressed in the

same strain. Figure 26C shows that ndc80^{14D}-RedStar2 co-localises with the wild-type protein Ndc80-GFP throughout the cell cycle.

The ChIP assay as well as the microscopical analysis demonstrate that the ndc80^{14D} protein correctly localises to the kinetochore and that it can compete for binding to the kinetochore with the Ndc80 wild-type protein present in the same cell.

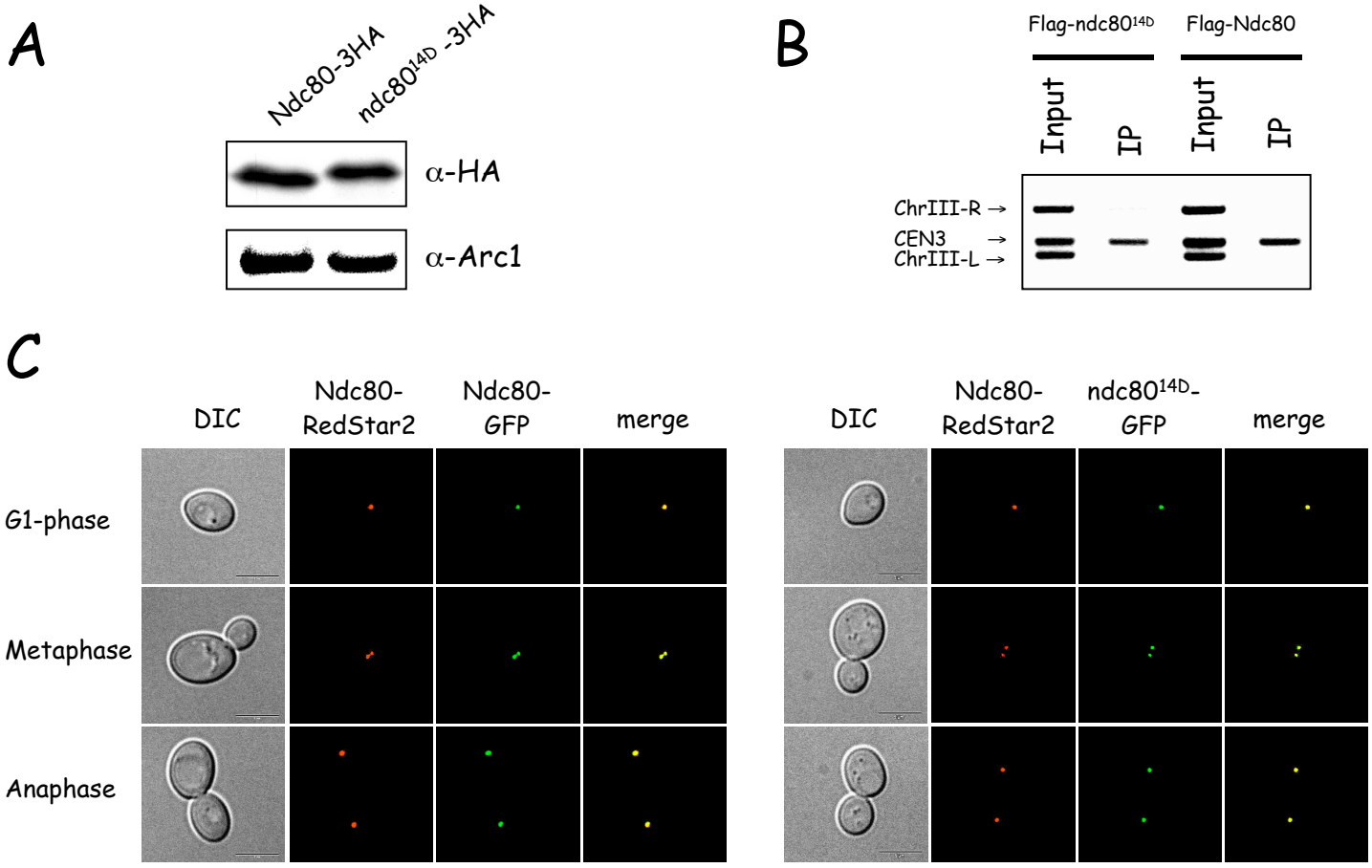

Figure 26. The ndc80^{14D} protein is stable and localises to the kinetochore.

(A) *Wild-type (NDC80) and ndc80^{14D} proteins are equally expressed and stable.* Logarithmically growing cells containing Ndc80-3HA or ndc80^{14D}-3HA were harvested and crude cell extracts were prepared. The Ndc80-protein levels were analysed by immunoblotting using α-HA antibody. α-Arc1 was used as a loading control.

(B) *ndc80^{14D} localises to the kinetochore by CHIP.* Wild-type cells (NDC80) containing Gal10-Flag-NDC80 or Gal10-Flag-ndc80^{14D} were grown to mid-logarithmic phase. After transient galactose induction, the association of Flag-Ndc80 or Flag-ndc80^{14D} with CEN3-DNA was analysed by Chromatin immunoprecipitation (CHIP). α-Flag M2 antibody was used for immunoprecipitation. The presence of CEN3 DNA and two flanking sequences (ChrIII-R and ChrIII-L) was analyzed by triplex PCR.

(C) *ndc80^{14D} localises to the kinetochore by fluorescence microscopy.* The subcellular localisation of Ndc80-GFP and ndc80^{14D}-GFP was analysed by fluorescence microscopy. A second copy of Ndc80 (Ndc80-RedStar2) serves as an internal control. Scale bar, 5 µm.

5.7 Detailed analysis of the ndc80^{14D} phenotype

5.7.1 A system for the analysis of the lethal ndc80^{14D} mutant

The ndc80^{14D} mutant is inviable (Figure 25, line 2). This fact makes it difficult to analyse the phenotype in more detail on the cellular level. In order to create a situation in which the ndc80^{14D} phenotype is present for a defined period of time, a strain containing the ndc80^{14D} mutant stably integrated into the LEU2-locus and an additional galactose inducible and glucose repressible copy of the NDC80 wild-type gene at the endogenous NDC80-locus was constructed. The NDC80 wild-type copy was fused to a ubiquitin followed by a single arginine residue (UbiR). This N-terminal tag results in an Ndc80-protein with an N-terminal arginine which renders the protein less stable. The efficiency of degradation of the fusion protein UbiR-Ndc80 is therefore increased.

To analyse the phenotype of the ndc80^{14D} mutant on the cellular level, the constructed strain (ndc80^{14D}-3HA pGal1-UbiR-NDC80-9myc) was first grown in media containing 0.1% galactose. The expression levels of Ndc80-9myc from the Gal-promoter under these conditions were slightly higher than those of Ndc80-9myc expressed form the endogenous NDC80-promoter (pNDC80-NDC80-9myc) (Figure 27).

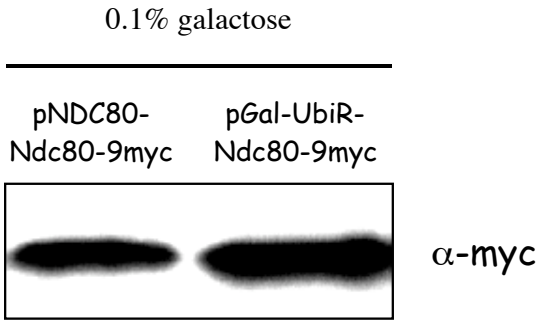

Figure 27. Expression analysis of the pGal1-UbiR-NDC80-9myc construct.

YMS398 (pNDC80-NDC80-9myc) and YSK1170 (ndc80^{14D}-3HA pGal1-UbiR-NDC80-9myc) were grown logarithmically in medium containing 0.1% galactose. Cultures were harvested and whole cell extracts were prepared. Proteins were separated by SDS-PAGE and blotted. The expression of NDC80-9myc was analysed by immunoblotting using the monoclonal α-myc antibody.

The increased Ndc80-levels were necessary for optimal growth of the ndc80^{14D}-3HA pGal1-UbiR-NDC80-9myc strain since the wild-type protein (Ndc80-9myc) has to compete for kinetochore-binding with ndc80^{14D}-3HA which is present in the same strain. To eliminate the Ndc80 wild-type protein, the strain was shifted to media containing 2% glucose to repress the Ndc80-9myc expression. As a consequence, only the ndc80^{14D}-3HA mutant protein was present in the cell and its physiological effects could be studied. The functionality of the Ndc80-depletion system was first tested by spotting serial dilutions of the ndc80^{14D} pGal1-UbiR-NDC80 strain onto plates containing either galactose (YPG) or glucose (YPD). The result is shown in Figure 28A. The Ndc80-depletion strain grows in the presence of galactose since the Ndc80 wild-type protein is expressed (as shown in Figure 27). In contrast, on glucose containing plates, Ndc80 wild-type expression from the Gal-promoter is repressed and the strain is no longer viable because only the lethal ndc80^{14D} copy is now present in the cell. The respective control strains containing Ndc80 wild-type or ndc80^{14A} in the pGal1-UbiR-NDC80 background were analysed as described above and were viable in the presence of galactose or glucose.

To distinguish between the wild-type and the ndc80^{14D} mutant protein, different tags were fused to their C-terminus. A 3HA-tag was fused to ndc80^{14D} and the wild-type protein was tagged with 9myc (ndc80^{14D}-3HA pGal1-UbiR-NDC80-9myc). To analyse the depletion of the NDC80-9myc protein, its repression by glucose was followed by immunoblotting (α-myc). As shown in Figure 28B, the Ndc80-9myc protein is almost completely depleted 3 hours after glucose addition.

The growth analysis of ndc80^{14D} and the α-myc immunoblot show that Ndc80 can be depleted efficiently, creating a suitable system for the analysis of the lethal ndc80^{14D} mutant.

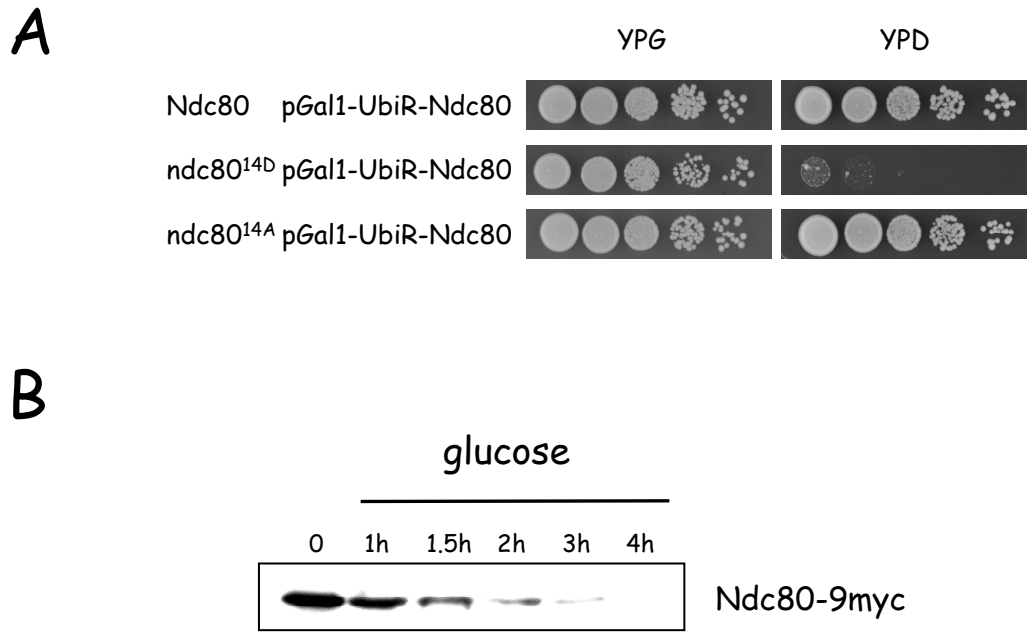

Figure 28. A tool for the analysis of the lethal ndc80^{14D} mutant: the Ndc80-depletion system.

(A) *Growth analysis of ndc80^{14D} and ndc80^{14A} mutants in the Ndc80-depletion strain.* Serial dilutions of the indicated strains were spotted onto YPG or YPD plates and incubated for 5 days (YPG) or 3 days (YPD) at 23°C.

(B) *Depletion of Ndc80 verified by immunoblotting.* Mid-log phase cells containing ndc80^{14D}-3HA pGal1-UbiR-NDC80-9myc were grown in YPGR (timepoint 0). 2% glucose was added to the culture to deplete Ndc80-expression and aliquots were taken at the indicated time points to analyse the Ndc80-9myc protein levels over time. NDC80-9myc was detected using an α-myc antibody.

5.7.2 The ndc80^{14D} mutant causes cell cycle arrest in mitosis

Using the described Ndc80-depletion system, the phenotype of the ndc80^{14D} mutant was analysed by light microscopy. An example of the morphology of cells possessing the ndc80^{14D} phenotype is shown in Figure 29A. A quantification of the observations is shown in Figure 29B. Cells containing the ndc80^{14D} mutant arrest in mitosis with a large bud. This observation is consistent with the idea that Ndc80 permanently activates the spindle checkpoint in its phosphorylated state (ndc80^{14D}). The corresponding Ndc80 wild-type control strain passed through the cell cycle as expected.

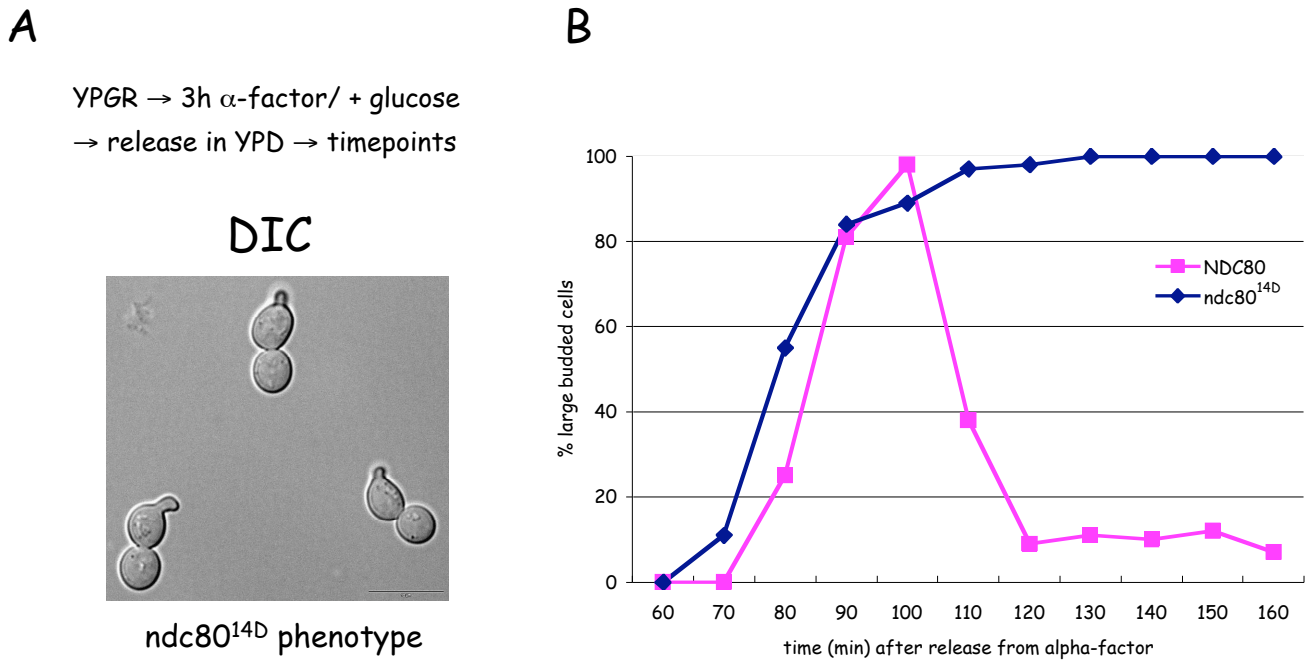

Figure 29. The ndc80^{14D} mutant causes cell cycle arrests in mitosis.

Logarithmically growing cells (NDC80 pGal1-UbiR-NDC80 or ndc80^{14D} pGal1-UbiR-NDC80) were grown to mid-logarithmic phase in media containing 0.1% galactose to allow for the expression of the Ndc80-9myc wild-type protein. The strain was synchronised in G_1 with α-factor. At the same time, Ndc80-9myc was depleted by the addition of 2% glucose. After 3 hours, cells were released from the G_1-arrest into glucose containing media (t=0). Samples were taken in 10 min intervals and analysed by light microscopy. An example of the morphological ndc80^{14D} phenotype 120 min after the release from α-factor is shown (A, Scale bar, 10 µm). The budding index of wild-type and ndc80^{14D} cells was determined at the indicated timepoints. The quantification is shown in (B). For each time point at least 100 cells were counted.

5.7.3 The spindle assembly checkpoint is permanently activated by the ndc80^{14D} mutant

To provide additional evidence that the ndc80^{14D} mutant indeed arrests with an active spindle assembly checkpoint, its Pds1 protein levels were analysed and compared to the wild-type situation to monitor the activation state of the checkpoint.

As described before (1.3.1), the meta-to-anaphase transition is regulated by the proteasome-dependent degradation of the Esp1-inhibitor Pds1. Therefore, the protein levels of Pds1 are a good indicator for the status of the spindle assembly checkpoint.

To analyse the spindle checkpoint in the ndc80^{14D} mutant, Pds1-levels were analysed in a timecourse experiment. Figure 30 summarises the result of this experiment. The FACS-analysis

shows that ndc80^{14D} arrests with a 2N DNA content even in the absence of the checkpoint inducing drug nocodazole (– nocodazole, ndc80^{14D}). This observation is consistent with the observed budding index (Figure 29) which showed that the ndc80^{14D} mutant arrests in mitosis. The Pds1-levels stay high throughout the timecourse which directly demonstrates that the spindle checkpoint is active. When the ndc80^{14D} mutant is released from the α-factor arrest in the presence of nocodazole (+ nocodazole, ndc80^{14D}), no difference is observed compared to the situation without nocodazole. The analysis of the wild-type strain in the absence of nocodazole shows the situation in the course of a normal cell cycle. Here, the Pds1-levels increase when cells enter mitosis (– nocodazole, NDC80, 60 min) and decrease upon exit from mitosis (– nocodazole, NDC80, 150 min). Since the cells are re-arrested in the G_1-phase of the following cell cycle by the re-addition of α-factor (100 min after the release from the initial α-factor arrest), the Pds1 protein levels stay low until the end of the timecourse. The analysis of the wild-type strain in the presence of nocodazole (+ nocodazole, NDC80) serves as a positive control for the state of an activated checkpoint. In this case, the checkpoint is artificially activated by the microtubule depolymerising drug which leads to unattached kinetochores and therefore to an activation of the spindle checkpoint with high Pds1-levels and a duplicated DNA content of 2N. The analysis of the Pds1 protein levels in the ndc80^{14D} mutant confirms the hypothesis after which Ndc80 in its phosphorylated state activates the checkpoint.

Many kinetochore mutants lead to an activation of the spindle checkpoint due to defective kinetochore-microtubule interactions, however they do not cause a permanent metaphase arrest. ndc80^{14D} is the first kinetochore mutant which constitutively activates the checkpoint in the presence of an intact kinetochore.

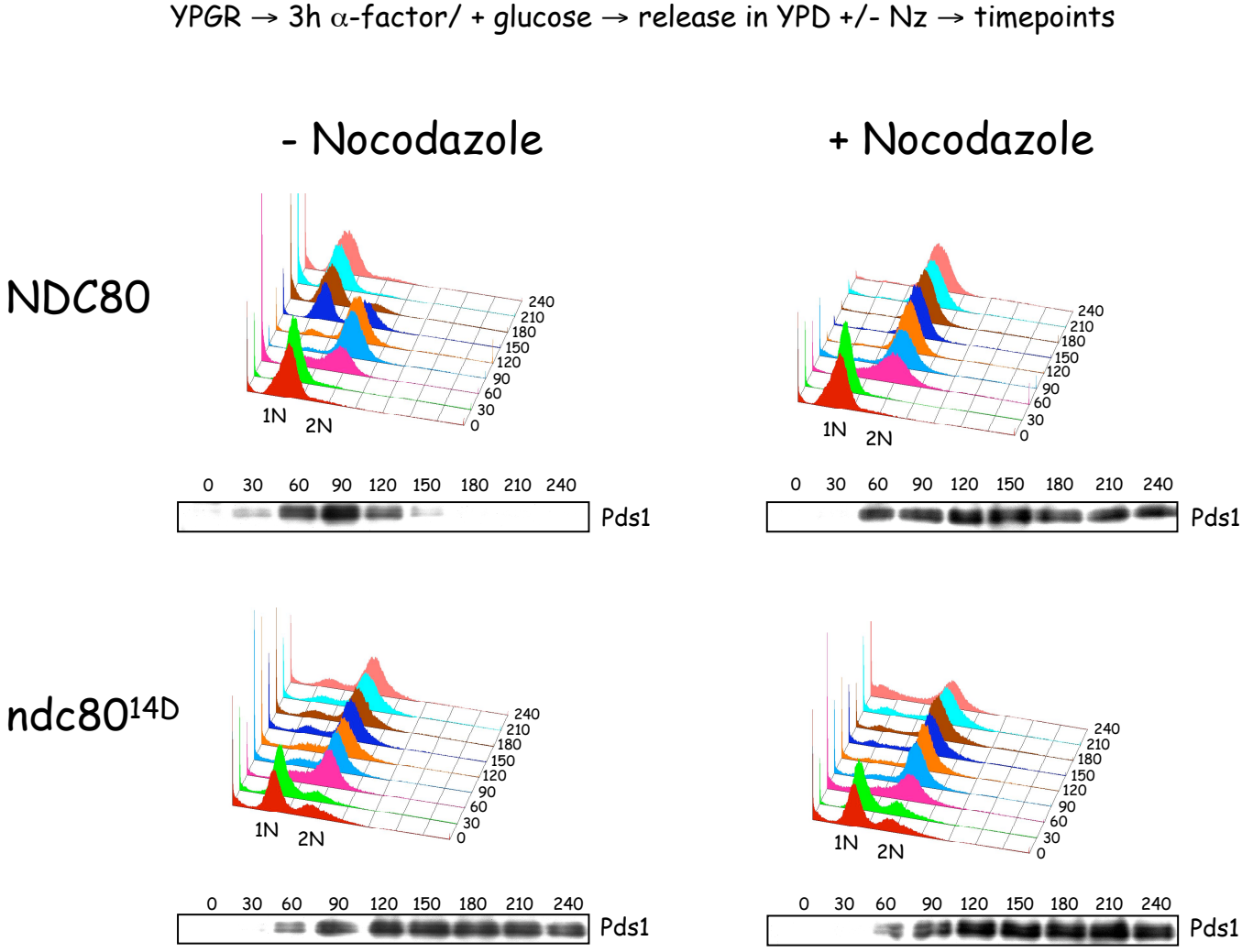

Figure 30. ndc80^{14D} constitutively activates the spindle checkpoint.

The spindle checkpoint was analysed in YSK1128 (NDC80 pGal1-UbiR-NDC80 PDS1-9myc) and YSK1174 (ndc80^{14D} pGal1-UbiR-NDC80 PDS1-9myc). Logarithmically growing cells were synchronised in G_1-phase with α-factor in the presence of glucose. After 3 hours, cells were released from the G_1-arrest into YPD in the presence or absence of 15 µg/ml nocodazole (Nz). When small buds emerged, α-factor was re-added to the culture in order to arrest the cells in the G_1-phase of the next cell cycle. At the indicated timepoints, samples were taken for immuno-detection of Pds1 (α-myc Western Blot) and FACS-analysis. In the histograms, the x-axis is the relative DNA content determined by propidium iodide fluorescence, and the y-axis is the relative number of cells. Protein loading was equal across the gels, as determined by Ponceau staining.

5.7.4 ndc80^{14D} cells arrest with short spindles and sister kinetochores under tension

The elevated Pds1-protein levels of the ndc80^{14D} mutant in the absence of nocodazole show that the spindle checkpoint is constitutively activated. If the kinetochores of the ndc80^{14D} mutant are intact, they should be able to support bipolar attachment and tension. Consequently, the cells should arrest in metaphase with the same phenotype as Cdc20-depleted cells. Cdc20 is the

substrate specifying subunit of the APC. If Cdc20 is depleted, the APC cannot be activated and target Pds1 for proteasome dependent degradation. Sister chromatids cannot be separated by the action of Esp1 and cells arrest in metaphase. At this stage of the cell cycle, the mitotic spindle is short and the sister kinetochores are bipolarly attached to microtubules and are consequently under tension. Since all 16 kinetochores of *S. cerevisiae* are clustered, they can be detected by fluorescence microscopy as one distinct signal. If tension is applied across the mitotic spindle apparatus, the two kinetochores of the sister chromatids are pulled towards the opposite poles. The distance between the two sister kinetochore clusters is big enough (about 1 µm) to be resolved by microscopy. Therefore, two distinct signals can be observed in the presence of tension. As described before, this situation is highly dynamic since the cohesin complex holds the sister chromatids together and therefore opposes the outward pulling forces of the spindle. As a consequence, at a given point in time a certain percentage of cells will have one signal whereas another subset of cells will show two signals ("chromosome breathing", Figure 31A).

To test the presence of tension in the ndc80^{14D} mutant, the mitotic spindle and the centromere region were labeled for the analysis by fluorescence microscopy. For the detection of the spindle, α-tubulin (tubulin1, TUB1), one of the subunits forming the microtubule polymers, was fused to Cherry (Cherry-TUB1), a fluorophore which emits light at 610 nm. To analyse the distribution of the kinetochores in the same strain, the centromere region of Chromosome 5 was labeled with GFP (CEN5-GFP) using the tetR/tetO-system (4.2.16).

The mitotic spindle (Cherry-TUB1) and the kinetochores (CEN5-GFP) of the ndc80^{14D} mutant were analysed by fluorescence microscopy. As a control for cells arrested with an active checkpoint, a Cdc20-depleted strain (pGal1-3HA-CDC20 Cherry-TUB1 CEN5-GFP) was cultured and analysed as described above. As shown in Figure 31A, the ndc80^{14D} mutant arrests with a short mitotic spindle indicative of the metaphase state. The cells showed either one or two CEN5-GFP signals. The latter indicates that kinetochores are under tension. The percentage of cells with one or two CEN5-GFP signals was determined and compared to the phenotype of the Cdc20-depleted cells. The quantification outlined in Figure 31B shows that the phenotype of the ndc80^{14D} mutant resembles the situation in Cdc20-depleted cells. Approximately two-third of the cells had two CEN5-GFP signals whereas one-third showed only one signal. The microscopically observed phenotype of the ndc80^{14D} mutant is consistent with the observation that Ndc80 in its phosphorylated state activates the checkpoint. In addition, the presence of bipolarity and tension

demonstrates that the kinetochore is intact which shows that the activation of the checkpoint is not caused by a general kinetochore defect but is rather a specific effect of Ndc80-phosphorylation.

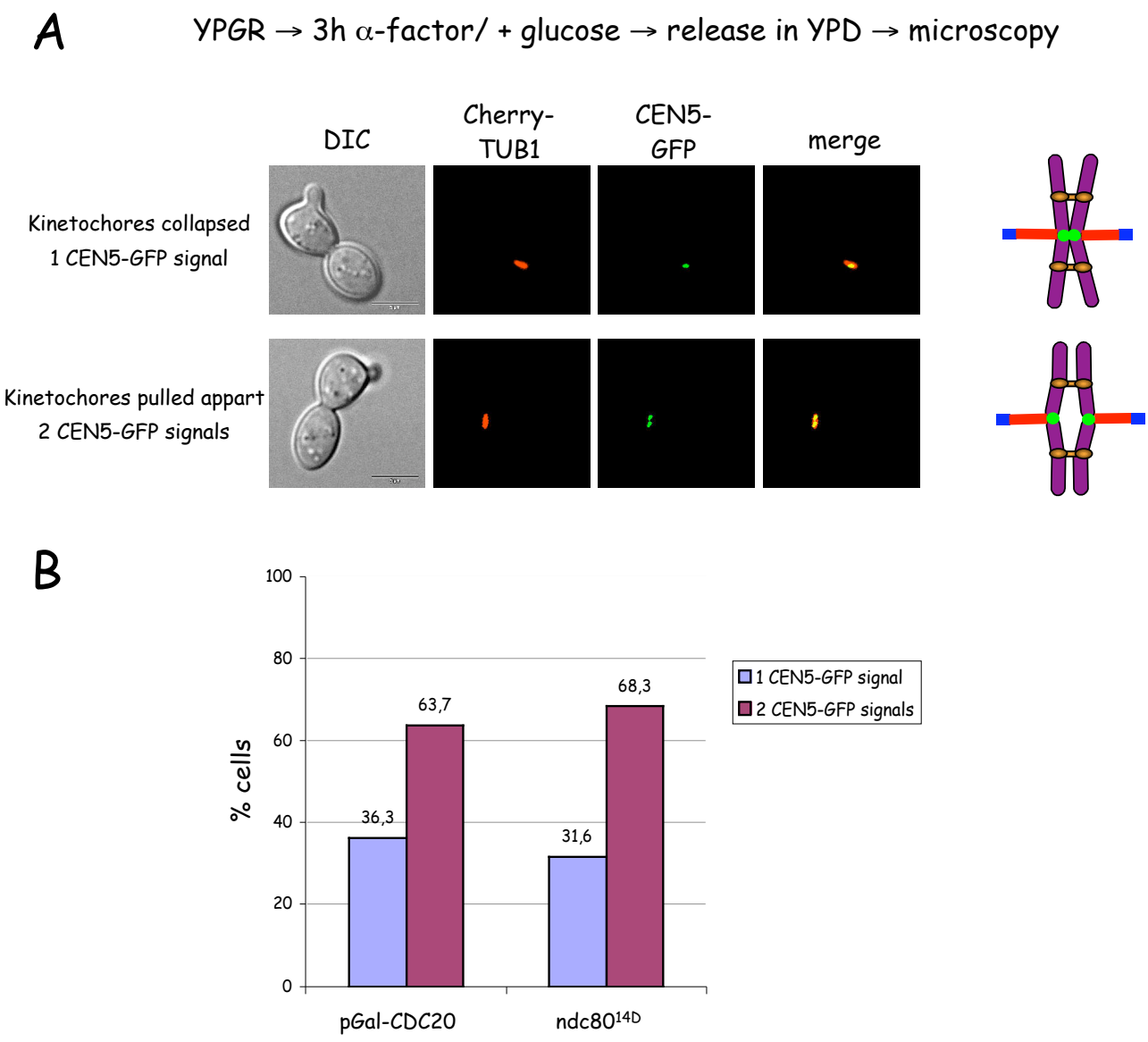

Figure 31. ndc80^{14D} arrests in mitosis with short metaphase spindles.

(A) *Phenotype of the ndc80^{14D} mutant.* Logarithmically growing cells (ndc80^{14D} pGal1-UbiR-NDC80 or pGal1-CDC20) were synchronised in G_1 with α-factor in the presence of glucose. After 3 hours, cells were released from the G_1-arrest into glucose containing media. 2 hours after the release, the spindle (Cherry-TUB1) and the kinetochores (CEN5-GFP) of the ndc80^{14D} mutant were analysed by fluorescence microscopy. Scale bar, 5 µm.

(B) *Quantification of CEN-signals.* The percentage of cells with and without tension at the kinetochores was determined by the number of CEN5-GFP signals. One signal indicates collapsed kinetochores and no tension, two signals indicate tension across the mitotic spindle. Cdc20-depleted cells arrest in metaphase with all sister kinetochores bipolarly attached (positive control). At least 100 cells were counted.

5.8 Mps1 is required for spindle checkpoint activation also downstream of Ndc80

The spindle checkpoint in the ndc80^{14D} mutant is activated although bipolar attachment is established as in wild-type, a situation which normally turns off the checkpoint. This observation indicates that Ndc80-phosphorylation by Mps1 is an intrinsic step in the spindle checkpoint signalling pathway. However, it is not known whether phosphorylation of Ndc80 is the only role of Mps1 in spindle checkpoint activation or whether Mps1 has more targets which have to be phosphorylated in order to activate the checkpoint.

To awnser this question, the ability of the ndc80^{14D} mutant to activate the checkpoint was analysed in Mps1-depleted cells. Mps1 is required for the activation of the checkpoint in response to spindle disruption (1.4.2). Therefore, wild-type cells depleted for Mps1 fail to arrest in the presence of nocodazole but instead undergo re-replication and aquire a DNA content of 4N. If Ndc80-phosphorylation was the only function of Mps1 in checkpoint activation, the checkpoint defect caused by the loss of Mps1 should be rescued in the ndc80^{14D} mutant and cells should arrest in metaphase even in the absence of Mps1 activity. On the other hand, if the activation of the checkpoint requires Mps1-activity downstream of Ndc80-phosphorylation, ndc80^{14D} cells should re-replicate their DNA in response to spindle damage by nocodazole.

Mps1 has two functions in the cell cycle (1.4.2). Its activity is required for spindle pole body (SPB) duplication at the G_1/S-transition as well as for the regulation of the spindle checkpoint. In order to analyse the checkpoint specific function of Mps1, wild-type (NDC80 pGal1-UbiR-NDC80 pGal1-3HA-MPS1) or ndc80^{14D} cells (ndc80^{14D} pGal1-UbiR-NDC80 pGal1-3HA-MPS1) were arrested with hydroxyurea (HU) which arrests the cells in S-phase. At this stage of the cell cycle, the duplication of the SPB has already been initiated and Mps1 is no longer required for this process. The protein expression of Mps1 and the Ndc80 wild-type copy was subsequently repressed by the addition of glucose and the spindle was disrupted by nocodazole in order to activate the checkpoint. Samples were taken in 1 hour intervals for the determination of the DNA content by FACS.

The FACS-analysis shows that Mps1-depleted Ndc80 wild-type cells aquire a 4N peak 3-4 hours after the release from the HU-arrest (Figure 32) which indicates that S-phase had been re-initiated in the absence of chromosome segregation. DNA-replication is also re-initiated the ndc80^{14D} mutant comparable to the Ndc80 wild-type cells. This result shows that the impaired checkpoint

of Mps1-depleted cells cannot be rescued in the ndc80^{14D} mutant indicating that Mps1 has a second role in checkpoint activation downstream of Ndc80-phosphorylation.

YPGR → 4h HU-arrest (after 3h15 min + glucose) → release in YPD + Noc → timepoints

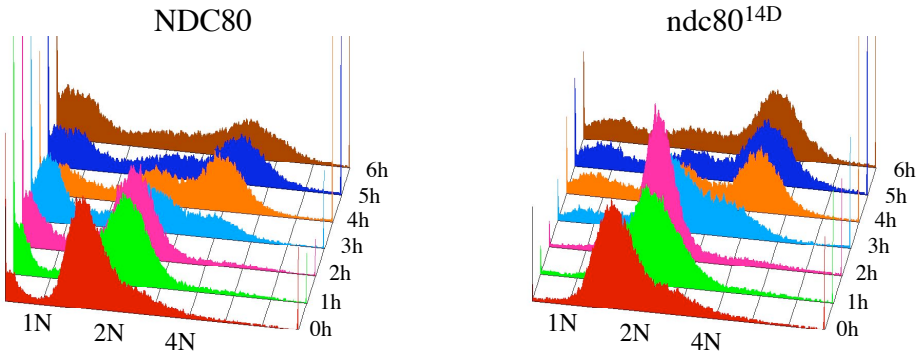

Figure 32. The ndc80^{14D} mutant is unable to activate the spindle checkpoint in Mps1-depleted cells.

YSK1158 (NDC80 pGal1-UbiR-NDC80 pGal1-3HA-MPS1) and YSK1176 (ndc80^{14D} pGal1-UbiR-NDC80 pGal1-3HA-MPS1) were synchronised in S-phase with hydroxyurea (HU) in galactose containing media to allow SPB-duplication. After 3h15 min, glucose was added to the culture to shut down Mps1- and Ndc80-protein expression. 4 hours after HU-addition, cells were released from the HU-arrest into YPD in the presence of nocodazole (Noc). At the indicated timepoints, samples were taken for FACS-analysis. In the histograms, the x-axis is the relative DNA content determined by propidium iodide fluorescence, and the y-axis is the relative number of cells.

5.9 The checkpoint of the non-phosphorylatable ndc80^{14A} mutant is deficient

The previous experiments demonstrate that Ndc80 in its pseudo-phosphorylated state (ndc80^{14D}) constitutively activates the spindle assembly checkpoint. If this working model is correct than non-phosphorylated Ndc80 should not be able to activate the checkpoint. To test this assumption, the non-phosphorylatable ndc80^{14A} mutant was analysed. This mutant contains 3 more mutations (T74,T79 and T82) than the ndc80^{11A} mutant which was shown to be sensitive to benomyl (Figure 24B). The 14 mutated Ser/Thr-sites correspond to the sites mutated in the ndc80^{14D} mutant. As outlined in Figure 25, the ndc80^{14A} mutant is viable. To test its checkpoint integrity, the viability of the strain in the presence of the checkpoint activating drug nocodazole was analysed and compared to the wild-type situation in a nocodazole survival assay. Cells were

exposed to nocodazole in order to disrupt the mitotic spindle and activate the checkpoint prior to plating the cells in the absence of nocodazole. Cells with a functional checkpoint arrest in metaphase and resume dividing when the drug is removed, thus retaining a high level of viability. In contrast, cells that lack an intact checkpoint undergo anaphase in the presence of nocodazole and missegregate their DNA, resulting in reduced cell viability. NDC80 and ndc80^{14A} strains were exposed to nocodazole for 0, 2 and 5 h and their viability was determined. Figure 33 shows that the ndc80^{14A} mutant lost viability when exposed to nocodazole for 5 hours, whereas NDC80 cells maintained a much higher level of viability. This result shows that if phosphorylation is abolished, Ndc80 can no longer activate the checkpoint. This observation is therefore consistent with the proposed model.

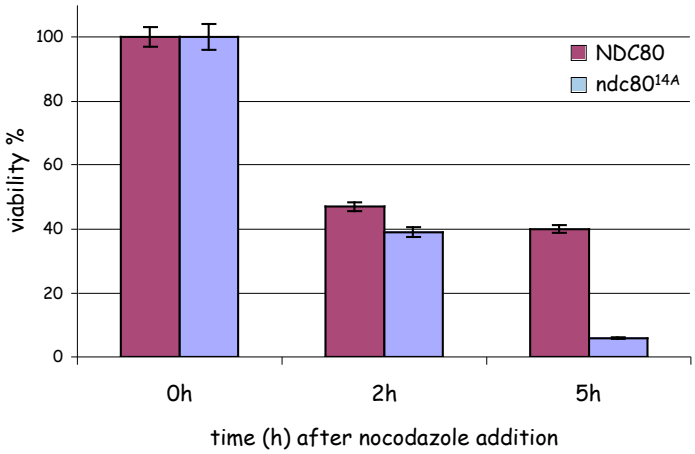

Figure 33. Ndc80 phosphorylation is required for the activation of the spindle checkpoint.

Nocodazole survival assay. NDC80 or ndc80^{14A} strains were exposed to nocodazole (15µg/ml) for 0, 2 and 5 hours and then plated onto YPD plates lacking the drug. The plates were incubated at 25°C for 3 days. Viability was calculated by dividing the number of colonies formed by cells treated with nocodazole for 2 or 5 h by the number of colonies formed by untreated cells (0 h).

6 DISCUSSION

The Ndc80-complex is a highly conserved, tetrameric complex composed of Ndc80, Nuf2, Spc24 and Spc25. It is a structural component of the *S. cerevisiae* kinetochore as shown by ChIP-analysis and fluorescence microscopy (Janke et al. 2001; Wigge et al. 2001).
A number of interesting observations from different groups indicated that the kinetochore might be a target for Mps1 and that its phosphorylation could have an influence on the activity of the spindle checkpoint. In general, phosphorylation events are known to be implicated in spindle checkpoint signalling (Andreassen et al. 1992). The presence of an unknown phospho-epitope at the mammalian kinetochore has been connected to the activity of the spindle checkpoint (Gorbsky and Ricketts 1993). Furthermore, the overexpression of Mps1 leads to cell cycle arrest in mitosis (Hartwick et al. 1996) and Mps1-depleted cells are not able to respond to the disruption of the mitotic spindle (Stucke et al. 2002). In mammalian cells, Mps1 transiently associates with the kinetochore during mitosis (Stucke et al. 2002). Finally, members of the Ndc80-complex have been implicated in the reguation of the spindle checkpoint (Janke et al. 2001) and are required for the recruitment of the checkpoint proteins Mad1 and Mad2 to the kinetochore in mammalian cells (Martin-Lluesma et al. 2002). Taken together, these observations were the basis for investigations concerning the relation between the Ndc80-complex and Mps1 in the context of spindle checkpoint regulation.

6.1 Ndc80 physically interacts with Mps1

In mammalian cells, the kinetochore localisation of Mps1 was shown to be dependent on the presence of the Ndc80-complex *in vivo* (Stucke et al. 2004). The present work provides two lines of experimental evidence that Mps1 directly interacts with Ndc80 in yeast. First, a weak interaction between endogenous Msp1 and the Ndc80-complex has been observed in *S. cerevisiae* (C. Jaeger, unpublished results). This interaction was shown to be enhanced when Mps1 is overexpressed to arrest the cells with an active spindle checkpoint (Figure 13). Second, the *in vitro* binding assay with His_{10}-$Ndc80^{1-257}$ as a bait demonstrated that the interaction between Ndc80 and Mps1 is mediated by the N-terminal globular domain of Ndc80 (Figure 16). These observations show that Mps1 physically interacts with Ndc80. However, they do not give any

information whether the observed physical interaction takes place at the kinetochore, in solution or both. To answer this question, the kinetochore localisation of Mps1 was studied.

The Mps1 kinetochore localisation could not be determined by fluorescence microscopy (Mps1-GFP and Mps1-3xGFP), most likely due to the low abundance of the protein and the transient nature of the interaction between kinases and their substrates. In contrast to the microscopical studies, the ChIP-analysis showed that Mps1 specifically associates with centromeric DNA (Figure 14). One possible explanation for the fact that Mps1 could be detected at the kinetochore by ChIP but not by fluorescence microscopy is that during the ChIP-assay, protein-protein interactions are covalently crosslinked using formaldehyde. Therefore, a potential transient association of Mps1 with the kinetochore is frozen at a particular point in time. This association can then be studied without having the problem of continuous association and dissociation of Mps1 from the kinetochore.

The results from the Spc24-ProA pull down, the *in vitro* binding assay with His_{10}-$Ndc80^{1-257}$ and the ChIP-analysis showed that Mps1 transiently associates with the yeast kinetochore via the N-terminal globular domain of Ndc80. These data are consistent with the observations made in the mammalian system.

6.2 Mps1 phosphorylates Ndc80 *in vitro* and *in vivo*

The kinase assays showed that Ndc80 is a target for Mps1 *in vitro* (Figure 15). When the entire Ndc80-complex was used as a substrate, Ndc80 was preferentially phosphorylated by Mps1. For the other three members of the complex (Nuf2, Spc24 and Spc25), only weak phosphorylation could be observed. The phosphorylation of Ndc80 by Mps1 was confirmed using recombinant proteins. It was shown that Mps1 itself was phosphorylated when purified from *E. coli*. Since *E. coli* does not express any Ser/Thr-protein kinases, this result indicates that Mps1 does not require a priming kinase for its own activation *in vitro*. This finding stands in contrast to the observation that Mps1 requires an initial phosphorylation by the cyclin-dependent kinase Cdc28 for its own activation *in vivo* (Jaspersen et al. 2004). One hypothetical explanation for this discrepancy would be that an inhibitory factor plays a role in Mps1-activation *in vivo*. Upon phosphorylation of Mps1 by Cdc28, the inhibitor dissociates from Mps1 which therefore gets active. Since

recombinantly expressed Mps1 is not associated with such an inhibitor, it is active in the absence of Cdc28-activity.

Interestingly, the globular N-terminus of Ndc80 was shown to be the main target of Mps1. This part of the protein contains the HEC-domain which is highly conserved throughout evolution. The data from the *in vitro* kinase assays indicate that the N-terminus of Ndc80 is regulated by phosphorylation. These findings could be confirmed *in vivo*. It was shown that Ndc80 gets phosphorylated in response to Mps1-overexpression (Figure 17), mainly at the globular N-terminus as verified by mass spectrometry (Figure 19). The observed Ndc80-band shift was shown to be due to the phosphate groups which are introduced into the protein by phosphorylation since Ndc80 collapses into one band upon phosphatase-treatment. However, the addition of one phosphate group increases the mass of the protein only about 98 Da. Even the presence of several phosphate groups would not explain the observed shift. This effect is rather due to the additional negative charges introduced by phosphorylation. These negative charges prevent also negatively charged SDS-molecules from binding to the denatured protein at these regions. The effect of the rejected SDS-molecules is stronger than the introduction of additional negative charges by the phosphate groups. The overall charge of the phosphorylated protein coated with SDS-molecules is therefore less negative than the unmodified protein. Therefore, the SDS-coated protein is retained during the gel electrophoresis. In total, 35 phosphorylation sites were identified for Ndc80. However, only a moderate Ndc80-band shift can be observed in response to Mps1-overexpression. The mass spectrometry analyses already implied, that not all Ndc80-molecules are phosphorylated on all identified phosphorylation sites at the same time indicating that a complex mixture of phosphorylated Ndc80-species is present *in vivo*. A second reason for the moderate shift of Ndc80 might be the fact that the majority of the identified Phospho-Serine and Phospho-Threonine residues are embedded in a hydrophilic amino acid environment. As mentioned above, the observed band shift is due to the rejected SDS-molecules which bind to hydrophobic streches of the polypeptide-chain. Since the amino acids around the phosphorylated residues in the Ndc80-protein are mainly hydrophilic, SDS binds to these regions with a low affinity even in the non-phosphorylated protein. Therefore, the addition of more negative charges by phosphorylation in a hydrophilic sequence has only a minor effect on the rejection of SDS-molecules in these regions and thus on the migration of phosphorylated Ndc80 in the SDS-electrophoresis. The small effect of additional negative charges on the running

behaviour of Ndc80 can also be seen for the ndc80^{14D}-protein. Although 14 negative charges are introduced by the Ser/Thr to Asp mutations, the ndc80^{14D}-protein migrates only slightly slower than the wild-type protein in the SDS-PAGE (Figure 26A).

As mentioned above, 35 *in vitro* phosphorylation sites were identified for Ndc80 by mass spectrometry (Table 2). The majority of these sites are located in the globular N-terminus of the protein which includes the evolutionary conserved HEC-domain (Figure 19). From these sites, 11 could be confirmed *in vivo*. One reason for the discrepancy between the number of identified *in vitro* and *in vivo* phosphorylation sites by mass spectrometry is the fact that the identification of phosphorylation sites is dependent on the amount of phosphorylated protein which is used for the analysis. For the *in vitro* analysis (kinase assays), recombinant Ndc80 could be easily produced in high amounts (microgram range). In contrast, kinetochore proteins like Ndc80 are low abundant proteins. Therefore, less protein was available for the identification of *in vivo* phosphorylation sites from the Spc24-ProA pull down. A second reason why not all *in vitro* sites could be confirmed *in vivo* is the fact that during the purification of the Ndc80-complex from yeast whole cell lysates, phosphate groups might be lost due to the residual activity of endogenous phosphatases despite the presence of phosphatase inhibitors. Furthermore, Ndc80 is present in a tetrameric complex *in vivo*. Therefore, some of the *in vitro* Ndc80-phosphorylation sites might not be accessible *in vivo* due to the interaction between Ndc80 and Nuf2. This idea is supported by the fact, that if the Ndc80-complex was used as a substrate in an Mps1-kinase assay, less phosphorylation sites could be identified than if Ndc80 alone was used. Finally, one has to consider that Ndc80 was purified as part of the Ndc80-complex for the identification of *in vivo* phosphorylation sites. However, free Ndc80 might be phosphorylated to a higher extend as complex-bound Ndc80.

The fact that a very high number of phosphorylated residues were identified by mass spectrometry raises the question about the specificity of Mps1. As mentioned in the introduction, several centrosomal Mps1-substrates (Spc98, Spc110 and Spc42) are described. From the identified Mps1-dependent phosphorylation-sites of these substrates, no clear Mps1-consensus sequence could be deduced indicating that Mps1 is a rather unspecific kinase. This finding is consistent with the fact that from the 35 Ndc80-phosphorylation sites which were identified in this study, no sequence preference of Mps1 could be derived.

Despite the unspecific nature of Mps1, there is also evidence that it has at least some degree of specificity. For example, when the entire tetrameric Ndc80-complex was used as a substrate in an *in vitro* kinase assay, Mps1 preferentially phosphorylated Ndc80. In contrast, the other three members of the complex (Nuf2, Spc24 and Spc25) were phosphorylated to a much lower extend. Furthermore, Ndc80 was heavily phosphorylated in the globular N-terminus (31 of 35 identified phosphorylation sites) but only weakly in the remaining C-terminal strech (4 phosphorylation sites) indicating that the phosphorylation by Mps1 is not completely random along the protein. In addition, the exogenous substrate BSA was not phosphorylatable by Mps1 at all which further indicates that Mps1 is not entirely unspecific.

Taken together, these findings confirm that Mps1 does not possess a stringent consensus sequence. The accessibility of a Ser/Thr-residue as well as conformational characteristics might be more important than the exact sequence environment around a particular site. In addition, regulatory factors might contribute to substrate specificity *in vivo*. Finally, the substrate specificity of Mps1 might simply be regulated by its own locatisation.

6.3 Mutagenesis strategy

To analyse the influence of Ndc80-phosphorylation on the spindle checkpoint, a reverse genetics approach was carried out which implied the identification of Ndc80-phosphorylation sites (Figures 18-22) and the analysis of Ndc80 mutants in which the identified phosphorylation sites were mutated either to Alanine to abolish phosphorylation or to Aspartic Acid to mimic phosphorylation. To simplify matters, the phosphorylation sites which are located in close proximity were mutated in groups. As mentioned above, in some cases it could not be clarified which of two adjacent sites (e.g. S73 or T74) carries the phosphate group or if both residues are phosphorylated. In these cases, both sites were mutated for two reasons. First, if a residue which is not phosphorylated *in vivo* is replaced by Alanine, most likely this mutation would be tolerated and not influence the function of the protein significantly. Second, a phosphate group introduces two negative charges into the protein whereas the mutation from Ser/Thr to Asp adds only one negative charge to the protein. Therefore, the replacement of one phosphorylated residue by two adjacent Ser/Thr to Asp mutations reflects the *in vivo* situation in terms of charge.

The first step in the functional characterisation of Ndc80-phosphorylation was the analysis of

non-phosphorylatable Ndc80-mutants. Instead of mutating 35 phosphorylation sites to Alanine individually, Ndc80 deletion mutants were constructed to eliminate several phosphorylation sites at once. Such preliminary analysis should give a first idea whether phosphorylation of the Ndc80 N-terminus is at all required for cell viability or spindle checkpoint function. The analysis showed, that even the deletion of the N-terminal 116 amino acids had no effect on cell viability, temperature sensitivity, protein expression or spindle checkpoint function (Figure 23). The respective mutant (ndc80 Δ1-116) lacks 24 of the identified phosphorylation sites. The deletion of the entire N-terminus including the HEC-domain however resulted in lethality of the respective strain (ndc80 Δ1-255) indicating an essential function of this conserved part of the protein.

6.4 Functional analysis of Ndc80-phosphorylation

6.4.1 Non-phosphorylatable Ndc80 (ndc80^{11A}) causes a defective spindle checkpoint

Since the deletion mutant ndc80 Δ1-116 already lacks the majority of the identified phosphorylation sites, this viable strain was a good starting point for the replacement of individual Serine or Threonine residues by Alanine using site-directed mutagenesis. The introduction of three Ser/Thr to Ala-mutations resulted in a benomyl sensitive phenotype of the respective strain (ndc80 Δ1-116 S205A T248A T252A; Figure 24B). As described above (5.5.2), low concentrations of benomyl interfere with kinetochore-microtubule attachments. Since the spindle checkpoint of this mutant is impaired, cells fail to delay their cell cycle progression and die because of genomic instability.

The cause of the benomyl sensitivity could be the three point mutations alone (S205A T248A T252A) or a combination of these mutations and a function in the deleted N-terminal stretch of the protein (Δ1-116 + S205A T248A T252A). Detailed analysis of numerous Ser/Thr to Ala mutants of Ndc80 showed that the latter is the case. In total, 11 sites are required for the benomyl sensitive phenotype of the respective Alanine mutant (ndc80 S205A T248A T252A S37A T38A T43A T21A S22A S4A T5A S6A or ndc80^{11A}) which clearly demonstrates that the benomyl sensitivity is exclusively caused by the elimination of phosphorylation of the Ndc80 N-terminus. This result indicated that the spindle checkpoint of the non-phosphorylatable Ndc80 protein is defect and that the checkpoint is regulated by Ndc80-phosphorylation.

6.4.2 Pseudo-phosphorylated Ndc80 activates the spindle checkpoint

Protein-phosphorylation is a reversible process. Typically, a phospho-protein fulfills opposite functions in its phosphorylated and unphosphorylated state. Therefore, the ndc80^{11D} mutant was generated and its phenotype was studied. The mutated phosphorylation sites of this mutant correspond to the residues of the ndc80^{11A} mutant. The replacement of Serine or Threonine residues by Aspartic Acid introduces a negative charge into the protein which is thought to mimic phosphorylation. The analysis of the ndc80^{11D} mutant on benomyl containing plates revealed that it is even more resistant to this drug than the wild-type strain and hence shows the opposite phenotype as the corresponding ndc80^{11A} mutant. This result indicated that Ndc80 in its phosphorylated form strongly activates the spindle checkpoint. The fact that the ndc80^{11D} mutant grows even better than the respective wild-type strain makes sence considering that a strong spindle checkpoint signal delays the cell cycle in metaphase until the cell has reached a state in which the mitotic spindle is properly assembled. If the spindle checkpoint is efficiently activated, a certain percentage of cells of a given population will reach this state even in the presence of higher concentrations of benomyl. These cells are able to segregate their DNA correctly and thus grow in the presence of high benomyl concentrations.

The analysis of the Ndc80 mutants on benomyl containing plates indicated that the ndc80^{11D} mutant strongly activates the spindle assembly checkpoint. One possible explanation would be that the negatively charged surface of the Ndc80 amino-terminus is responsible for this effect. It seemed therefore possible, that the strength of this signal is determined by the number of negative charges. Consequently, the addition of more negative charges should enhance the checkpoint signal. This hypothesis was tested by relpacing three more Threonine residues in the HEC-domain by Aspartic Acid. The resulting strain (ndc80^{14D}) is inviable (Figure 25).

It was tested whether all 14 mutated sites are required for the lethal phenotype of this strain. For this purpose, groups of mutated residues were again converted back to the wild-type sequence. However, the resulting strains (YSK868, YSK894, YSK949, YSK998, YSK999) were viable indicating that the mutation of all clusters of phosphorylated sites is required for the lethal phenotype (Table 3).

The lethality of the ndc80^{14D} mutant could be explained by the fact that the negative surface of the N-terminal part of the protein signals the checkpoint to arrest the cells in metaphase. Since

this checkpoint activation is constitutive, the respective strain cannot proceed through the cell cycle, stays permanently arrested in mitosis and eventually dies. The fact that the corresponding Alanine mutant ndc80^{14A} is viable (Figure 25, line 7) indicates that the lethality is not caused by the high number of mutations *per se* but is rather a specific effect of the negatively charged Ndc80-surface. Furthermore, the lethality of the ndc80^{14D} mutant can be rescued by the elimination of the spindle checkpoint pathway (Δmad2 or Δbub1) which shows that this phenotype is caused by permanent checkpoint activation. At this point it should be noted, that the growth of the respective strains (ndc80^{14D} Δmad2 or ndc80^{14D} Δbub1) is not competely restored to the wild-type level (Figure 25, compare line 3 and 5 with line 1). This observation indicates that there is a yet unidentified factor or process which contributes to the lethal phenotype of ndc80^{14D}. The specificity of the described genetic interaction between ndc80^{14D} and the spindle checkpoint is further supported by the fact that the re-introduction of a wild-type copy of MAD2 or BUB1 on a plasmid into the respective strains (ndc80^{14D} Δmad2 or ndc80^{14D} Δbub1) restores the lethality of the ndc80^{14D} mutant. In addition, the lethality of the Ndc80 knock-out mutant (Δndc80) cannot be rescued by the deletion of a checkpoint protein clearly demonstrating that the presence of the ndc80^{14D} protein is responsible for the observed effect.

Ndc80 in its phosphorylated form activates the spindle checkpoint. However, it is unclear whether the negatively charged surface of the phosphorylated protein is responsible for this effect or whether the 14 sites in particular are important for the observed checkpoint activation. There is evidence for both possibilities. On the one hand, if three particular point mutations (T74D, T79D, T82D) of the lethal ndc80^{14D} mutant (YSK869) are replaced by three other mutations (T54D, S56D, T58D) which are located in the same domain of the protein, the resulting strain (YSK975) is no longer lethal (Table 3). Although the two mutant proteins carry the same number of negative charges in the same region of the protein, one mutant is lethal whereas the other mutant is viable indicating that the three original sites (T74D, T79D, T82D) specifically contribute to the lethality of the ndc80^{14D} mutant and are not replaceable by other identified phosphorylation sites in the vicinity. This finding indicates that the checkpoint activation by the ndc80^{14D} mutant is a specific effect of the 14 mutated sites. However, there is also evidence that the negative surface of the protein *per se* triggers checkpoint activation. One mutant was created which carries 17 Ser/Thr to Asp mutations (ndc80^{17D}, YSK925) and activates the spindle checkpoint like the ndc80^{14D} mutant. The ndc80^{17D} mutant carries 6 different mutations as the ndc80^{14D} mutant. Both

mutants are lethal and can be rescued by the elimination of the spindle checkpoint. This result indicates that the negatively charged Ndc80-surface *per se* is responsible for the lethal phenotype. These findings indicate that some of the mutations of the ndc80^{14D} mutant are absolutely required for the observed phenotype whereas others are replaceable by alternative point mutations.

The genetic interaction studies indicate, that the phosphorylation status of Ndc80 signals the spindle checkpoint the correct assembly of the mitotic spindle. If there is a spindle defect, Ndc80 stays phosphorylated and arrests the cell in metaphase until bipolar attachment of all kinetochores is achieved. This arrest is dependent on MAD2 or BUB1. In addition, it could be shown that the ndc80^{14D} mutant is not involved in the regulation of the spindle positioning checkpoint, since deletion of BUB2, a key regulator of this pathway does not rescue the lethality of the ndc80^{14D} mutant (Figure 25, line 13). This observation is another indication that the activation of the spindle assembly checkpoint by Ndc80-phosphorylation is a specific effect.

The described findings are consistent with the fact that a phospho-epitope is present at unattached kinetochores in prometaphase cells when no tension across the mitotic spindle is applied (Gorbsky and Ricketts 1993).

The microscopical analysis revealed that the ndc80^{14D} mutant arrests with large buds indicating a cell cycle arrest in mitosis (Figure 29). This observation confirms the benomyl-analysis which indicated that the viable ndc80^{11D} mutant induces a strong spindle checkpoint signal (Figure 24). Furthermore, these data are consistent with the finding that the ndc80^{14D} mutant causes a lethal phenotype which can be rescued by the elimination of the spindle assembly checkpoint (Figure 25). The fact that the Pds1-protein levels in the ndc80^{14D} mutant remain high over a long period of time even in the absence of nocodazole provides evidence on the molecular level that cells arrest in metaphase as a consequence of a constitutively activated spindle checkpoint (Figure 30).

In contrast to the ndc80^{14D} mutant, many temperature-sensitive kinetochore mutants (kinetochore defect) or Scc1-depleted cells (tension deficient) cause a mitotic arrest with high Pds1-levels which are less stable and therefore start to decline when cells are kept at restrictive conditions over a longer period of time.

Furthermore, the FACS-analysis of the ndc80^{14D} mutant is consistent with the high Pds1-protein levels and the observed budding index. If the checkpoint was non-functional, cells would re-replicate their DNA and aquire a 4N peak. However, ndc80^{14D} cells arrest with a DNA-content of 2N in the absence of nocodazole indicating a fully functional checkpoint. The fact that the

ndc80^{14D} mutant arrests with an active spindle checkpoint in the presence of nocodazole is expected because both the ndc80^{14D} mutant and nocodazole cause the same effect, namely the activation of the checkpoint.

Finally, ndc80^{14D} cells arrest with short spindles and sister kinetochores under tension (Figure 31), a situation which normally inactivates the checkpoint. This phenotype confirms that Ndc80-phophorylation is an intrinsic step in spindle checkpoint activation.

Experiments with non-phosphorylatable Ndc80-mutants confirm this model. In the presence of nocodazole, the viability of the ndc80^{14A} mutant was reduced compared to the wild-type control strain which shows that if phosphorylation is abolished, Ndc80 can no longer activate the checkpoint (Figure 33). This observation is consistent with the observed benomly-sensitivity of the ndc80^{11A} mutant and confirms that Ndc80 is able to activate the checkpoint only in its phosphorylated form.

6.5 The ndc80^{14D} protein is part of a functional kinetochore

Several observations indicate that the ndc80^{14D} protein is part of a functional kinetochore which in turn shows that the observed checkpoint activation of the ndc80^{14D} mutant is not simply caused by a defective kinetochore.

The viability of the ndc80^{14A} mutant already indicates that the lethality of ndc80^{14D} is a specific effect of the negative charges introduced by the Ser/Thr to Asp mutations and is not caused by the high number of point mutations *per se*. Furthermore, the ndc80^{14D} protein is expressed in equal amounts as the wild-type protein (Figure 26A). When the ndc80^{14D} mutant and the wild-type are expressed in the same strain, both forms of Ndc80 can bind to the kinetochore, as determined by ChIP-analysis and fluorescence microscopy (Figure 26B and C). This finding indicates that the ndc80^{14D} protein can compete with the wild-type protein for binding sites at the kinetochore which in turn shows that the ndc80^{14D} protein is functional in respect to expression, stability and subcellular localisation.

The lethal phenotype of the ndc80^{14D} mutant can be rescued by the elimination of the spindle checkpoint (Δmad2 or Δbub1). This is not the case for the Δndc80 mutant (Figure 25) which indicates that the presence of the ndc80^{14D} protein is required for the permanent activation of the

spindle checkpoint. This finding further shows that the ndc80^{14D} protein fulfills a specific function rather than causing a general kinetochore defect.

Taken together, these data indicate that the ndc80^{14D} protein itself is intact. However, they do not provide evidence that the overall kinetochore integrity is intact. An impaired kinetochore structure could be the cause for the observed checkpoint activation. In this case, the kinetochores would not be able to resist the tension which is created by the pulling forces of the mitotic spindle. As a consequence, defective kinetochores collapse if tension is applied. This has been shown to be the case for several temperature sensitive kinetochore mutants. However, the microscopical analysis of the spindle and the GFP-labeled centromers in the ndc80^{14D} mutant indicated that the overall kinetochore function is intact. Kinetochores of ndc80^{14D} cells are under tension (Figure 31), an indirect indication of bipolarity. In contrast, kinetochores of Δndc80-cells are completely detached from the mitotic spindle.

The length of the mitotic spindle is an additional evidence that the overall structure of the kinetochore is intact since kinetochore mutants (like Δndc80) which impair the kinetochore structure show elongated metaphase spindles and cannot fully resist the tension applied by the mitotic spindle apparatus. In the ndc80^{14D} mutant however, the spindle is short indicative of the metaphase state and an active checkpoint.

The short spindle and the presence of tension in the ndc80^{14D} mutant finally confirms the proposed model according to which Ndc80 in its phosphorylated state activates the checkpoint.

6.6 Mps1 is required for spindle checkpoint activation also downstream of Ndc80

The FACS-analysis of Mps1-depleted cells showed that the impaired checkpoint in the absence of Mps1-activity cannot be rescued in ndc80^{14D} cells (Figure 32). This result indicates that Mps1 has a second function in checkpoint activation downstream of Ndc80-phosphorylation. One possible target of Mps1 which is involved in spindle checkpoint signalling is Mad1. It has been shown that Mad1 is phosphorylated in mitosis (Hartwick et al. 1995) and that Mad1-phosphorylation is dependent on Mps1-overexpression (Hartwick et al. 1996). These findings indicate that Mad1 is an Mps1-substrate whose phosphorylation might contribute to the proper activation of the spindle checkpoint.

In the present work, some preliminary analyses has been carried out in order to characterise the relation between Mps1 and Mad1 in more detail. After overexpression of Mps1, the phosphorylation status of Mad1 was analysed by mass spectrometry. This way, seven *in vivo* phosphorylation sites of Mad1 were identified (T240, S474, T502, S514, S516, T529 and S530). In the future, it will be interessting to investigate whether Mad1-phosphorylation by Mps1 contributes to the regulation of spindle checkpoint activity.

There is another evidence that Mps1 acts downstream of the kinetochore. As mentioned in the introduction, overexpression of Mps1 causes cell cycle arrest in mitosis. Unlike the checkpoint arrest in response to spindle depolymerising drugs such as benomyl, this arrest can be established and maintained even in the absence of intact kinetochores (*ndc10-1*). This result indicates that Mps1 has another non-kinetochore target which is involved in the activation of the spindle checkpoint independent on the kinetochore itsself (Fraschini et al 2001; Poddar et al. 2004).

6.7 A second role of Ndc80-phosphorylation

It was shown that Ndc80 is phosphorylated by the Aurora B-type kinase Ipl1 in yeast and mammals (Cheeseman et al. 2002; De Luca et al. 2006). Ipl1 acts in resolving syntelic attachments of sister kinetochores. The phosphorylation of Dam1 and Ndc80 by Ipl1 is proposed to weaken the interaction between the Dam1-complex and the Ndc80-complex thereby facilitating the formation of bipolar connections between chromosomes and the spindle (Shang et al. 2003). These data indicate that phosphorylation of Ndc80 plays a role in regulating the attachment/detachment dynamics of kinetochore microtubules. This aspect of Ndc80-phosphorylation is distinct from the described checkpoint-activating function of Ndc80-phosphorylation since the pseudo-phosphorylated ndc80^{14D} protein is able to resist the tension which is established as a consequence of bipolarly attached sister kinetochores. This result indicates that the 14 mutated phosphorylation sites of the ndc80^{14D} protein do not contribute to the weakening of kinetochore-microtubule attachments. Strikingly, these sites do not include Ipl1-consensus sites.

6.8 A Model for spindle checkpoint regulation by Ndc80-phosphorylation

The data which were accumulated during this work add new information to the current model of the spindle assembly checkpoint of *S. cerevisiae*. It is known for some time that the kinetochore serves as a platform for the spindle checkpoint pathway since many of the checkpoint proteins like Mad1, Mad2 or Bub1 localise to this structure during mitosis. However, up to now it remained unclear which is the actual signal that transmits the information of the presence of unattached kinetochores and the absence of tension to the checkpoint proteins like Mad2 which finally inhibit the APC through Cdc20.

The present work provides evidence that the signal which leads to an activation of the checkpoint is the phosphorylation of the globular domain of the integral kinetochore component Ndc80 by the kinase Mps1. According to this model (Figure 34), Mps1 phosphorylates the globular N-terminus of Ndc80 in response to unattached kinetochores or the lack of tension in prometaphase. This observation is consistent with the finding that a phospho-epitope is present at unattached kinetochores in mammalian cells (Gorbsky and Ricketts 1993). Ndc80 in its phosphorylated state activates the spindle assembly checkpoint via the spindle checkpoint proteins which in turn leads to the inhibition of the APC^{Cdc20}. Since Pds1 cannot be degraded in the absence of APC^{Cdc20}-activity, the separase Esp1 is kept inactive and thus cannot cleave the cohesin complex to initiate anaphase. As a consequence, the cell arrests in metaphase. Once bipolarity is achieved in metaphase, tension is build up across the mitotic spindle apparatus. This situation is proposed to lead to the dephosphorylation of Ndc80 by a yet unidentified phosphatase. This part of the model is highly speculative since a Ndc80-specific phosphatase has not been identified so far. Cdc14 or Glc7 are phosphatases which have been shown to regulate mitotic events and are therefore candidates for this step. Ndc80 in its unphosphorylated state is no longer able to activate the spindle checkpoint. Consequently, the APC^{Cdc20} gets active, Pds1 is degraded by the proteasome system and Esp1 cleaves the cohesins which leads to sister chromatid segregation in anaphase. The proteasome dependent proteolysis of Mps1 irreversibly inactivates the checkpoint in anaphase. Therefore, Mps1 has multiple functions in spindle checkpoint signalling. It contributes to checkpoint activation via the phosphorylation of Ndc80 and possibly other substrates downstream of Ndc80. In addition, APC^{Cdc20} dependent Mps1-degradation leads to checkpoint silencing in anaphase.

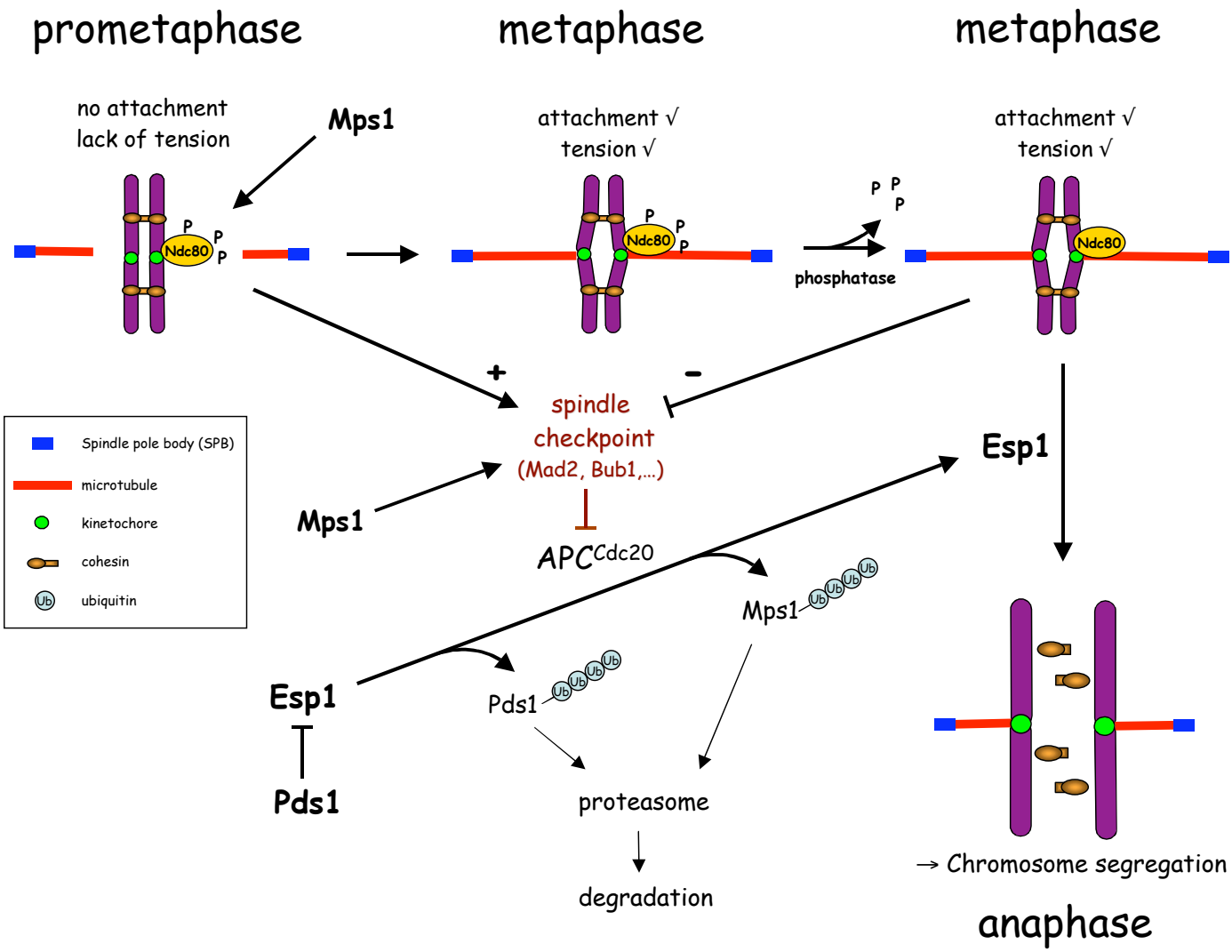

Figure 34: Mps1-dependent phosphorylation of Ndc80 as a mechanism for checkpoint activation and silencing during mitotic progression.

In prometaphase, unattached kinetochores are present in the cell and tension cannot be generated across the mitotic spindle apparatus. In this state, the action of Mps1 kinase is proposed to lead to the phosphorylation of the kinetochore component Ndc80 and possibly other substrates downstream of Ndc80 which in turn activates the spindle assembly checkpoint via Mad2, a checkpoint protein which inhibits the substrate specifying APC-subunit Cdc20 and therefore APC-activity. As a consequence, the cell cycle is delayed until all kinetochores become attached to microtubules. When all kinetochores are properly attached in metaphase, tension is built up across the mitotic spindle which is thought to induce dephosphorylation of Ndc80 by a yet unidentified phosphatase. As a consequence, the checkpoint is no longer activated by Ndc80-phosphorylation which leads to the inactivation of MAD2 and therefore to the activation of APC^{Cdc20}, the ubiquitin ligase responsible for the proteasome dependent degradation of the Esp1-inhibitor Pds1. Esp1 is a protease which cleaves the cohesin complex thereby initiating anaphase and allowing sister chromatids to seperate and segregate to the opposite spindle poles. Increased APC^{Cdc20} activity also leads to the degradation of Mps1 which contributes to the irreversible inactivation of the checkpoint at the onset of anaphase (Palframan et al. 2006).

7 REFERENCES

Abrieu,A., Magnaghi-Jaulin,L., Kahana,J.A., Peter,M., Castro,A., Vigneron,S., Lorca,T., Cleveland,D.W., and Labbe,J.C. (2001). Mps1 is a kinetochore-associated kinase essential for the vertebrate mitotic checkpoint. *Cell* 106, 83-93.

Ahonen LJ, Kallio MJ, Daum JR, Bolton M, Manke IA, Yaffe MB, Stukenberg PT, Gorbsky GJ. (2005). Polo-like kinase 1 creates the tension-sensing 3F3/2 phosphoepitope and modulates the association of spindle-checkpoint proteins at kinetochores. *Curr Biol* 15:1078-89.

Akhmanova, A. and Hoogenraad, C. C. (2005). Microtubule plus-end-tracking proteins: mechanisms and functions. *Curr Opin Cell Biol* 17, 47-54.

Andreassen,P. AND Margolis, R. (1992). 2-Aminopurine overrides multiple cell cycle checkpoints in BHK cells. *Proc Nati Acad Sci USA* Vol. 89, pp. 2272-2276.

Bloecher, A., Venturi, G. M. and Tatchell, K. (2000). Anaphase spindle position is monitored by the BUB2 checkpoint. *Nat Cell Biol* 2, 556-8.

Bardin, A. J., Visintin, R. and Amon, A. (2000). A mechanism for coupling exit from mitosis to partitioning of the nucleus. *Cell* 102, 21-31.

Bram, R. J. and Kornberg, R. D. (1987). Isolation of a Saccharomyces cerevisiae centromere DNA-binding protein, its human homolog, and its possible role as a transcription factor. *Mol Cell Biol* 7, 403-9.

Baker, R. E., Fitzgerald-Hayes, M. and O'Brien, T. C. (1989). Purification of the yeast centromere binding protein CP1 and a mutational analysis of its binding site. *J Biol Chem* 264, 10843-50.

Baker, R. E. and Masison, D. C. (1990). Isolation of the gene encoding the Saccharomyces cerevisiae centromere-binding protein CP1. *Mol Cell Biol* 10, 2458-67.

Bernard P, Maure JF, Javerzat JP. (2001). Fission yeast Bub1 is essential in setting up the meiotic pattern of chromosome segregation. *Nat Cell Biol* 3, 522-6.

Buvelot, S., Tatsutani, S. Y., Vermaak, D. and Biggins, S. (2003). The budding yeast Ipl1/Aurora protein kinase regulates mitotic spindle disassembly. *J Cell Biol* 160, 329-39.

Bouck, D. and Bloom, K. (2005a). The role of centromere-binding factor 3 (CBF3) in spindle stability, cytokinesis, and kinetochore attachment. *Biochem Cell Biol* 83, 696-702.

Bouck, D. C. and Bloom, K. S. (2005b). The kinetochore protein Ndc10p is required for spindle stability and cytokinesis in yeast. *Proc Natl Acad Sci U S A* 102, 5408-13.

Biggins, S., Severin, F. F., Bhalla, N., Sassoon, I., Hyman, A. A. and Murray, A. W. (1999). The conserved protein kinase Ipl1 regulates microtubule binding to kinetochores in budding yeast. *Genes Dev* 13, 532-44.

Biggins, S. and Murray, A. W. (2001). The budding yeast protein kinase Ipl1/Aurora allows the absence of tension to activate the spindle checkpoint. *Genes Dev* 15, 3118-29.

Bradford M. (1976). *Anal Biochem* 72, 248.

Cerutti, L. and Simanis, V. (1999). Asymmetry of the spindle pole bodies and spg1p GAP segregation during mitosis in fission yeast. *J Cell Sci* 112 (Pt 14), 2313-21.

Cai, M. and Davis, R. W. (1990). Yeast centromere binding protein CBF1, of the helix-loop-helix protein family, is required for chromosome stability and methionine prototrophy. *Cell* 61, 437-46.

Campbell L, Hardwick KG (2003). Analysis of Bub3 spindle checkpoint function in Xenopus egg extracts. *J Cell Sci*. 116, 617-28.

Castillo,A.R., Meehl,J.B., Morgan,G., Schutz-Geschwender,A., and Winey,M. (2002). The yeast protein kinase Mps1p is required for assembly of the integral spindle pole body component Spc42p. *J Cell Biol* 156, 453-465.

Chen, R. H., Waters, J. C., Salmon, E. D. and Murray, A. W. (1996). Association of spindle assembly checkpoint component XMAD2 with unattached kinetochores. *Science* 274, 242-6.

Ciferri C, Musacchio A, Petrovic A. (2007). The Ndc80 complex: hub of kinetochore activity. *FEBS Lett* 581(15):2862-9.

Ciosk R, et al. (1998). An ESP1/PDS1 complex regulates loss of sister chromatid cohesion at the metaphase to anaphase transition in yeast. *Cell* 93, 1067-76.

Connelly, C. and Hieter, P. (1996). Budding yeast SKP1 encodes an evolutionarily conserved kinetochore protein required for cell cycle progression. *Cell* 86, 275-85.

Cheeseman, I. M., Brew, C., Wolyniak, M., Desai, A., Anderson, S., Muster, N., Yates, J. R., Huffaker, T. C., Drubin, D. G. and Barnes, G. (2001). Implication of a novel multiprotein Dam1p complex in outer kinetochore function. *J Cell Biol* 155, 1137-45.

Cheeseman, I. M., Anderson, S., Jwa, M., Green, E. M., Kang, J., Yates, J. R., 3rd, Chan, C. S., Drubin, D. G. and Barnes, G. (2002a). Phospho-regulation of kinetochore-microtubule attachments by the Aurora kinase Ipl1p. *Cell* 111, 163-72.

Cheeseman, I. M., Drubin, D. G. and Barnes, G. (2002b). Simple centromere, complex kinetochore: linking spindle microtubules and centromeric DNA in budding yeast. *J Cell Biol* 157, 199-203.

Clarke, L. and Carbon, J. (1980). Isolation of a yeast centromere and construction of functional small circular chromosomes. *Nature* 287, 504-9.

Cooper, T.G. (1981). *Biochemische Arbeitsmethoden, W.de Gruyter-Verlag, Berlin, 49-51.*

Cyert, M. , Andmarc,T., Kirschner W. (1988). Monoclonal Antibodies Specific for Thiophosphorylated Proteins Recognize Xenopus MPF Developmental Biology 129,209-216

De Wulf, P., McAinsh, A. D. and Sorger, P. K. (2003). Hierarchical assembly of the budding yeast kinetochore from multiple subcomplexes. *Genes Dev* 17, 2902-21.

DeLuca J.G., Gal W.E., Ciferri C., Cimini D. ,Musacchio A. and Salmon, E.D. (2006). Kinetochore Microtubule Dynamics and Attachment Stability Are Regulated by Hec1 *Cell* 127, 969-982.

Douville,E.M., Afar,D.E., Howell,B.W., Letwin,K., Tannock,L., Ben David,Y., Pawson,T., and Bell,J.C. (1992). Multiple cDNAs encoding the esk kinase predict transmembrane and intracellular enzyme isoforms. *Mol Cell Biol* 12, 2681-2689.

Doheny, K. F., Sorger, P. K., Hyman, A. A., Tugendreich, S., Spencer, F. and Hieter, P. (1993). Identification of essential components of the S. cerevisiae kinetochore. *Cell* 73, 761-74.

De Antoni, A., Pearson, C. G., Cimini, D., Canman, J. C., Sala, V., Nezi, L., Mapelli, M., Sironi, L., Faretta, M., Salmon, E. D. et al. (2005). The Mad1/Mad2 complex as a template for Mad2 activation in the spindle assembly checkpoint. *Curr Biol* 15, 214-225.

Espelin, C. W., Kaplan, K. B. and Sorger, P. K. (1997). Probing the architecture of a simple kinetochore using DNA-protein crosslinking. *J Cell Biol* 139, 1383-96.

Enquist-Newman, M., Cheeseman, I. M., Van Goor, D., Drubin, D. G., Meluh, P. B. and Barnes, G. (2001). Dad1p, third component of the Duo1p/Dam1p complex involved in kinetochore function and mitotic spindle integrity. *Mol Biol Cell* 12, 2601-13.

Euskirchen, G. M. (2002). Nnf1p, Dsn1p, Mtw1p, and Nsl1p: a new group of proteins important for chromosome segregation in Saccharomyces cerevisiae. *Eukaryot Cell* 1, 229-40.

Elledge SJ (1996). Cell cycle checkpoints: preventing an identity crisis. *Science* 274:1664-1671.

Fisk,H.A. and Winey,M. (2001). The mouse Mps1p-like kinase regulates centrosome duplication. *Cell* 106, 95-104.

Friedman,D.B., Kern,J.W., Huneycutt,B.J., Vinh,D.B., Crawford,D.K., Steiner,E., Scheiltz,D., Yates,J., III, Resing,K.A., Ahn,N.G., Winey,M., and Davis,T.N. (2001). Yeast Mps1p phosphorylates the spindle pole component Spc110p in the N-terminal domain. *J Biol Chem 276*, 17958-17967.

Fraschini R, Beretta A, Lucchini G, Piatti S. (2001). Role of the kinetochore protein Ndc10 in mitotic checkpoint activation in Saccharomyces cerevisiae. *Mol Genet Genomics* 1,115-25.

Furge, K. A., Wong, K., Armstrong, J., Balasubramanian, M. and Albright, C. F. (1998). Byr4 and Cdc16 form a two-component GTPase-activating protein for the Spg1 GTPase that controls septation in fission yeast. *Curr Biol* 8, 947-54.

Fitzgerald-Hayes, M., Clarke, L. and Carbon, J. (1982). Nucleotide sequence comparisons and functional analysis of yeast centromere DNAs. *Cell* 29, 235-44.

Goshima, G. and Yanagida, M. (2000). Establishing biorientation occurs with precocious separation of the sister kinetochores, but not the arms, in the early spindle of budding yeast. *Cell* 100, 619-33.

Gorbsky, G. and Ricketts, W. (1993). Differential Expression of a Phosphoepitope at the Kinetochores of Moving Chromosomes The Journal of Celi Biology, Volume 122, Number 6, 1311-1321

Goh, P. Y. and Kilmartin, J. V. (1993). NDC10: a gene involved in chromosome segregation in Saccharomyces cerevisiae. *J Cell Biol* 121, 503-12.

Gardner, R. D., Poddar, A., Yellman, C., Tavormina, P. A., Monteagudo, M. C. and Burke, D. J. (2001). The spindle checkpoint of the yeast Saccharomyces cerevisiae requires kinetochore function and maps to the CBF3 domain. *Genetics* 157, 1493-502.

Geymonat, M., Spanos, A., Smith, S. J., Wheatley, E., Rittinger, K., Johnston, L. H. and Sedgwick, S. G. (2002). Control of mitotic exit in budding yeast. In vitro regulation of Tem1 GTPase by Bub2 and Bfa1. *J Biol Chem* 277, 28439-45.

Güldener, U., Heck, S., Fiedler, T., Beinhauer, J. and Hegemann, J. (1996). A new efficient gene disruption cassette for repeated use in budding yeast. *Nucleic Acids Res* 24, 2519-2524.

Hardwick,K.G. and Murray,A.W. (1995). Mad1p, a phosphoprotein component of the spindle assembly checkpoint in budding yeast. *J Cell Biol* 131, 709-20.

Hardwick,K.G., Weiss,E., Luca,F.C., Winey,M., and Murray,A.W. (1996). Activation of the budding yeast spindle assembly checkpoint without mitotic spindle disruption. *Science* 273, 953-956.

Hardwick,K.G. (1998). The spindle checkpoint. Trends Genet. 1998 Jan;14(1):1-4.

Hanahan, D. (1983). Studies on transformation of Escherichia coli with plasmids. *J Mol Biol* 166, 557-80.

He,X., Jones,M.H., Winey,M., and Sazer,S. (1998). mph1, a member of the Mps1-like family of dual specificity protein kinases, is required for the spindle checkpoint in *S.pombe*. *J Cell Sci* 111, 1635-47.

He, X., Asthana, S. and Sorger, P. K. (2000). Transient sister chromatid separation and elastic deformation of chromosomes during mitosis in budding yeast. *Cell* 101, 763-75.

He, X., Rines, D. R., Espelin, C. W. and Sorger, P. K. (2001). Molecular analysis of kinetochore-microtubule attachment in budding yeast. *Cell* 106, 195-206.

Hecht, A. and Grunstein, M. (1999). Mapping DNA interaction sites of chromosomal proteins using immunoprecipitation and polymerase chain reaction. *Methods Enzymol* 304, 399-414.

Hildebrandt, E. R. and Hoyt, M. A. (2000). Mitotic motors in Saccharomyces cerevisiae. *Biochim Biophys Acta* 1496, 99-116.

Hoyt, M. A., He, L., Loo, K. K. and Saunders, W. S. (1992). Two Saccharomyces cerevisiae kinesin-related gene products required for mitotic spindle assembly. *J Cell Biol* 118, 109-20.

Hunter AW, Wordeman L. (2000). How motor proteins influence microtubule polymerization dynamics. *J Cell Sci* 113, 4379-89.

Hoyt, M. A., Totis, L. and Roberts, B. T. (1991). *S. cerevisiae* genes required for cell cycle arrest in response to loss of microtubule function. *Cell* 66, 507-17.

Howell BJ, Moree B, Farrar EM, Stewart S, Fang G, Salmon ED. (2004). Spindle checkpoint protein dynamics at kinetochores in living cells. *Curr Biol* 14(11):953-64.

Ito, T., Chiba, T., Ozawa, R., Yoshida, M., Hattori, M. and Sakaki, Y. (2001). A comprehensive two-hybrid analysis to explore the yeast protein interactome. *Proc Natl Acad Sci U S A* 98, 4569-74.

Janke, C., Ortiz, J., Lechner, J., Shevchenko, A., Shevchenko, A., Magiera, M. M., Schramm, C. and Schiebel, E. (2001). The budding yeast proteins Spc24p and Spc25p interact with Ndc80p and Nuf2p at the kinetochore and are important for kinetochore clustering and checkpoint control. *Embo J* 20, 777-91.

Janke, C., Ortiz, J., Tanaka, T. U., Lechner, J. and Schiebel, E. (2002). Four new subunits of the Dam1-Duo1 complex reveal novel functions in sister kinetochore biorientation. *Embo J* 21, 181-93.

Jiang W, Lechner J, Carbon J. (1993). Isolation and characterization of a gene (CBF2) specifying a protein component of the budding yeast kinetochore. *J Cell Biol* 121(3):513-9.

Jones, M. H., He, X., Giddings, T. H. and Winey, M. (2001). Yeast Dam1p has a role at the kinetochore in assembly of the mitotic spindle. *Proc Natl Acad Sci U S A 98*, 13675-80.

Kallio MJ, Beardmore VA, Weinstein J, Gorbsky GJ. (2002). Rapid microtubule-independent dynamics of Cdc20 at kinetochores and centrosomes in mammalian cells. *J Cell Biol* 158, 841-7.

Knop, M., Siegers, K., Pereira, G., Zachariae, W., Winsor, B., Nasmyth, K. and Schiebel, E. (1999). Epitope tagging of yeast genes using a PCR-based strategy: more tags and improved practical routines. *Yeast* 15, 963-72.

Lampson MA, Kapoor TM. (2005). The human mitotic checkpoint protein BubR1 regulates chromosome-spindle attachments. *Nat Cell Biol* 7(1):93-8.

Laemmli UK. (1970). Cleavage of structural proteins during the assembly of the head of bacteriophage T4. *Nature* 15;227

Li, Y. and Benezra, R. (1996). Identification of a human mitotic checkpoint gene: hsMAD2. *Science* 274, 246-8.

Li, X. and Nicklas, R. B. (1995). Mitotic forces control a cell-cycle checkpoint. *Nature* 373, 630-2.

Li, R. and Murray, A. W. (1991). Feedback control of mitosis in budding yeast. Cell 66, 519-31.

Li, Y., Bachant, J., Alcasabas, A. A., Wang, Y., Qin, J. and Elledge, S. J. (2002). The mitotic spindle is required for loading of the DASH complex onto the kinetochore. *Genes Dev* 16, 183-97.

Lindberg,R.A., Fischer,W.H., and Hunter,T. (1993). Characterisation of a human protein threonine kinase isolated by screening an expression library with antibodies to phosphotyrosine. *Oncogene* 8, 351-359.

Lechner, J. and Carbon, J. (1991). A 240 kd multisubunit protein complex, CBF3, is a major component of the budding yeast centromere. *Cell* 64, 717-25.

Murray,A.W. (1994). Cyclin-dependent kinases: regulators of the cell cycle and more. *Chem Biol* 1, 191-195.

Martin-Lluesma, S., Stucke, V. M. and Nigg, E. A. (2002). Role of Hec1 in spindle checkpoint signaling and kinetochore recruitment of Mad1/Mad2. *Science* 297, 2267-70.

Michaelis, C., Ciosk, R. and Nasmyth, K. (1997). Cohesins: chromosomal proteins that prevent premature separation of sister chromatids. *Cell* 91, 35-45.

Millband,D.N. and Hardwick,K.G. (2002). Fission yeast Mad3p is required for Mad2p to inhibit the anaphase-promoting complex and localizes to kinetochores in a Bub1p-, Bub3p-, and Mph1p-dependent manner. *Mol Cell Biol* 22, 2728-2742.

Mills,G.B., Schmandt,R., McGill,M., Amendola,A., Hill,M., Jacobs,K., May,C., Rodricks,A.M., Campbell,S., and Hogg,D. (1992). Expression of TTK, a novel human protein kinase, is associated with cell proliferation. *J Biol Chem* 267, 16000-16006.

McEwen, B. F., Heagle, A. B., Cassels, G. O., Buttle, K. F. and Rieder, C. L. (1997). Kinetochore fiber maturation in PtK1 cells and its implications for the mechanisms of chromosome congression and anaphase onset. *J Cell Biol* 137, 1567-80.

McIntosh, J. R. (1991). Structural and mechanical control of mitotic progression. *Cold Spring Harb Symp Quant Biol* 56, 613-9.

Meluh, P. B., Yang, P., Glowczewski, L., Koshland, D. and Smith, M. M. (1998). Cse4p is a component of the core centromere of Saccharomyces cerevisiae. *Cell* 94, 607-13.

Meluh, P. B. and Koshland, D. (1995). Evidence that the MIF2 gene of Saccharomyces cerevisiae encodes a centromere protein with homology to the mammalian centromere protein CENP-C. *Mol Biol Cell* 6, 793-807.

McCleland, M. L., Gardner, R. D., Kallio, M. J., Daum, J. R., Gorbsky, G. J., Burke, D. J. and Stukenberg, P. T. (2003). The highly conserved Ndc80 complex is required for kinetochore assembly, chromosome congression, and spindle checkpoint activity. *Genes Dev* 17, 101-14.

Measday, V., Hailey, D. W., Pot, I., Givan, S. A., Hyland, K. M., Cagney, G., Fields, S., Davis, T. N. and Hieter, P. (2002). Ctf3p, the Mis6 budding yeast homolog, interacts with Mcm22p and Mcm16p at the yeast outer kinetochore. *Genes Dev* 16, 101-13.

Müller-Reichert, T., Sassoon, I., O'Toole, E., Romao, M., Ashford, A. J., Hyman, A. A. and Antony, C. (2003). Analysis of the distribution of the kinetochore protein Ndc10p in Saccharomyces cerevisiae using 3-D modeling of mitotic spindles. *Chromosoma* 111, 417-28.

Moore, A. and Wordeman, L. (2004). The mechanism, function and regulation of depolymerizing kinesins during mitosis. *Trends Cell Biol* 14, 537-46.

Michaelis C, et al. (1997) Cohesins: chromosomal proteins that prevent premature separation of sister chromatids. *Cell* 91, 35-45.

Musacchio A, Salmon ED (2007). The spindle-assembly checkpoint in space and time. *Nat Rev Mol Cell Biol* 8, 379-93.

McAinsh, A. D., Tytell, J. D. and Sorger, P. K. (2003). Structure, function, and regulation of budding yeast kinetochores. *Annu Rev Cell Dev Biol* 19, 519-39.

Nicklas, R. B., Waters, J. C., Salmon, E. D. and Ward, S. C. (2001). Checkpoint signals in grasshopper meiosis are sensitive to microtubule attachment, but tension is still essential. *J Cell Sci* 114, 4173-4183.

Ng, R. and Carbon, J. (1987). Mutational and in vitro protein-binding studies on centromere DNA from Saccharomyces cerevisiae. *Mol Cell Biol* 7, 4522-34.

Nekrasov, V. S., Smith, M. A., Peak-Chew, S. and Kilmartin, J. V. (2003). Interactions between centromere complexes in Saccharomyces cerevisiae. *Mol Biol Cell* 14, 4931-46.

Ortiz, J., Stemmann, O., Rank, S. and Lechner, J. (1999). A putative protein complex consisting of Ctf19, Mcm21, and Okp1 represents a missing link in the budding yeast kinetochore. Genes Dev 13, 1140-55.

Osborne MA, Schlenstedt G, Jinks T, Silver PA. (1994). Nuf2, a spindle pole body-associated protein required for nuclear division in yeast. *J Cell Biol* 125(4):853-66.

Palmer, R. E., Sullivan, D. S., Huffaker, T. and Koshland, D. (1992). Role of astral microtubules and actin in spindle orientation and migration in the budding yeast, Saccharomyces cerevisiae. *J Cell Biol* 119, 583-93.

Palframan WJ, Meehl JB, Jaspersen SL, Winey M, Murray AW. (2006). Anaphase inactivation of the spindle checkpoint. *Science* 4;313(5787):680-4.

Pereira, G. and Schiebel, E. (2003). Separase regulates INCENP-Aurora B anaphase spindle function through Cdc14. *Science* 302, 2120-4.

Pereira, G., Hofken, T., Grindlay, J., Manson, C. and Schiebel, E. (2000). The Bub2p spindle checkpoint links nuclear migration with mitotic exit. *Mol Cell* 6, 1-10.

Pereira,G., Knop,M., and Schiebel,E. (1998). Spc98p directs the yeast gamma-tubulin complex into the nucleus and is subject to cell cycle-dependent phosphorylation on the nuclear side of the spindle pole body. Mol. Biol. *Cell* 9, 775-793.

Pinsky, B. A., Tatsutani, S. Y., Collins, K. A. and Biggins, S. (2003). An Mtw1 complex promotes kinetochore biorientation that is monitored by the Ipl1/Aurora protein kinase. *Dev Cell* 5, 735-45.

Pinsky, B. A., Kung, C., Shokat, K. M. and Biggins, S. (2006). The Ipl1-Aurora protein kinase activates the spindle checkpoint by creating unattached kinetochores. *Nat Cell Biol* 8, 78-83.

Puig, O., Caspary, F., Rigaut, G., Rutz, B., Bouveret, E., Bragado-Nilsson, E., Wilm, M. and Seraphin, B. (2001). The tandem affinity purification (TAP) method: a general procedure of protein complex purification. *Methods* 24, 218-29.

Poddar A, Daniel JA, Daum JR, Burke DJ. (2004). Differential kinetochore requirements for establishment and maintenance of the spindle checkpoint are dependent on the mechanism of checkpoint activation in Saccharomyces cerevisiae. *Cell Cycle* 3, 197-204.

Rieder, C. L., Cole, R. W., Khodjakov, A. and Sluder, G. (1995). The checkpoint delaying anaphase in response to chromosome monoorientation is mediated by an inhibitory signal produced by unattached kinetochores. *J Cell Biol* 130, 941-8.

Rout MP, Kilmartin JV. (1990). Components of the yeast spindle and spindle pole body. *J Cell Biol* 111(5 Pt 1):1913-27.

Sambrook, J., Fritsch, E. F. and Maniatis, T. (2001). Molecular cloning - A laboratory manual (3rd edition). *Cold Spring Harbor Laboratory Press, Cold Spring Harbor, New York.*.

Sandall S, Severin F, McLeod IX, Yates JR 3rd, Oegema K, Hyman A, Desai A. (2006). A Bir1-Sli15 complex connects centromeres to microtubules and is required to sense kinetochore tension. *Cell* 127, 1179-91.

Schiestl, R. H. and Gietz, R. D. (1989). High efficiency transformation of intact yeast cells using single stranded nucleic acids as a carrier. *Curr Genet* 16, 339-46.

Stucke,V.M., Sillje,H.H., Arnaud,L., and Nigg,E.A. (2002). Human Mps1 kinase is required for the spindle assembly checkpoint but not for centrosome duplication. *EMBO J* 21, 1723-1732.

Stucke VM, Baumann C, Nigg EA. (2004). Kinetochore localization and microtubule interaction of the human spindle checkpoint kinase Mps1. *Chromosoma* 113(1):1-15.

Strunnikov, A. V., Kingsbury, J. and Koshland, D. (1995). CEP3 encodes a centromere protein of Saccharomyces cerevisiae. *J Cell Biol* 128, 749-60.

Scharfenberger, M., Ortiz, J., Grau, N., Janke, C., Schiebel, E. and Lechner, J. (2003). Nsl1p is essential for the establishment of bipolarity and the localization of the Dam-Duo complex. *Embo J* 22, 6584-97.

Shang C., Hazbun T.R., Cheeseman I.M., Aranda J., Fields S., Drubin D.G. and Barnes G. (2003). Kinetochore Protein Interactions and their Regulation by the Aurora Kinase Ipl1p. *Mol. Biol. Cell* 14, 3342-3355.

Stemmann, O. and Lechner, J. (1996). The Saccharomyces cerevisiae kinetochore contains a cyclin-CDK complexing homologue, as identified by in vitro reconstitution. *Embo J* 15, 3611-20.

Stern, B. M. and Murray, A. W. (2001). Lack of tension at kinetochores activates the spindle checkpoint in budding yeast. *Curr Biol* 11, 1462-7.

Schuyler, S. C. and Pellman, D. (2001a). Microtubule "plus-end-tracking proteins": The end is just the beginning. Cell 105, 421-4.

Schuyler, S. C. and Pellman, D. (2001b). Search, capture and signal: games microtubules and centrosomes play. *J Cell Sci* 114, 247-55.

Stoler, S., Keith, K. C., Curnick, K. E. and Fitzgerald-Hayes, M. (1995). A mutation in CSE4, an essential gene encoding a novel chromatin-associated protein in yeast, causes chromosome nondisjunction and cell cycle arrest at mitosis. *Genes Dev* 9, 573-86.

Schutz,A.R. and Winey,M. (1998). New alleles of the yeast MPS1 gene reveal multiple requirements in spindle pole body duplication. *Mol Biol Cell* 9, 759-74.

Sullivan, M., Lehane, C. and Uhlmann, F. (2001). Orchestrating anaphase and mitotic exit: separase cleavage and localization of Slk19. *Nat Cell Biol* 3, 771-7.

Skoufias, D. A., Andreassen, P. R., Lacroix, F. B., Wilson, L. and Margolis, R. L. (2001). Mammalian mad2 and bub1/bubR1 recognize distinct spindleattachment and kinetochore-tension checkpoints. *Proc Natl Acad Sci USA 98*, 4492-4497.

Segal, M. and Bloom, K. (2001). Control of spindle polarity and orientation in Saccharomyces cerevisiae. *Trends Cell Biol* 11, 160-6.

Taylor,S.S., Hussein,D., Wang,Y., Elderkin,S., and Morrow,C.J. (2001). Kinetochore localization and phosphorylation of the mitotic checkpoint components Bub1 and BubR1 are differentially regulated by spindle events in human cells. *J Cell Sci* 114, 4385-4395.

Tanaka, T. U., Rachidi, N., Janke, C., Pereira, G., Galova, M., Schiebel, E., Stark, M. J. and Nasmyth, K. (2002). Evidence that the Ipl1-Sli15 (Aurora kinase-INCENP) complex promotes chromosome bi-orientation by altering kinetochore-spindle pole connections. *Cell* 108, 317-29.

Tanaka, K., Mukae, N., Dewar, H., van Breugel, M., James, E. K., Prescott, A. R., Antony, C. and Tanaka, T. U. (2005). Molecular mechanisms of kinetochore capture by spindle microtubules. *Nature* 434, 987-94.

Tang Z, Bharadwaj R, Li B, Yu H. (2001). Mad2-Independent inhibition of APCCdc20 by the mitotic checkpoint protein BubR1. *Dev Cell* 227-37.

Tytell, J. D. and Sorger, P. K. (2006). Analysis of kinesin motor function at budding yeast kinetochores. *J Cell Biol* 172, 861-74.

Uetz, P., Giot, L., Cagney, G., Mansfield, T. A., Judson, R. S., Knight, J. R., Lockshon, D., Narayan, V., Srinivasan, M., Pochart, P. et al. (2000). A comprehensive analysis of protein-protein interactions in *Saccharomyces cerevisiae*. *Nature* 403, 623-7.

Uhlmann F, et al. (2000). Cleavage of cohesin by the CD clan protease separin triggers anaphase in yeast. *Cell* 103, 375-86.

Vagnarelli, P. and Earnshaw, W. C. (2004). Chromosomal passengers: the four-dimensional regulation of mitotic events. *Chromosoma* 113, 211-222.

Westermann, S., Cheeseman, I. M., Anderson, S., Yates, J. R., 3rd, Drubin, D. G. and Barnes, G. (2003). Architecture of the budding yeast kinetochore reveals a conserved molecular core. *J Cell Biol* 163, 215-22.

Wigge, P. A. and Kilmartin, J. V. (2001). The Ndc80p complex from Saccharomyces cerevisiae contains conserved centromere components and has a function in chromosome segregation. J Cell Biol 152, 349-60.

Wassmann, K., Liberal, V. and Benezra, R. (2003). Mad2 phosphorylation regulates its association with Mad1and the APC/C. *EMBO J* 22, 797-806.

Winey,M., Goetsch,L., Baum,P., and Byers,B. (1991). MPS1 and MPS2: novel yeast genes defining distinct steps of spindle pole body duplication. *J Cell Biol* 114, 745-754.

Wigge,P.A., Jensen,O.N., Holmes,S., Soues,S., Mann,M., and Kilmartin,J.V. (1998). Analysis of the Saccharomyces spindle pole by matrix-assisted laser desorption/ionization (MALDI) mass spectrometry. *Journal of Cell Biology* 141, 967-977.

Weiss,E. and Winey,M. (1996). The Saccharomyces cerevisiae spindle pole body duplication gene MPS1 is part of a mitotic checkpoint. *J Cell Biol* 132, 111-23.

Waters,J.C., Chen,R.H., Murray,A.W., and Salmon,E.D. (1998). Localization of Mad2 to kinetochores depends on microtubule attachment, not tension. *J Cell Biol* 141, 1181-91.

Xiao Z, McGrew JT, Schroeder AJ, Fitzgerald-Hayes M. (1993). CSE1 and CSE2, two new genes required for accurate mitotic chromosome segregation in Saccharomyces cerevisiae. *Mol Cell Biol* (8):4691-702.

Yin H, You L, Pasqualone D, Kopski KM, Huffaker TC. (2002). Stu1p is physically associated with beta-tubulin and is required for structural integrity of the mitotic spindle. *Mol Biol Cell* 13, 1881-92.

Yu H. (2006). Structural activation of Mad2 in the mitotic spindle checkpoint: the two-state Mad2 model versus the Mad2 template model. *J Cell Biol* 24;173(2):153-7.

Zeng, X., Kahana, J. A., Silver, P. A., Morphew, M. K., McIntosh, J. R., Fitch, I. T., Carbon, J. and Saunders, W. S. (1999). Slk19p is a centromere protein that functions to stabilize mitotic spindles. *J Cell Biol* 146, 415-25.

Zachariae W and Nasmyth K (1999). Whose end is destruction: cell division and the anaphase-promoting complex. *Genes Dev* 13, 2039-58.

ACKNOWLEDGEMENTS

I would like to acknowledge the following people for their support in the accomplishment of this work:

Johannes Lechner for giving me the opportunity to work in his laboratory, for numerous experimental ideas, scientific discussions and for permanent support.

Michael Brunner for being my first referee.

Jens Pfannstiel and Jürgen Reichert for extensive support in the identification of Ndc80-phosphorylation sites.

Eileen Diezel, Maria Knapp and Barbara Lang for excellent technical support.

My lab collegues for experimental support, fruitful discussions and technical advice.

Daniel Spengler and Vikram Panse for constructive discussions and helpful advice.

All members of the BZH for their cooperativeness and technical support.

Ndc80 for carrying phosphate-groups which are physiologically relevant!

My parents, my sister and my friends who have given me great support in every respect.